The University of Texas at Dallas
Center for Quantum Electronics
The Gamma-Ray Laser Project
Quarterly Report
July-September 1987

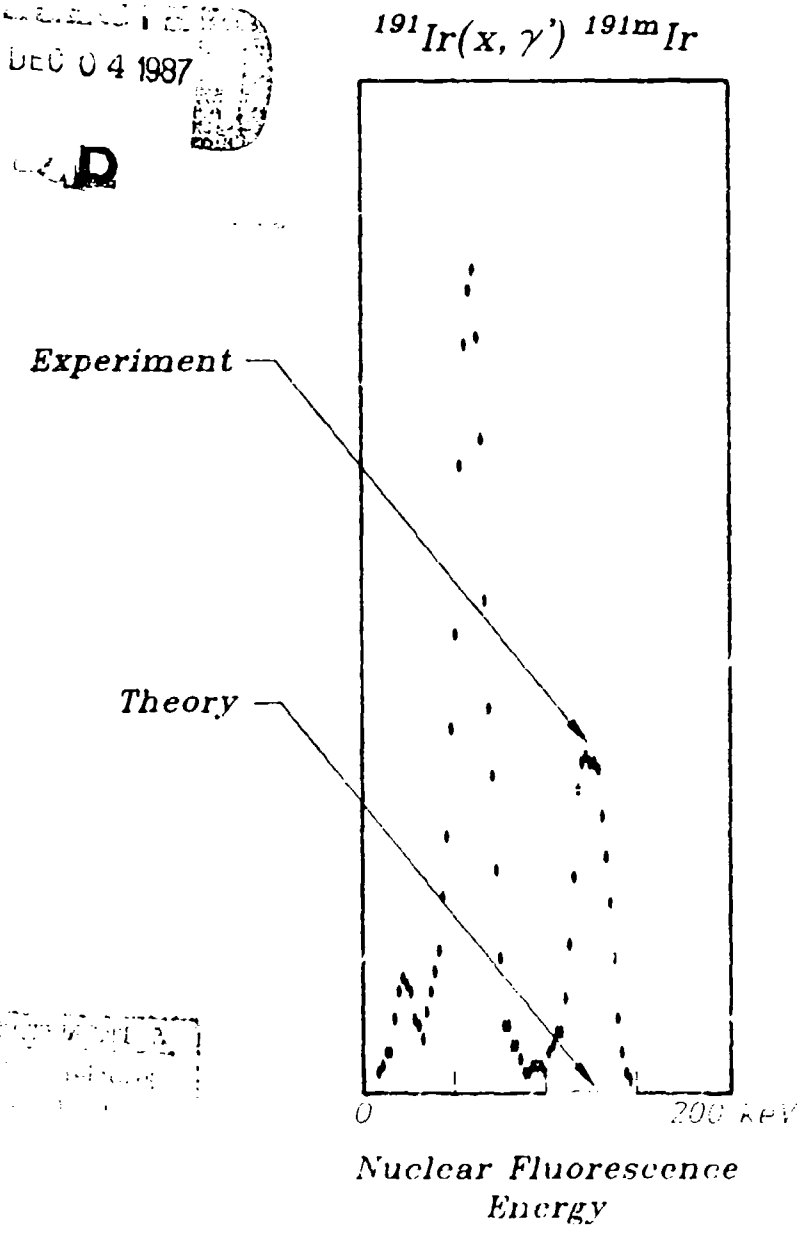

Report GRL/8702

PROOF OF THE FEASIBILITY OF COHERENT AND INCOHERENT SCHEMES FOR PUMPING A GAMMA-RAY LASER

Principal Investigator: Carl B. Collins
The University of Texas at Dallas
Center for Quantum Electronics
P.O. Box 830688
Richardson, Texas 75083-0688

October 1987

Quarterly Technical Progress Report
1 July 1987 through 30 September 1987
Contract Number N00014-86-C-2488

Prepared for
INNOVATIVE SCIENCE AND TECHNOLOGY DIRECTORATE
OF STRATEGIC DEFENSE INITIATIVE ORGANIZATION

Contracting Officer's Technical Representative
Dr. Paul Kepple, Code 4720
Naval Research Laboratory
4555 Overlook Avenue, SW
Washington, DC 20375-5000

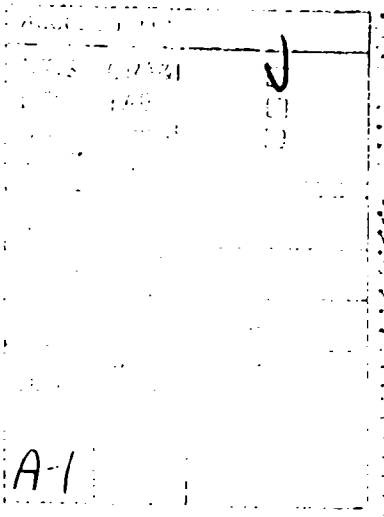

SECURITY CLASSIFICATION OF THIS PAGE (When Data Entered)

REPORT DOCUMENTATION PAGE

READ INSTRUCTIONS BEFORE COMPLETING FORM

1. REPORT NUMBER: GRL/8702	2. GOVT ACCESSION NO.
3. RECIPIENT'S CATALOG NUMBER	
4. TITLE (and Subtitle): PROOF OF THE FEASIBILITY OF COHERENT AND INCOHERENT SCHEMES FOR PUMPING A GAMMA-RAY LASER	5. TYPE OF REPORT & PERIOD COVERED: Quarterly Technical Progress 7/1/87 - 9/30/87
	6. PERFORMING ORG. REPORT NUMBER
7. AUTHOR(s): C. B. Collins	8. CONTRACT OR GRANT NUMBER(s): N00014-86-C-2488
9. PERFORMING ORGANIZATION NAME AND ADDRESS: University of Texas at Dallas, Center for Quantum Electronics, P.O.Box 830688/ Richardson, TX 75083-0688	10. PROGRAM ELEMENT, PROJECT, TASK AREA & WORK UNIT NUMBERS
11. CONTROLLING OFFICE NAME AND ADDRESS: INNOVATIVE SCIENCE AND TECHNOLOGY DIRECTORATE OF STRATEGIC DEFENSE INITIATIVE ORGANIZATION	12. REPORT DATE: October 1987
	13. NUMBER OF PAGES: 105
14. MONITORING AGENCY NAME & ADDRESS (if different from Controlling Office): Dr. Paul Kepple, Code 4720, Naval Research Laboratory, 4555 Overlook Avenue, SW, Washington, DC 20375-5000	15. SECURITY CLASS. (of this report): Unclassified
	15a. DECLASSIFICATION/DOWNGRADING SCHEDULE

16. DISTRIBUTION STATEMENT (of this Report)

This document has been approved for public release and sale; its distribution is unlimited.

17. DISTRIBUTION STATEMENT (of the abstract entered in Block 20, if different from Report)

18. SUPPLEMENTARY NOTES

19. KEY WORDS (Continue on reverse side if necessary and identify by block number)

20. ABSTRACT (Continue on reverse side if necessary and identify by block number)

Recent approaches to the problem of the gamma-ray laser have focused upon upconversion techniques in which metastable nuclei are pumped with long wavelength radiation. At the nuclear level the storage of energy can approach tera-Joules (10^{12} J) per liter for thousands of years. However, any plan to use such a resource for a gamma-ray laser poses problems of a broad interdisciplinary nature requiring the fusion of concepts taken
(continued next page)

DD FORM 1 JAN 73 1473 EDITION OF 1 NOV 65 IS OBSOLETE

SECURITY CLASSIFICATION OF THIS PAGE (When Data Entered)

20. Abstract (continued)

from relatively unrelated fields of physics. Our research group has described several means through which this energy might be coupled to the radiation fields with cross sections for stimulated emission that could reach 10^{-17} cm^2. Such a stimulated release could lead to output powers as great as 3×10^{21} Watts/liter. Since 1978 we have pursued an approach for the upconversion of longer wavelength radiation incident upon isomeric nuclear populations that can avoid many of the difficulties encountered with traditional concepts of single photon pumping. Recent experiments have confirmed the general feasibility and have indicated that a gamma-ray laser is feasible if the right combination of energy levels and branching ratios exists in some real material. Of the 1886 distinguishable nuclear materials, the present state-of-the-art has been adequate to identify 29 first-class candidates, but further evaluation cannot proceed without remeasurements of nuclear properties with higher precision. A laser-grade database of nuclear properties does not yet exist, but the techniques for constructing one have been developed under this contract and are now being utilized. Resolution of the question of the feasibility of a gamma-ray laser now rests upon the determination of: 1) the identity of the best candidate, 2) the threshold level of laser output, and 3) the upconversion driver for that material.

This ~~quarter's~~ report focuses upon continued development of one of the new technologies being developed for the screening of the laser candidates. It is the nuclear analog of the optical double resonance methods which produced much of the database at the molecular level that was of such essential use in the development of conventional lasers. Applied most recently to the study of levels which might be used in dumping isomeric populations into freely radiating states, it produced an unexpected result of major importance. In several test isotopes, a class of extremely useful states was discovered that could radiatively couple to both normal and isomeric states of a nucleus.

The achievements of this quarter have a clear significance. Two strong mechanisms were demonstrated for the elusive "interband transfer" of nuclear populations. As many as four quanta of angular momenta were transferred by an intense pulse of x-rays used to pump nuclei from the initial to the fluorescent state with integrated cross sections that varied from 10 to 10,000 on the scale in which unity results in a large yield. One technique funneled population through a level of mixed single particle states, and the other utilized a funneling level at the head of a complex cascade to the fluorescent level. Both considerably strengthen the probabilities that a suitable candidate for a gamma-ray laser exists in reality.

TABLE OF CONTENTS

PREFACE

The nuclear analog of the ruby laser embodies the simplest concepts for a gamma-ray laser. Not surprisingly, the greatest rate of achievement in the quest for a subAngstrom laser has developed in that direction.

The past fiscal year saw the major milestone demonstration of substantial amounts of nuclear fluorescence pumped by flash x-rays. Proving our concept of bandwidth funneling, we achieved eleven orders of magnitude more output than could have been obtained by pumping the fluorescent level directly. In the first quarter of FY-87, we showed a scale-up of fluorescence intensities when demonstration targets were pumped with x-rays from a nuclear simulator. Funneled outputs increased linearly with input for another four orders of magnitude, showing no evidence of detrimental saturation or loss of efficiency. In this second quarter of FY-87 scientific momentum has continued along this line and has resulted in another notable achievement. *It has been shown that intense x-rays were able to create and destroy large amounts of angular momenta possessed by the nuclei being pumped.*

Nuclei to be used in the analog of the ruby laser can start in either ground or isomeric states. In addition to the obvious need to transfer energy in order to reach the fluorescence level to be populated for lasing, there must also be a substantial transfer of angular momentum. Last year's major breakthrough proved that the energy could be transferred, and now in this quarter we report that the angular momentum can be pumped in amounts as large as $\Delta J = 3$, and even $\Delta J = 4$. The integrated cross sections for the excitation of fluorescence in such cases as ^{167}Er and ^{191}Ir were found to be as large as had been reported for other species in which $\Delta J = 1$. This is extremely important as a contrast with the depressingly negative results from attempts to transfer $\Delta J = 3$ in a more complicated scheme pursued elsewhere. *We find that large amounts of angular momentum can be transferred to a nucleus by "optically pumping" with x-rays through an appropriate funneling process.* A detailed review of the data and analyses are found in one of the several manuscripts following.

Continuing the preparation of this report as an "in-house" journal, this series presents material to reflect the individual contributions of the teams of research faculty and graduate students involved in these

phases of the research. In this regard I wish to thank all our staff for their splendid efforts in supporting the preparation of these manuscripts to a rather demanding timetable.

- C. B. Collins
- Director
- Center for Quantum Electronics

INTRODUCTION

Levels of nuclear excitation which might be efficiently stimulated in a gamma-ray laser are very difficult to pump directly. To have sharply-peaked cross sections for stimulated emission, such levels must have very narrow widths for interaction with the radiation field. This is a fundamental attribute that has led to the facile criticism that "absorption widths in nuclei are too narrow to permit effective pumping with x-rays."

The same concerns were voiced in atomic physics before Maiman's great discovery, and it has been useful to pursue this analogy between ruby and gamma-ray lasers. Identification and exploitation of a bandwidth funnel in ruby were the critical keys in the development of the first laser. There was a broad absorption band exciting a state of Cr^{3+} which quickly decayed by cascading its population into levels of lower energy. A reasonably favorable pattern of branching insured that much of the cascading populated the narrow level. At the core of our simplest proposal[1] for pumping a gamma-ray laser is the use of the analog of this effect at the nuclear level as shown in Fig. 1. A detailed analysis of this option was reviewed in the previous quarterly reports[2,3] together with the breakthrough report actually demonstrating the great utility of bandwidth funneling at the nuclear level. Yields of gamma-ray fluorescence in ^{77}Se and ^{79}Br were enhanced by eleven orders of magnitude by this effect.[4]

Also shown in Fig. 1 is a further refinement of the incoherent pumping scheme benefiting from upconversion. As has been often discussed[5,6] upconversion as shown in Fig. 1c has many advantages. Most prior reports have emphasized those tending to enhance performance and efficiencies; however, upconversion also makes threshold itself much more accessible. Higher energy isomers need less pump energy to reach the broad collective states that would optimize bandwidth funneling, and the required pump energies can fall in the range where strong x-ray lines may be found to concentrate the spectral intensity.

At first seeming to temper the strong advantages of upconversion is a concern for the conservation of angular momenta. In the simplest perceptions, radiative transitions are expected to exchange no more than unit quanta of angular momenta with the fields. At this level of understanding, it would be unlikely that J_f in Fig. 1c could differ from

J_i by more than 2ħ. Most of the isomeric states derive their long lifetimes for the storage of excitation energy from the larger differences in angular momenta they would have to transfer to reach the ground state. A common occurrence is

$$|J_i - J_o| \geq 4 \quad , \tag{1}$$

for the candidate isomers for a gamma-ray laser. Then, in this simplistic view the fluorescent level should have

$$|J_f - J_o| \geq 2 \quad , \tag{2}$$

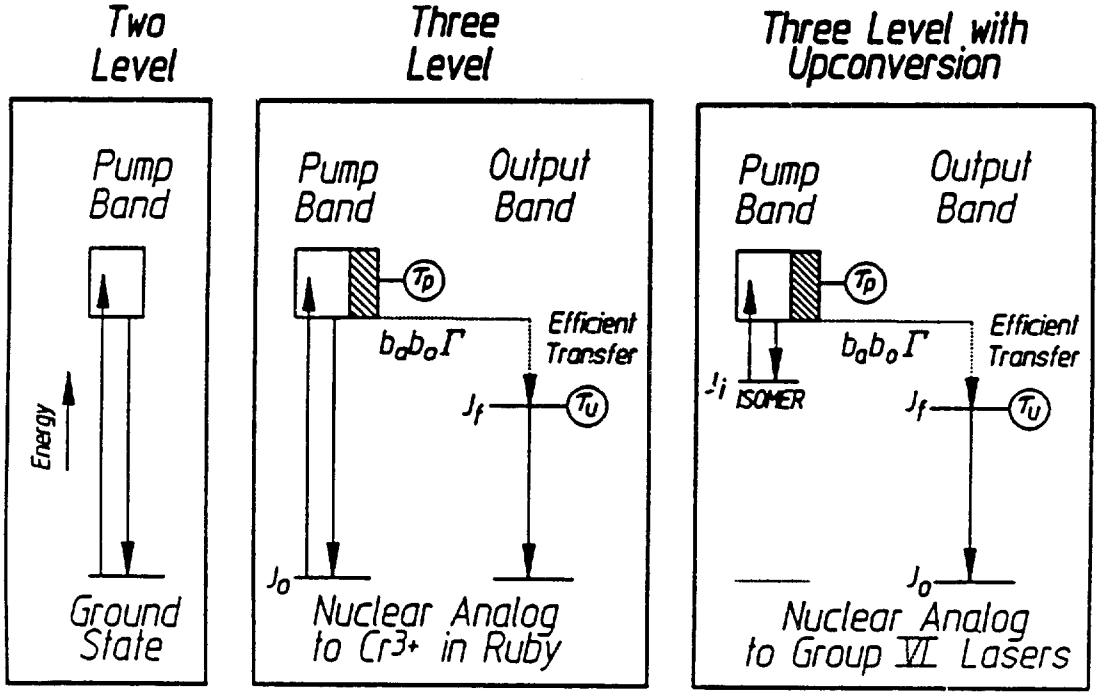

Figure 1: Schematic representation of the energetics of the priority schemes for pumping a gamma-ray laser with flash x-rays. The large width of the level defining the pump band is implied by the height of the rectangle representing the level, and the shaded portion indicates that fraction b_o which is attributed to the transition to the upper laser level. Angular momenta of the ground, isomeric, and fluorescent levels are denoted by J_o, J_i, and J_f, respectively.
(a) Traditional two-level approach.
(b) Three-level analog of the ruby laser serving to illustrate the important concept of bandwidth funneling.
(c) Refinement of the three-level scheme which incorporates upconversion in order to lessen the energy per photon which must be supplied in the pumping step.

and so, itself, might have too long a lifetime τ_u to be usable in a laser. At a finer level of perception, many factors can be seen to remedy the situation. Two particularly effective ones have been demonstrated during this most recent quarter.

Many of the interesting isomers belong to nuclei deformed from the normally spherical shape. For those systems, there is an additional quantum number of dominant importance, K, the projection of individual nucleonic angular momenta upon the axis of elongation. To this is added the collective rotation of the nucleus to obtain the total angular momentum J. The resulting system of energy levels resembles those of a diatomic molecule for which

$$E_x(K,J) = E_x(K) + B_x J(J+1) \quad , \tag{3}$$

where

$$J \geq K \geq 0 \quad , \tag{4}$$

and

$$J = |K|, \ |K|+1, \ |K|+2, \ldots \quad . \tag{5}$$

In these expressions B_x is a rotational constant, and $E_x(K)$ is the lowest value for any level in the resulting "band" of energies identified by other quantum numbers x. For such systems it becomes much easier to satisfy the restrictions on ΔJ because of the possibility of intraband transitions occurring during the cascade to the fluorescence level. However, a new problem arises from restrictions upon ΔK.

For the deformed nuclei, the J_y in Fig. 1 must be replaced by K_y, where y denotes i, f, or o. Then, the analogous concerns and constraints upon K must also be satisfied during interactions with the radiation field. In most cases of interest it is the condition

$$|K_i - K_o| \geq 4 \quad , \tag{6}$$

that makes an actual laser candidate isomeric. For perfectly pure quantum states of the deformed nuclei, we would not expect bandwidth funneling to transfer effectively more than $\Delta K = 2$ in the two steps shown in Figs. (1b) or (1c).

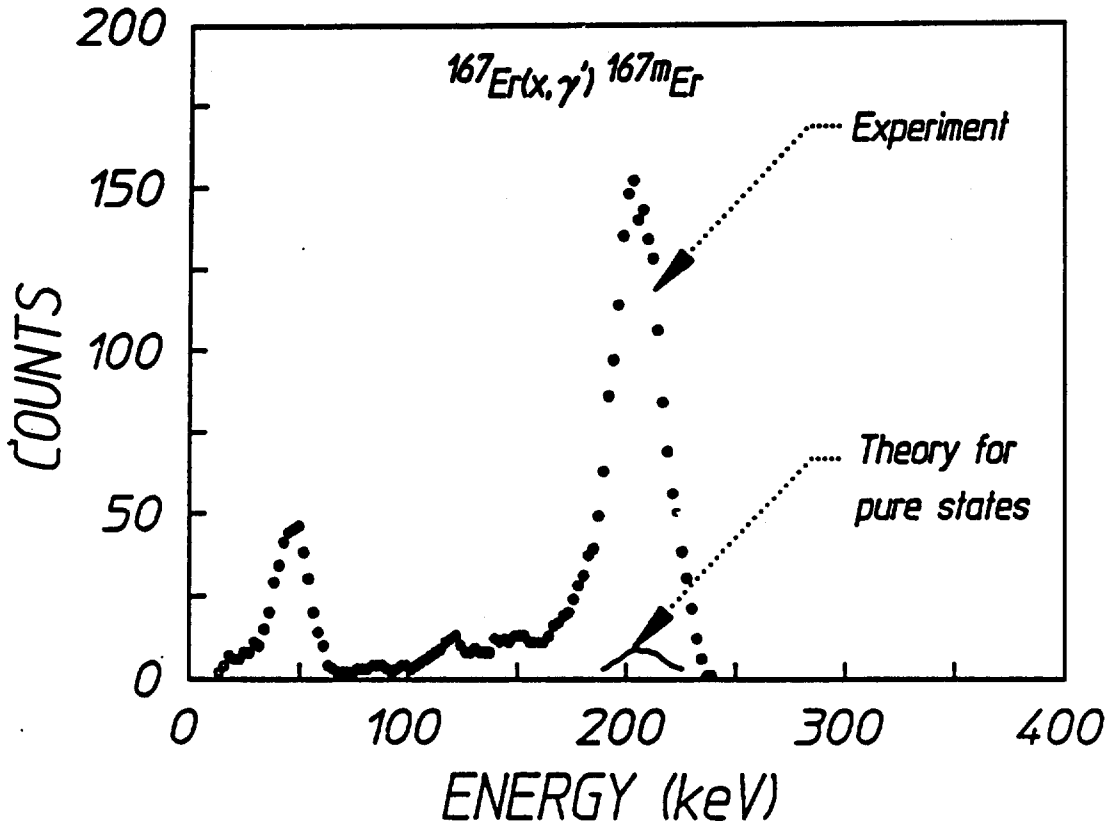

Figure 2: Arrows identify the nuclear component of the spectrum of fluorescence of Er_2O_3 in comparison with model predictions based upon pure states whose nuclear parameters were taken from the extant database. Data were obtained from a single irradiation of 2.8 g of Er_2O_3 in natural isotopic abundance with about 10^{16} keV/keV of bremsstrahlung from the DNA/PITHON nuclear simulator.

One key to realizing larger transfers of the critical K-projection is to *avoid systems afflicted with a high purity of single particle states*. Figure 2 shows fluorescence from the K = $1/2^-$ level of ^{167}Er pumped from the ground K = $7/2^+$ by an intense flash of bremsstrahlung. Shown there is the yield expected theoretically from bandwidth funneling through the pure states whose properties[7] are known to require $|\Delta K| = 2$ in the cascading step. The intensity actually radiated was measured to be 1700% in excess of theory as shown in Fig. 2. Evidence is discussed in the following manuscript that this drastic increase in yield results from bandwidth funneling through a mixed state with finite probabilities for having both K = $1/2^-$ and K = $5/2^-$. The pumping to this mixed level would occur from the $7/2^+$ ground state to the $5/2^-$ component, while

cascading to the $1/2^-$ fluorescent level would proceed from the $1/2^-$ component. In the first step $|\Delta K| = 1$ while $|\Delta K| = 0$ in the second; neither is hindered by an excessive $|\Delta K|$.

Just such a mixed state of ^{167}Er was proposed[8] in 1971. The $1/2^-[510]$ Nilsson state for the odd neutron was supposed to be mixed with the $5/2^-[512]$ by a collective quadrupole vibration of the core of the nucleus. Such a vibration is a perturbation of the Hamiltonian for which K is conserved in pure stationary states, so the mixing of states with K differing by two is not surprising. However, until the present emphasis was placed upon our nuclear experiments analogous to the optical double resonance methods, such a sensitive test for the degree of mixing had not been performed upon the ^{167}Er system. Other indications of mixing had been obtained from particle reactions, and the entire question is now being restudied with an intent to guide systematic studies designed to determine the frequency of occurrence and energetics of such usefully mixed states.

For a simple figure-of-merit it seems the question to ask is how large can be the transfer of J or K before the integrated cross section for the process is reduced. In subsequent manuscripts it will be shown that currently $\Delta J = 4$ can be optically pumped through the funneling process with no noticeable loss of efficiency. The nuclei at this current frontier, ^{179}Hf, ^{191}Ir, and ^{197}Au, may be benefiting either from bandwidth funneling through a mixed state, the process for which ^{167}Er is the archetype, or from a complexity of the cascade from the pumped state to the fluorescent level. This latter is the second of the processes demonstrated this quarter for pumping large changes in angular momentum. The important consequence is that *complex cascades can be pumped while maintaining viable branching ratios both to the initial and fluorescent levels.*

In real nuclei, the shortest lifetimes and greatest widths are found for spurious states of collective excitation of nucleons.[9] Instead of a single nucleon generating the transition moment coupling to the radiation field, for these states a collective oscillation of a number of core nucleons contributes a much larger transition moment. Moreover, there is the general characteristic that the larger the excitation energy at which this or any other type of funneling state is found, the larger is the width over which pump continua can be absorbed. As a consequence, there is an instinctive desire to incorporate as

highly excited a state as possible into funneling schemes for pumping a gamma-ray laser. The quantitative concern, then, is whether the useful width increases with excitation energy in sufficient strength to offset other negative aspects of a more highly excited transfer level.

In resolving concerns as to the quantitative boundaries on the efficacy of funneling through long cascades from highly excited levels, it is important to be able to relate the fluorescent yield seen in the output transition to the nuclear parameters critical to the schemes of Fig. 1. The general controversy surrounding such computations of yield has been recently resolved[10] both theoretically and experimentally. For a sample which is optically thin at the pump wavelength, the number of nuclei produced in the levels of Figs. 1b and 1c from which the fluorescence will be radiated over the lifetime τ_u is given by

$$S = N \sum_i \frac{(\pi b_a b_o \sigma_o \Gamma/2)_i}{E_i} \frac{\phi(E_i)}{A} \quad , \qquad (7)$$

where N is the number of absorbing nuclei in the sample, and the summation is taken over the properties and pump energy E_i. Only one such pump band is shown in the schemes of Fig. 1, but there could be several at different E_i, each funneling its population into the same output level.

In Eq. (7) the first ratio in the summation is composed of the nuclear parameters, while the second describes the intensities of the pump x-rays which are assumed to be continuous, at least without structure on the fine scale of the nuclear absorption. In particular, the combination $\phi(E_i)/A$ is the spectral fluence at the energy E_i in units of keV/keV/cm^2. Tacitly, it has been assumed[10] that the duration of the pump source is less than the fluorescence lifetime τ_u.

Of the nuclear parameters, Γ is the natural width in keV of the i-th pump band, as shown in Fig. 1,

$$\Gamma = \hbar/\tau_p \quad , \qquad (8)$$

and the branching ratios, b_a and b_o, give the probabilities for the decay of the broad level back into the initial and fluorescence (laser) level, respectively. The pump energy E_i is in keV, and σ_o is the Breit-Wigner cross section for the absorption transition,

$$\sigma_o = \frac{\lambda^2}{2\pi} \quad \frac{2I_e+1}{2I_g+1} \quad \frac{1}{\alpha_p+1} \quad , \tag{9}$$

where λ is the wavelength in cm of the gamma ray at the resonant energy E_f; I_e and I_g are the nuclear spins of the excited and ground states, respectively; and α_p is the total internal conversion coefficient for the two-level system shown in Fig. 1a.

Equation (7) is the basic expression for evaluating the number of fluorescent nuclei produced by either of the two schemes of Fig. 1 that can benefit from bandwidth funneling. The numerator of the first term of Eq. (7) is usually termed the integrated cross section for the photoexcitation of the fluorescent level from the initial state. It is convenient to discuss this quantity in units of 10^{-29} cm^2 keV. On this scale, unity would describe a funneling process of strength sufficient to give the clear level of nuclear fluorescence described in the major milestone report[2] from a few grams of material pumped with a source of laboratory scale. For example, the excitation of isomeric ^{77m}Se is mediated by funneling transitions whose strengths total to the order of unity ($\times 10^{-29}$ cm^2 keV) for excitation energies below 1 MeV.

Variability of the integrated cross section is contributed mostly by the product of branching ratios and level widths, $(b_e b_o \Gamma)$, indicated schematically by the shaded and unshaded portions of the funneling levels in Fig. 1. While it has been clear from the beginning that broader funneling levels could be found at higher excitation energies, the concern persisted that the increase in width might be associated only with a stronger transition to the ground state so that the branching ratio to the fluorescent level, b_o, would decrease as Γ increased. This situation is shown schematically in Fig. 3a by the funneling levels denoted #1 and #2. The resulting insensitivity of the integrated cross section to the excitation energy of funnel state #2 is shown by the dashed curve in Fig. 3b. The converse possibility is typified by funnel #3 in Fig. 3a, where it is assumed that branching ratios are little affected between #1 and #3. In that case, the integrated cross section would increase drastically with increases in excitation energy of the funneling level, as shown by the solid curve of Fig. 3b.

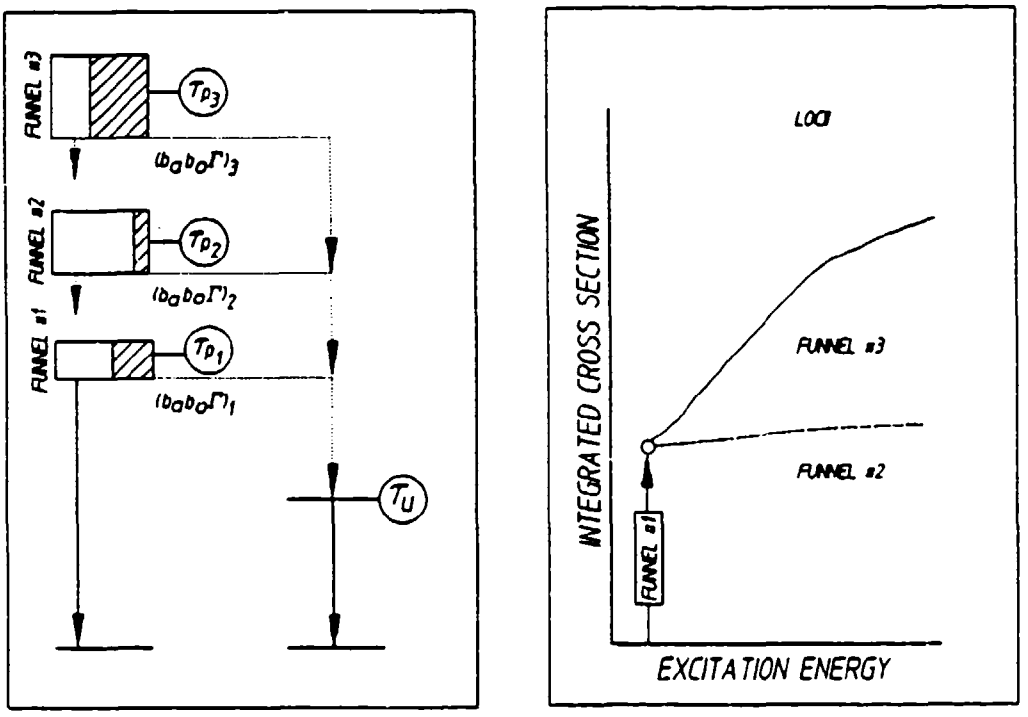

Figure 3: (a) Left: Schematic representation of the energetics of the nuclear analog to the ruby laser for excitation through several possible funneling states subject to different model assumptions. Branchings of the decay back to ground and to the cascade leading to the isomer are indicated by the unshaded and shaded portions, respectively, of the rectangle representing the funneling state.

(b) Right: Graph of the dependence of the locii of the integrated cross section for photoexcitation of the isomer through the funneling states shown in the left panel as functions of the possible excitation energies of the gateway (funneling) state. Solid and dashed curves contrast the functional dependences expected, respectively, when the branching ratio is largely unaffected by the excitation energy and conversely, when the excitation transition contributes most of the width to the funneling state so that the branching ratio to the isomer decreases as the level width increases.

A second major achievement of this reporting period was the experimental measurement of integrated cross sections conforming to the solid curve of Fig. 3b. Preliminary analysis[11] of the mass of data obtained in the June series of experiments with the DNA/PITHON nuclear simulator showed that at 1005 keV a funneling state could be excited in ^{77}Se with an integrated cross section of 30 in the usual units ($\times 10^{-29}$ cm^2 keV). Reported in a following manuscript is a further interpretation of more

of that data[12] which shows that in ^{191}Ir the cross section for excitation of the isomer exceeds 40 between 1.0 and 1.4 MeV. Shown in Fig. 4 is the newest data we obtained in the September series of experiments at the University of Texas Southwestern Medical Center at Dallas, in which nuclear targets were pumped with bremsstrahlung from their 6 MeV linear accelerator. Of particular interest in the context discussed here is the fluorescence line at 337 keV from ^{115m}In that was obtained by pumping 2.2 g of natural indium with a time-integrated fluence of the order of 1.8×10^{14} keV/keV/cm^2. The yield seen in Fig. 4 proves the integrated cross section to be of the order of 10,000 ($\times 10^{-29}$ cm^2 keV) for excitation of the $\Delta J = 4$ transition to the fluorescence level through a funneling state having an excitation energy between 1 and 5 MeV. Clearly there are some cases following the solid curve of Fig. 3b.

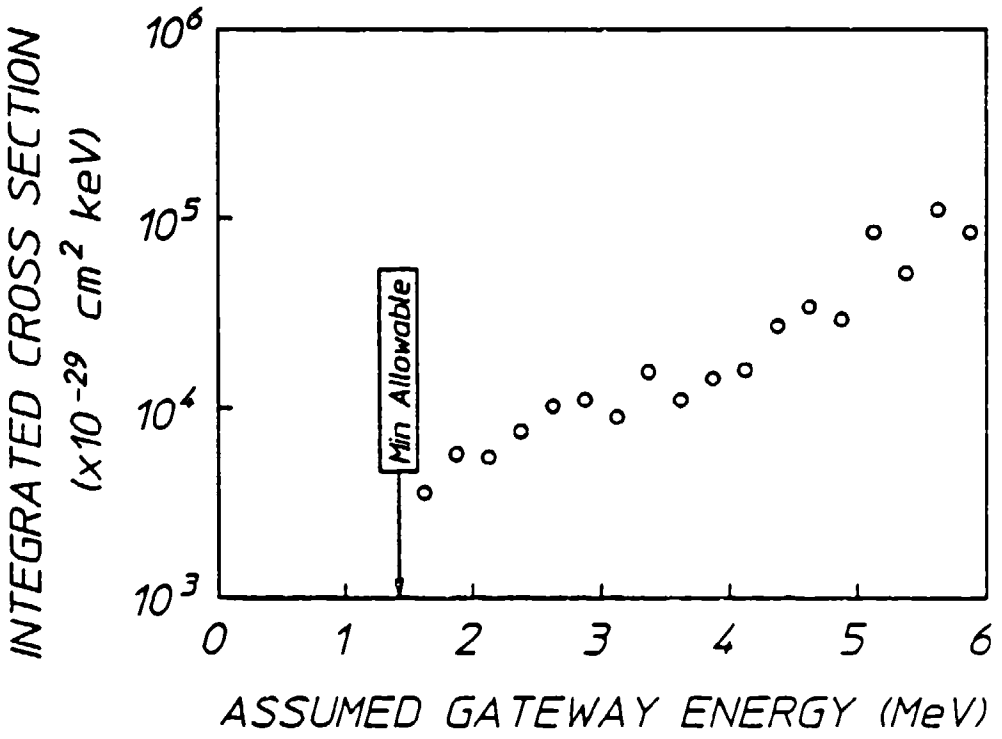

Figure 4: Plot of the envelope of the integrated cross section measured for the reaction $^{115}In(\gamma,\gamma')^{115m}In$ as a function of the value assumed for the first γ transition to the gateway state.

Contained in this quarterly report are details of the September experiments on the linear accelerator. Other manuscripts describe the final recapitulation of the concerns and procedures for the use of the x-ray activation of nuclei (XAN) to calibrate large impulsive sources of bremsstrahlung and the detailed reconciliation of the integrated cross sections for excitation of ^{115m}In and ^{111m}Cd that were needed in the calibration activity.

The achievements of this quarter have a clear significance. Two strong mechanisms have been demonstrated for the elusive "interband transfer" of nuclear populations. As many as four quanta of angular momenta can be transferred by an intense pulse of x-rays used to pump nuclei from the initial to the fluorescent state with integrated cross sections that vary from 10 to 10,000 on the scale in which unity results in a large yield. One technique funnels population through a level of mixed single particle states, and the other utilizes a funneling level at the head of a complex cascade to the fluorescent level. Both considerably strengthen the probabilities that a suitable candidate for a gamma-ray laser exists in reality.

References

1. Both the dressed state (coherent) scheme and the flash x-ray (incoherent) pumping techniques still appear feasible just as we originally proposed in C. B. Collins, F. W. Lee, D. M. Shemwell, B. D. DePaola, S. Olariu, and I. I. Popescu, J. Appl. Phys. 53, 4645 (1982). However, the latter, being simpler, is developing at a more dramatic rate.

2. C. B. Collins, Proof of the Feasibility of Coherent and Incoherent Schemes for Pumping a Gamma-Ray Laser, University of Texas at Dallas, Report #GRL/8602, Innovative Science and Technology Directorate of Strategic Defense Initiative Organization, April 1987, pp. 1-28.

3. Proof of the Feasibility of Coherent and Incoherent Schemes for Pumping a Gamma-Ray Laser, University of Texas at Dallas, Report #GRL/8701, Innovative Science and Technology Directorate of Strategic Defense Initiative Organization, July 1987, pp. 1-10.

4. J. A. Anderson and C. B. Collins, Proof of the Feasibility of Coherent and Incoherent Schemes for Pumping a Gamma-Ray Laser, University of Texas at Dallas, Report #GRL/8602, Innovative Science and Technology Directorate of Strategic Defense Initiative Organization, April 1987, pp. 29-46.

5. C. B. Collins, F. W. Lee, D. M. Shemwell, B. D. DePaola, S. Olariu, and I. I. Popescu, J. Appl. Phys. 53, 4645 (1982).

6. C. B. Collins, Proof of the Feasibility of Coherent and Incoherent Schemes for Pumping a Gamma-Ray Laser, University of Texas at Dallas, Report #GRL/8601, Innovative Science and Technology Directorate of Strategic Defense Initiative Organization, January 1987, pp 1-14.

7. Evaluated Nuclear Structure Data File (Brookhaven National Laboratory, Upton, New York, 1986).

8. M. E. Bunker and C. W. Reich, Rev. Mod. Phys. 43, 348 (1971)

9. A. deSchalit and H. Feshbach, Theoretical Nuclear Physics Vol. I: Nuclear Structure (J. Wiley, New York, 1974) Ch. 6, Section 14.

10. C. B. Collins, Proof of the Feasibility of Coherent and Incoherent Schemes for Pumping a Gamma-Ray Laser, University of Texas at Dallas, Report #GRL/8603, Innovative Science and Technology Directorate of Strategic Defense Initiative Organization, June 1987, pp. 1-30.

11. J. A. Anderson and C. B. Collins, Proof of the Feasibility of Coherent and Incoherent Schemes for Pumping a Gamma-Ray Laser, University of Texas at Dallas, Report #GRL/8701, Innovative Science and Technology Directorate of Strategic Defense Initiative Organization, July 1987, pp. 11-34.

12. C. B. Collins and J. A. Anderson, Proof of the Feasibility of Coherent and Incoherent Schemes for Pumping a Gamma-Ray Laser, University of Texas at Dallas, Report #GRL/8701, Innovative Science and Technology Directorate of Strategic Defense Initiative Organization, July 1987, pp. 35-53.

OPPORTUNITIES FOR NUCLEAR ACTIVATION

by C. B. Collins, J. M. Carroll, and J. A. Anderson

Recent manuscripts[1,2] have reported how effectively the technique of X-Ray Activation of Nuclei (XAN) can be used to calibrate the spectral intensities found in a single pulse of intense bremsstrahlung. Essential to determining the pump intensities used in schemes for exciting a gamma-ray laser,[3] XAN has also been validated as a means of calibrating nuclear simulators.

As currently implemented, three isotopes, ^{77}Se, ^{79}Br, and ^{115}In, are used to sample narrow spectral slices of the fluence illuminating a target. Information is stored as isomeric excitations to be "read out" later. With three isotopes, XAN accommodates measurements at three photon energies, 433, 761, and 1078 keV.

The key to the development of that technique was the use of a large number of shots to activate test samples in order to resolve experimentally the level of self-consistency among values of basic nuclear parameters in the current database.[4] Five of six critical parameters for these three isotopes were found to be consistent[5] and the sixth was repaired. Lest this give a false sense of security in the use of the existing database for the description of other laser-related processes, it must be recognized that these three materials were chosen because it appeared a priori that they were the materials most precisely characterized by the study of particle reactions reported in the literature. The resulting score of 83% for consistency should be considered representative of only the very best group of test nuclei. Fortunately, the level of consistency was this high, or XAN could not have been validated in a practical number of test shots.

The next logical step would be to add more isotopes to the calibration target in order to improve both resolution and coverage, and a number of candidates suggest themselves. During the same series of experiments on the PITHON nuclear simulator during which self-consisten-

cy of the basic three was demonstrated, 29 other isotopes were irradiated in a survey mode. Four, ^{167}Er, ^{179}Hf, ^{191}Ir, and ^{197}Au, were found to be particularly promising and others were certainly interesting. The opportunity for using those four to add four more energies to the list for which XAN is applicable was discussed[6] in the previous quarterly report. Unfortunately, of the ten nuclear parameters of importance, *at least five accepted values were found to be drastically erroneous*. An error rate in excess of 50% for this part of the nuclear database, coupled with the lack of foreknowledge of which of the materials should have borne greatest scrutiny, resulted in insufficient data to extract the self-consistent parameters needed for the application of XAN at four additional energies. Nevertheless, partial analysis of the data for these four species was both interesting and provocative. Those results are reported again[6] here, together with the analyses of additional data taken during this most recent quarter with our own e-beam accelerator, APEX-I.

In the case of ^{167}Er these extensions of the fluorescence experiments have been particularly effective, allowing us to find a new gateway state of major importance. *However, the greatest significance lies in the lesson taught by the unexpected strength of the* $^{167}Er(\gamma,\gamma')^{167m}Er$ *reaction*. Evidently, interband transfers of population occur with much greater probability than allowed by the restrictive K-selection rules, which are often considered of paramount importance. The results of this work support the hypothesis that strong channels for (γ,γ') reactions connecting isomers to ground states may arise through levels for which the angular momentum projection K is not a conserved quantity because of core vibrations.

Methods

In a previous report[1,2] it was shown that the uncertainty in the absolute value of the geometric coefficient coupling the source of pump radiation to the absorbing target could be eliminated by normalizing both the pump fluence and the fluorescence counts to some standard material having a monochromatic excitation spectrum. The reaction $^{79}Br(761,\gamma')^{79m}Br$ was found to be an ideal standard, having an integrated cross section of 6.2×10^{-29} cm^2 keV. Following the formalism reported earlier, the number of isomeric nuclei, S(x), of material x which could

be excited by a flash of intense bremsstrahlung can be conveniently expressed[1] as a ratio,

$$R(\text{model}) = \left.\frac{S(x)/N(x)}{S(Br)/N(Br)}\right|_{\text{Model}} = \sum_E \frac{\xi_E(x)}{\xi_{761}(Br)}\,\zeta(E) \quad , \qquad (1)$$

where S(x) and N(x) are the number of nuclei produced and the number of target nuclei of material x, respectively; $\zeta(E)$ is the ratio of pumping intensity at E keV to the intensity at 761 keV; and the $\xi_E(x)$ are the combinations of nuclear parameters involved in the excitation of the gateway level at energy E,

$$\xi_E(x) = \frac{(\pi b_a b_o \sigma_o \Gamma/2)_E}{E} \quad . \qquad (2)$$

The collection of terms in parenthesis in Eq. (2) comprises the integrated cross section for excitation as usually reported. They are summarized in Table I for the nuclei whose energy levels are found in Figs. 1 and 2.

The source of excitation in the initial experiments was the bremsstrahlung produced by the PITHON nuclear simulator at Physics International. The nominal end point energy of the electrons producing the bremsstrahlung was 1.3 MeV with relatively small shot-to-shot variance. For those particular experiments the nominal firing parameters were deliberately perturbed so that successive irradiations could be obtained with end point energies varying from 0.9 to 1.5 MeV.

Intensities at the target were determined by measuring the nuclear activation of the ^{79}Br component of a sample of LiBr containing isotopes in natural abundance. This calibrating target was run in a pneumatic transfer system which enabled the population of ^{79m}Br produced by a single irradiation to be subsequently counted at a quiet location 10 m removed from the source. Activation lost during the 1.0 s transit time could be readily corrected during analysis.

The sample material x was placed in a second pneumatic shuttle and transferred after irradiation to a NaI(Tl) well counter. The analyzer system was capable of simultaneously producing a record of counting rate as a function of time, together with the spectrum as a function of energy. In that way both the decay spectrum and the lifetime of the activation could be obtained in a single experiment.

Table I

Summary of literature values for nuclear parameters important to the excitation of isomeric fluorescence. These were not confirmed by the results of this experiment.

Nuclide	Ref.	E_{out} (keV)	E_{in} (keV)	$\pi b_a b_o \sigma_o \Gamma/2$ ($\times 10^{-29}$ cm^2 keV)
^{167}Er	Ref. 7	207	532	0.074
			667	0.036
			745	0.49
^{179}Hf	a	214*	650	0.057
			880	0.082
			1030	0.25
			1160	0.22
			1400	2.0
^{191}Ir	Ref. 4	129**	659	0.037
^{197}Au	Ref. 4	279***	No known levels	

*cascading from the isomer at 375 keV
**cascading from the isomer at 171 keV
***cascading from the isomer at 409 keV

a. E. A. Henry, Nuc. Data Sheets 17, 287 (1976). In contrast to the other data shown here, these are experimentally determined values. Note that they do not correspond to individual levels in Fig. 2.

Figure 1: (opposite) Energy level diagram of the spheroidal nucleus ^{167}Er showing a band structure reminiscent of the energy levels of diatomic molecules. Each column shows the ladder of rotational levels built upon the single particle state whose Nilsson quantum numbers given by Ref. 4 are shown in the box at the top of that column. Transitions to the isomeric state that are listed in Ref. 4 are shown by the arrows. Branching ratios are shown in boxes for two principal transitions for the (γ,γ') channels expected to be important in this work. Dotted levels plot energies of higher members of known bands from rotational constants determined from the lower levels of each.

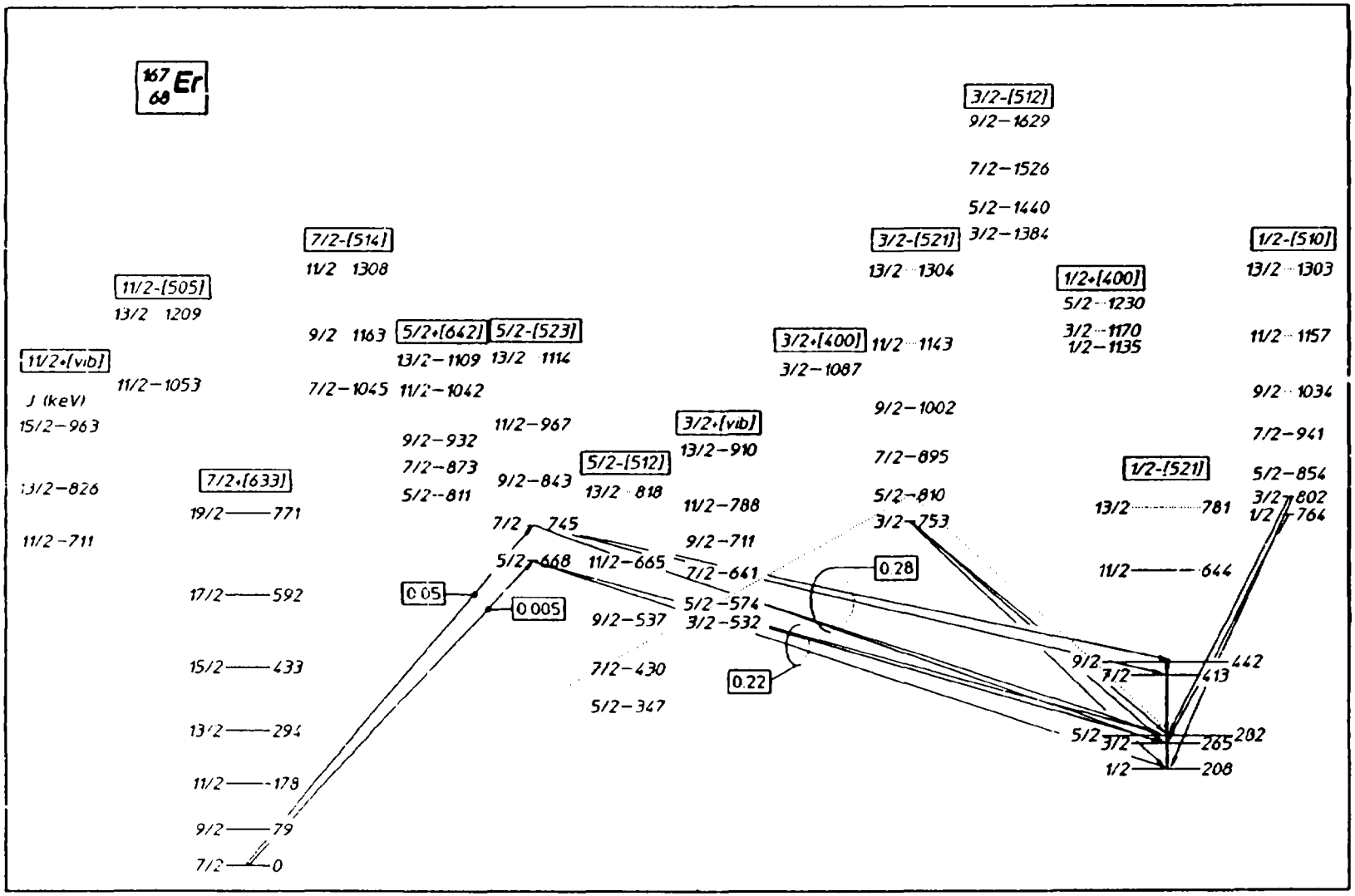
167 68 Er
11/2+[vib]
J (keV)
15/2−963
13/2−826
11/2−711
11/2-[505]
13/2 1209
11/2−1053
7/2+[633]
19/2 771
17/2 592
15/2 433
13/2 294
11/2 178
9/2 79
7/2 0
7/2-[514]
11/2 1308
9/2 1163
7/2−1045
5/2+[642]
13/2−1109
11/2−1042
9/2−932
7/2−873
5/2−811
5/2-[523]
13/2 1114
11/2−967
9/2−843
7/2 745
5/2 668
0.05
0.005
5/2-[512]
13/2 818
11/2−788
9/2−711
7/2−641
11/2−665
5/2−574
3/2−532
9/2−537
7/2−430
5/2−347
3/2+[vib]
13/2−910
0.22
3/2-[512]
9/2−1629
7/2−1526
5/2−1440
3/2−1384
3/2-[521]
13/2 1304
3/2+[400]
3/2−1087
11/2 1143
9/2−1002
7/2−895
5/2−810
3/2−753
0.28
1/2+[400]
5/2 1230
3/2 1170
1/2 1135
1/2-[521]
13/2 781
11/2 644
9/2 442
7/2 413
5/2 282
3/2 265
1/2 208
1/2-[510]
13/2 1303
11/2 1157
9/2 1034
7/2−941
5/2−854
3/2 802
1/2 764

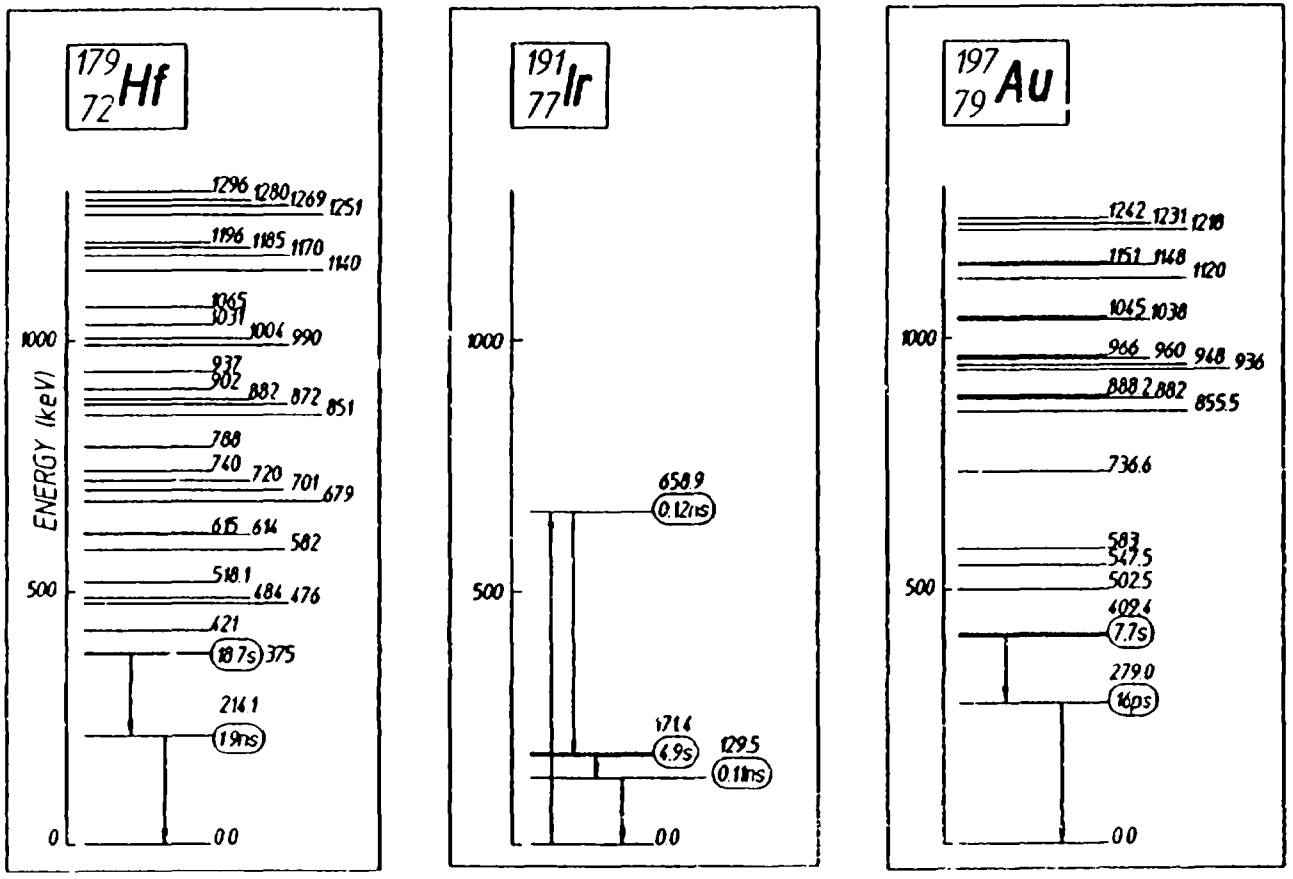

Figure 2: Energy level diagrams of the excited states of these nuclei that might be pumped from their ground states to cascade to their respective isomers. Arrows show paths of known (γ,γ') reactions.

In a subsequent series of experiments performed in September, the source of excitation was the bremsstrahlung from our "in-house" accelerator APEX-I, described in a previous report.[7] A schematic diagram of that apparatus is shown in Fig. 3. Samples were exposed to the bremsstrahlung radiation and then automatically transferred to a counting chamber as shown. The arrival of the sample at the NaI(Tl) detector triggered dual analyzers and caused simultaneous time- and energy-resolved spectra to be obtained for each shot.

The APEX-I electron beam facility in our Center for Quantum Electronics has a nominal 1 MeV, 100 kA output pulse lasting 26 ns. This machine can be fired every two minutes. An anode of 0.25 mm tungsten foil was used as a transmission-type bremsstrahlung converter. As noted above, the calibration of the x-ray output from such converters is a difficult matter. Shot-to-shot variability of the machine performance was recorded with two 7912AD transient digitizers separately monitoring the output voltage and the output x-ray fluence delivered to a fast, large-volume silicon PIN diode.

Samples were transferred from the irradiation cell to the counting chamber with the same pneumatic shuttle (rabbit system) we fielded for the PITHON experiments. A synchronization signal from the APEX-I machine triggered the transfer system and started a transit-time clock, which was then stopped by an arrival sensor at the detector. Typical transit times were 700 ms or less because of our shorter distances. The rabbits and the transfer tube were made of polyethylene and acrylic plastic, which presented negligible x-ray attenuations at the energies involved here. Total sample volume in each rabbit was about 7.5 cm^3. The cylindrical axis of the rabbit was approximately 2.8 cm behind the converter target during irradiation.

The counting system for the work done in September comprised a NaI(Tl) detector, its associated preamp/amplifier, and a dual analyzer that obtained both pulse height spectra and multichannel scaler data for each shot. Counting was initiated by the arrival of the sample at 7.6 × 7.6 cm, well-type NaI(Tl) detector. The analyzers were ORTEC 918 multichannel buffers running on an IEEE-488 bus. Although ORTEC provides the IEEE interface as a listed option, no software is currently commercially available to control them in this mode; and a special, in-house software package was developed for this application. An

IEEE-488 configuration was chosen because of the severe RFI/EMI environments we encounter in many of our experiments. The detector and analyzers were mounted in shielded enclosures and communicated via a serial link with the PC/AT that served as the system controller.

The photographs of Figs. 4 and 5 show the APEX-I electron beam facility, pneumatic transfer system, counting chamber, and data acquisition electronics.

Standard procedures were employed for determining the detection efficiency and the self-absorption correction. Correction was also made for the loss of activity during the individual transit time of the sample after each irradiation.

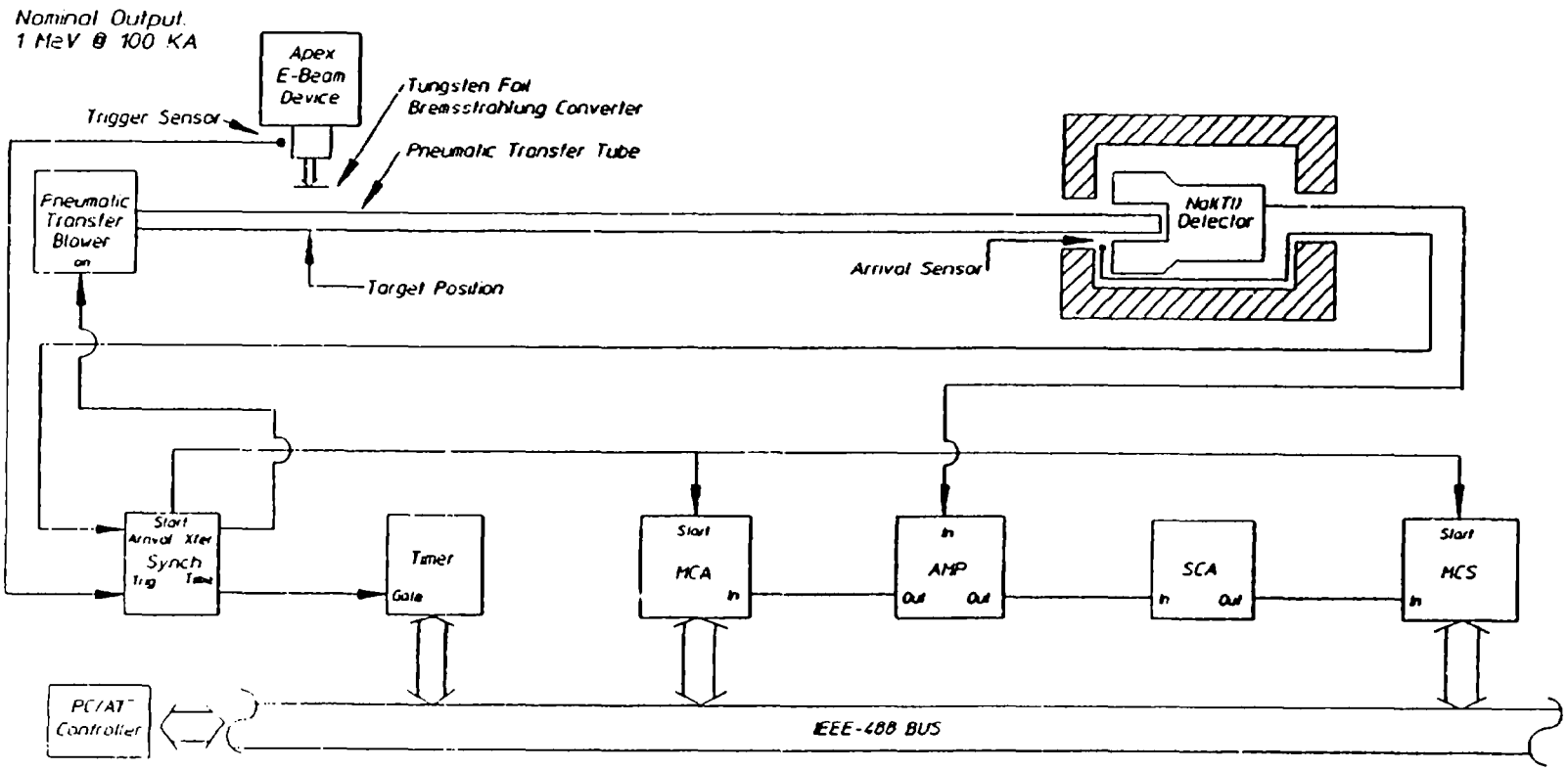

Figure 3: Schematic diagram of the UTD nuclear fluorescence experiment. Samples were irradiated and then automatically transferred to a dual analyzer to obtain time and energy spectra.

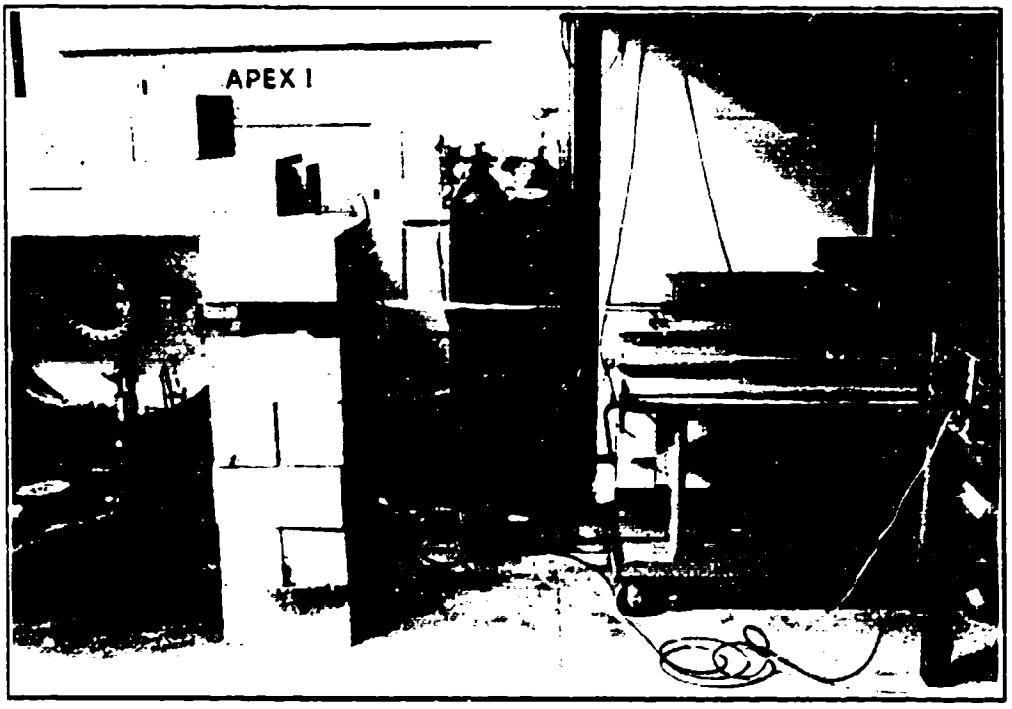

Figure 4(a): APEX-I electron beam facility, bremsstrahlung cell, and counting chamber used in the nuclear fluorescence experiment shown schematically in Fig 3. The RFI enclosure that normally contains the counting shield is shown in Fig. 5. (b): Keyed illustration. 1. APEX-I electron beam facility. 2. Irradiation cell 3. Sample position during irradiation. 4. Air supply for pneumatic system. 5. Transfer tube. 6. Counting chamber. 7. Detector electronics (in actual use, electronics and detector are enclosed in a Faraday cage).

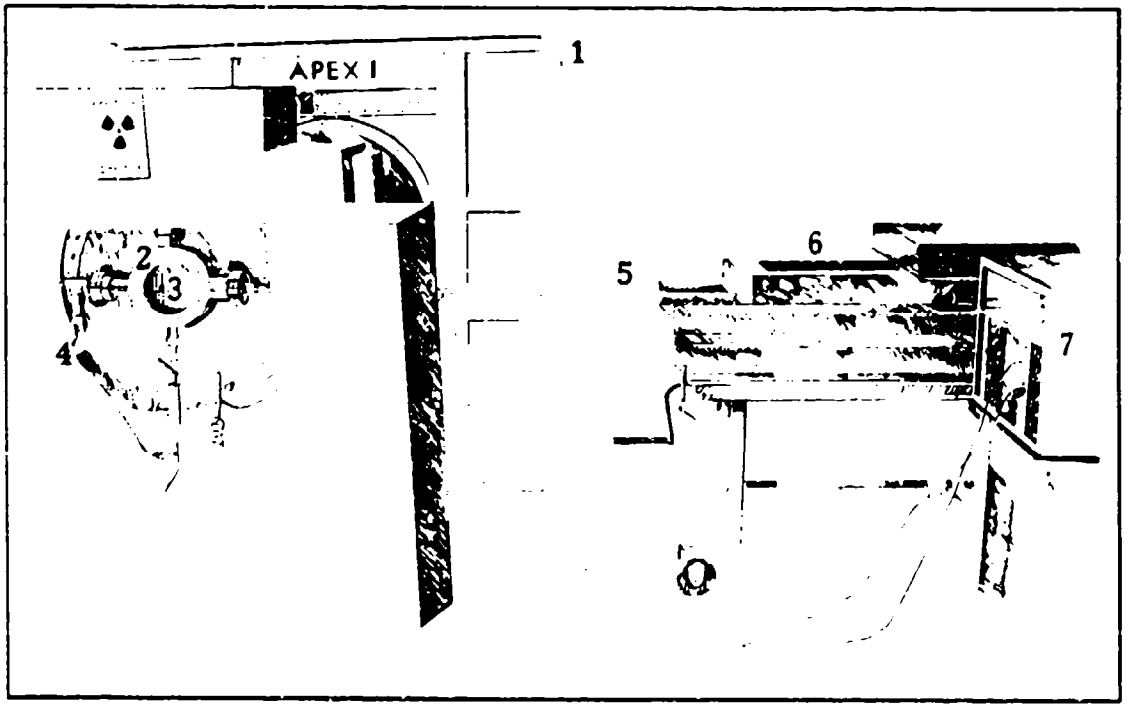

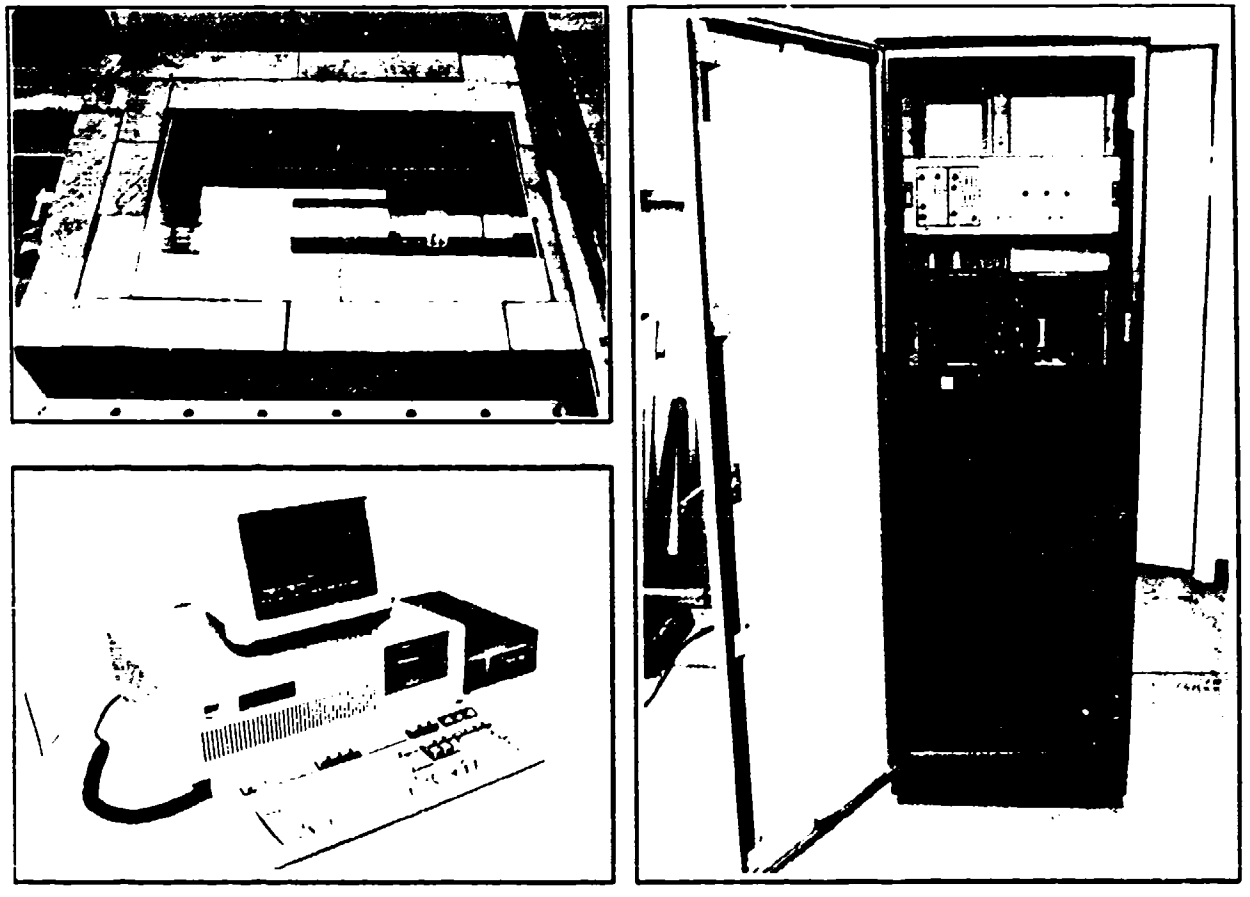

Figure 5: Counting chamber detail (top left) showing the Na'(Tl) detector and transfer tube. The sensor that detects the arrival of the sample rabbit is not shown. RFI instrument enclosure (right) contains the analog electronics, the multichannel analyzers, and the fiber optics IEEE-488 bus extender. Operator's console for the data acquisition system is shown bottom left. The fiber optics link allows the IEEE-488 controller to be well removed from the RFI pulse associated with the bremsstrahlung source.

Results

In the PITHON experiments, a physical displacement existed between the shuttle system for the test material and the mixed $^{79}Br/^{77}Se$ target used for providing calibration. The relative radiation delivered to the two samples was corrected for this separation by mounting thermoluminescent diodes (TLD's) at both positions and then comparing the total dose recorded at the different points for each shot. The number of photons from the test materials was scaled by the value of relative dose received at the test shuttle and at the calibrating positions. These corrections varied on a shot-to-shot basis because of the instability of the position of the "hot spot" in the pinched diode used on the PITHON machine.

For the APEX-I experiments described here, the high-intensity region was not large enough to accomodate both a calibration sample and the test sample. However, shot-to-shot variations in output beam morphology were not believed to be significant in APEX-I because it is not a pinched diode device. This assumption is being tested in current experiments using TLD arrays that, unfortunately, were unavailable for the September work. While it was reasonable to postulate that the radiation pattern was stable, its intensity and spectral content were not. With no intentional change of firing parameters, the diode voltage was found to vary by up to 200 keV. Subsequent work on the machine has greatly improved its reproducibility, but for the erbium experiments discussed here it was necessary to sort shot results by their measured output potential. This was crucial since the spectra of approximately 10 shots were stacked to obtain acceptable signal levels at each value of V_{max}. In practice, the shots were sorted into bins that were 100 keV wide.

Figure 6a shows the result of photoactivation of ^{79m}Br with the APEX-I device for various end point energies. The data plotted correspond to the number of photoactivation counts recorded per shot of the x-ray device. As can be seen, the count rate increases smoothly as the end point energy is moved above the 761 keV gateway state in ^{79}Br. This plot evidences the effects of both the opening of the gateway and the increase of the x-ray output at 761 as the end point is raised. In Fig. 6b, the same data has been normalized to the output of the machine as

mea ured in arbitrary units by the x-ray PIN diode. The sharp rise seen near 750 keV again demonstrates the presence of the gateway state. In this representation, as the end point energy increases, the response flattens since the proportional change in the intensity of 761 keV decreases as the separation between this energy and the end point energy widens. Figure 6c illustrates the corresponding situation for ^{77m}Se. Here the data quality is poorer due to a lower isotopic abundance and less favorable branching ratios for the detection transition, but a sharp transition is demonstrated in the vicinity of 1 MeV. Previous work[2] with PITHON led us to assign this contribution in ^{77}Se to a gateway state at 1005 keV. From these graphs, we can conclude that the voltage calibration for APEX-I is reasonable and that we can locate gateway states within 100 keV or better by use of this type of presentation.

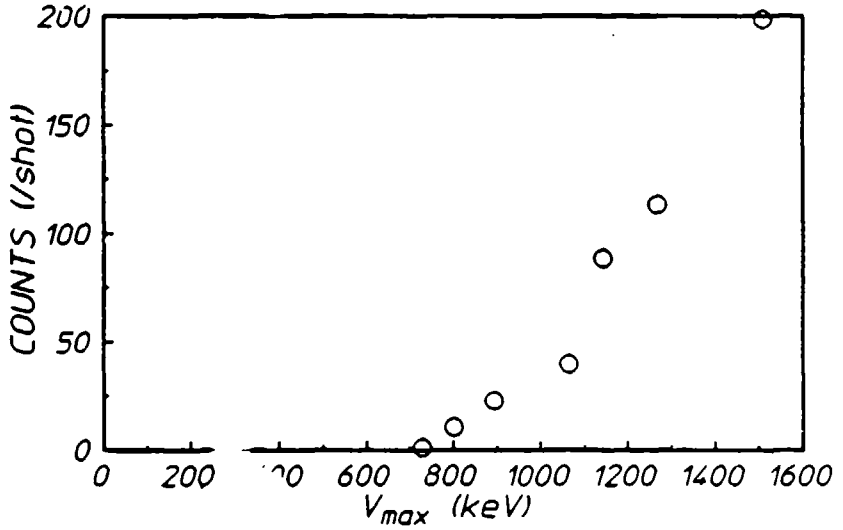
200
150
100
50
0
COUNTS (/shot)
0
200
600
800
1000
1200
1400
1600
V_{max} (keV)

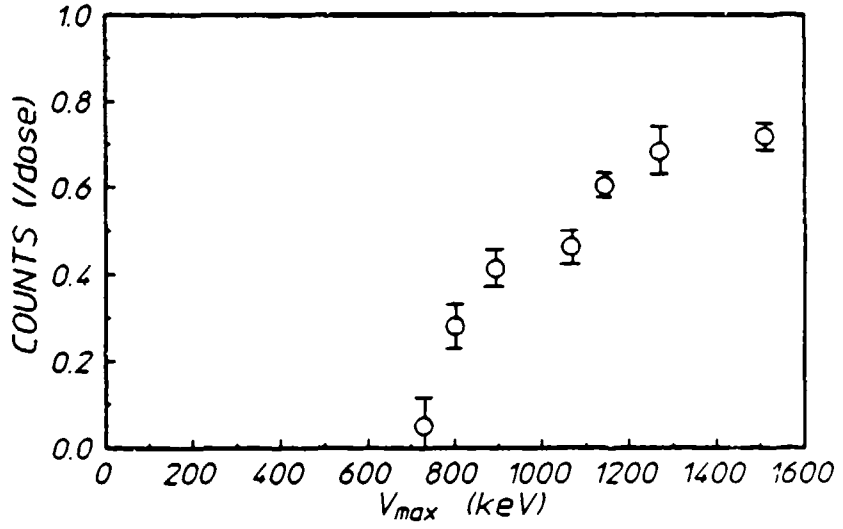
1.0
0.8
0.6
0.4
0.2
0.0
COUNTS (/dose)
0
200
400
600
800
1000
1200
1400
1600
V_{max} (keV)

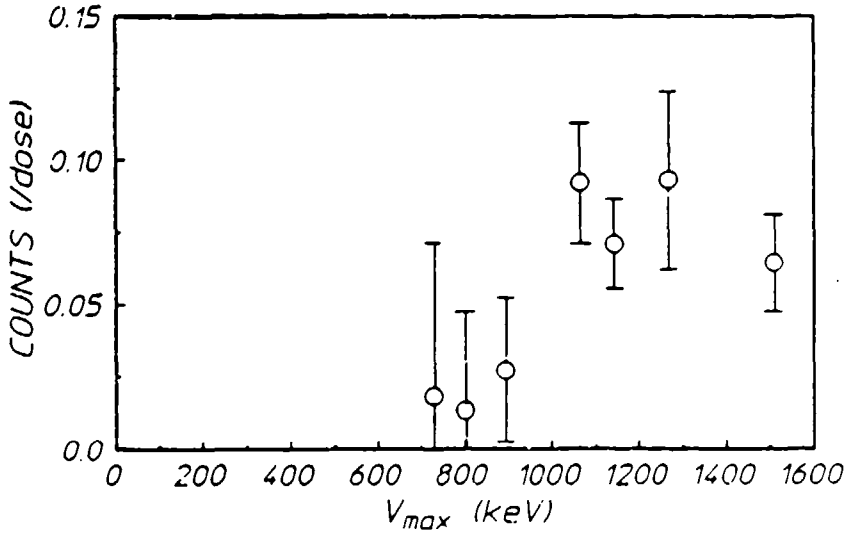
0.15
0.10
0.05
0.0
COUNTS (/dose)
0
200
400
600
800
1000
1200
1400
1600
V_{max} (keV)

Figure 6(a): (Opposite) Plot of the average number of photoactivation counts per shot of the APEX-I device for ^{79m}Br. Data represent average values obtained from approximately 10 shots at each value of V_{max}. The onset of excitation through the 761 keV gateway state is clearly demonstrated.

(b): Plot of the average number of photoactivation counts per unit dose (arbitrary units) for ^{79m}Br. The data of Fig. 6(a) were normalized with respect to the x-ray PIN diode output monitor to eliminate the effects of the overall increase in x-ray output with voltage.

(c): Plot of the average number of photoactivation counts per unit dose (arbitrary units) for ^{77m}Se. In all three figures, raw counts (no corrections for decay or detection efficiency) are plotted.

ERBIUM

The sample of erbium run in the test shuttle in the PITHON experiments consisted of 2.76 g of Er_2O_3 containing natural isotopic abundances. The fluorescence spectrum is shown in Fig. 7, together with the result expected on the basis of Eq. (1). As can be seen, the experimental results exceed expectations by a factor of 17.

From Fig. 7 it can be immediately concluded that either one or more of the parameters for ^{167}Er listed in Table I are grossly incorrect or there is an excitation channel above 745 keV which is substantially more effective than those listed. Figure 1 shows a high density of states which might seem to offer numerous possibilities. However, ^{167}Er is the most elongated of the stable nuclei and hence the one most nearly conforming to the Nilsson model of structure.[8] The energy level diagram of Fig. 1 is dominated by rotational bands built upon an initial value of K, the quantum number for the projection of nucleonic angular momentum upon the axis of elongation. The situation is very analogous to that for diatomic molecules.

Transitions must not only satisfy selection rules upon changes in J, the total angular momentum, but also upon K, both ΔJ and ΔK being limited by the multipolarity of the transition. The limitations upon ΔK are understood to comprise the restrictive "K-selection rules" which would seem to impede some of the otherwise attractive systems for a gamma-ray laser. Laser candidates suffering a large ΔK are currently excluded from serious consideration, automatically. Now, here is a K-hindered analog where the fluorescence yield is 17 times expectations.

The change in K from ground to isomer in ^{167}Er is a negative three. It is not immediately clear from Fig. 1 that there could be a reasonable path containing three steps for which $\Delta K = -1$ and $\Delta J = \pm 1$ or 0. Failing that, it is not clear how there could be a two-step (γ,γ') reaction through which $\Delta K = -2$ for one component that would be any more probable than the known[4] E2 and M2 channels shown in Fig. 1. Those give the result which is too small by a factor of seventeen. Of course, there could be a more favorable E2 route if transitions to one of the states were enhanced by a collective quadrupole vibration, but the one band for which this is predicted is not reported[4] to be radiatively connected to both ground and isomeric states.

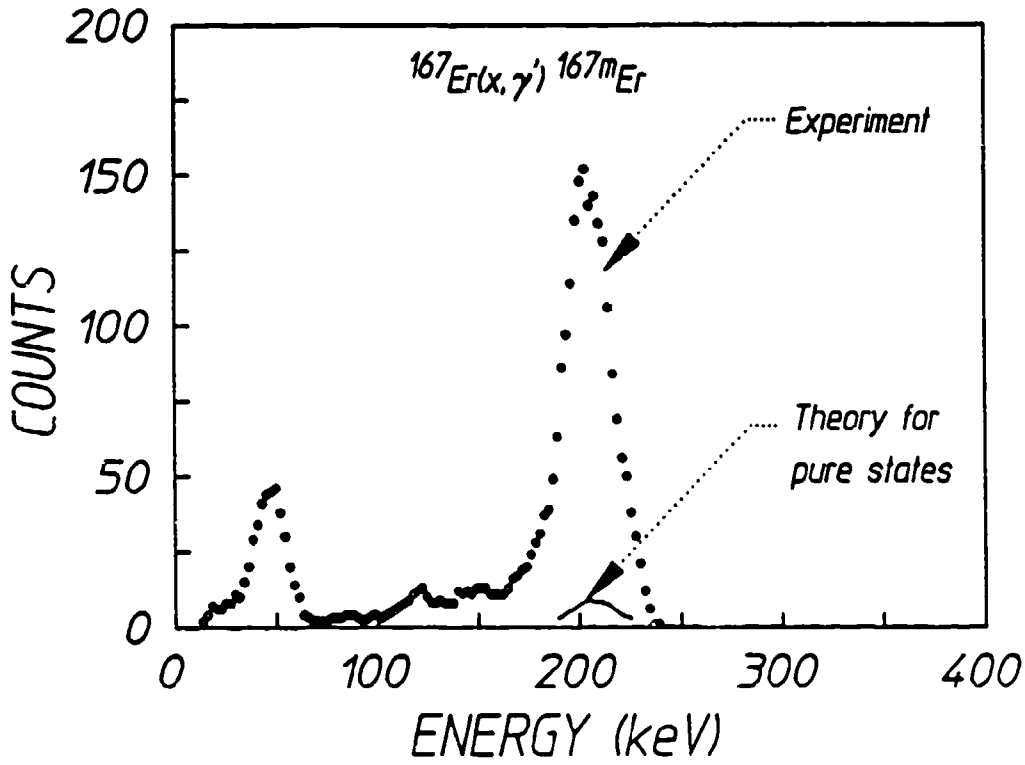

Figure 7: Arrows identify the nuclear component of the spectrum of fluorescence of Er_2O_3 in comparison with model predictions based upon nuclear parameters input from the extant database. Data were obtained from a single irradiation of 2.8 g of Er_2O_3 in natural isotopic abundance.

Earlier studies[9] of the structure of ^{167}Er were more generous in the identification of mixed states. For example, the $1/2^-[510]$ Nilsson state giving rise to the band in the rightmost column of Fig. 1 was originally considered to be a mixture of that state with $5/2^-[512]$ coupled to a 2+ quadrupole vibration of the core.[10] If that were the case, transitions from the ground $7/2^+[633]$ to the mixed states lying between 854 and 1034 keV might not actually be hindered because the transition would not be purely $\Delta K = 2$. The changes in ΔJ are quite low in that energy range, and the selection rule $\Delta J = \pm 1$ or 0 is easily satisified. Moreover, some cascades from the mixed state to the rotational system built on the isomer have been assigned,[4] and those are shown in Fig. 1. Such a sequence of steps in the reaction $^{167}Er(\gamma,\gamma')^{167m}Er$ would provide an intrinsic mechanism for the interband transfer of population. *Whatever the reason, the experimental fact is*

that an excitation sequence exists which has the effect of short-circuiting the K-selection rules as usually applied in excluding low priority candidates for a gamma-ray laser.

In principle, the particularly effective (γ,γ') sequence in ^{167}Er can be identified through the same iterative procedures used to discover and characterize the dominant $^{77}Se(1005\ keV,\ \gamma')^{77m}Se$ channel in the presence of the three other known reactions producing the same product.[1,2] In implementation it requires a sequence of measurements of fluorescence yield be made with successively differing values of end point energies of the bremsstrahlung. Because of the survey nature of the PITHON series of experiments reported here, only a single, fully instrumented measurement was obtained for which the reduced excitation ratio of Eq. (1) was found to be,

$$R(Er) = 1.90 \quad , \tag{3a}$$

for irradiation at an end point energy of

$$V_{max}(Er) = 1470\ keV \quad . \tag{3b}$$

If it is assumed that ^{167m}Er is activated through a single gateway, the right-hand side of Eq. (1) consists of a single term,

$$R(Er) = \frac{\xi_E(Er)}{\xi_{761}(Br)}\ \zeta(E) \quad , \tag{4}$$

where E is the unknown energy of the gateway. Of course, both R and ζ depend upon the end point energy, which in this case is given by Eq. (3b). The intensity ratio is a known function[2] of E for the PITHON accelerator, so Eq. (4) can be solved for $\xi_E(Er)$. From Eq. (2) it can be seen that the integrated cross section $(\pi b_s b_o \sigma_o \Gamma/2)$ can be readily obtained from $\xi_E(Er)$. The result is shown in Fig. 8. If the energy of the gateway were known, the integrated cross section for the reaction $^{167}Er(\gamma,\gamma')^{167m}Er$ could be simply read from the figure.

In an attempt to determine the gateway energy, experiments were continued during this past quarter with APEX-I. To compensate partially for the lower pump fluence, a larger target of isotopically enriched ^{167}Er was used. In these experiments, the pneumatic transfer shuttle contained 9.08 g of erbium enriched to 91.5% abundance in the form of an oxide. Corrections for self-absorption of the fluorescence were calculated for completeness, but only relative measurements were needed.

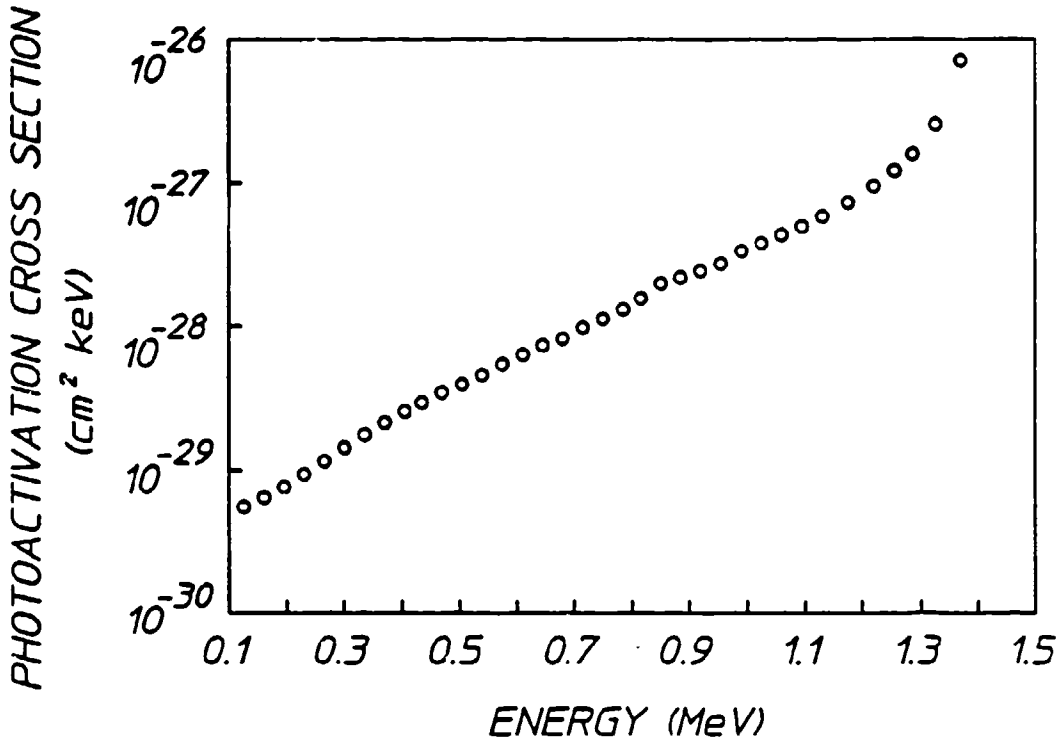

Figure 8: The integrated cross section for the photoactivation of ^{167m}Er through a single dominant gateway state as a function of the energy at which it could be assumed to lie.

As in the calibrations with ^{77}Se and ^{79}Br discussed above, data had to be sorted into bins identified by the end point voltage actually measured for that individual irradiation. To obtain reasonable signal-to-noise ratios, the bins had to be enlarged to a width of 100 keV. The resulting data are plotted in Fig. 9. Each datum represented the number of active nuclei obtained from averaging nominal samples of 10 irradiations per bin.

The data of Fig. 9 show a clear trend toward an intercept between 800 and 1000 keV. The linear approximation corresponds to a least squares fit and gives an intercept of 902 keV, but it is more reasonable to conclude

$$E = 900 \pm 100 \text{ keV} \quad . \qquad (5)$$

If there is no larger gateway at a higher energy, $900 \leq E \leq 1470$ keV, then Eq. (5) gives the energy at which it can be determined from Fig. 8 that,

$$\pi b_a b_0 \sigma_0 \Gamma/2 = 23 \times 10^{-29} \text{cm}^2 \text{ keV} \quad . \qquad (6)$$

The remaining question is whether the gateway seen in Fig. 9 is the same one characterized in Fig. 8. However, if it is not, then there must be one at higher energies having a cross section even greater than the value of Eq. (6), as can be seen from Fig. 8. In any case, one exists which is much more effective than the largest shown in Table I, recording initial expectations.

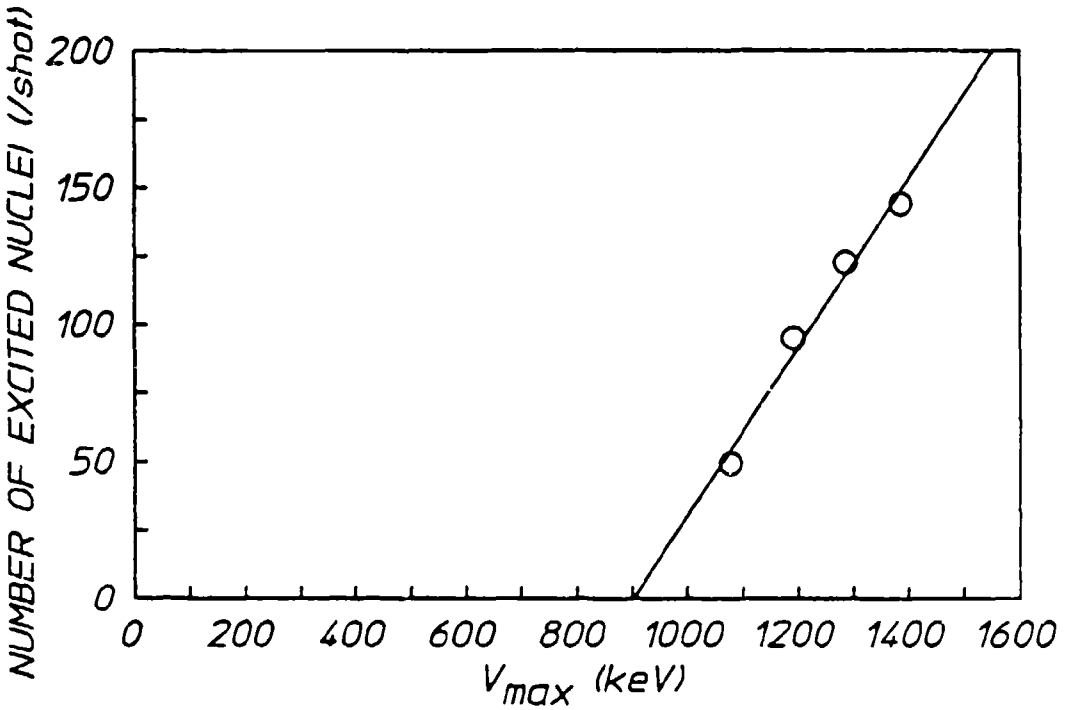

Figure 9. Plot of the average numbers of activations of ^{167m}Er produced by single discharges of APEX-I corrected for the finite duration of the counting period and plotted as functions of the end point energies of the electrons producing the bremsstrahlung. Data were averaged over several shots at similar end point energies to improve statistics.

It is extremely interesting that at 900 keV, the gateway is 48 times the expected value at 745 keV and occurs just where states of mixed K would be expected as discussed above. Here seems a reasonable indication that collective quadrupole vibrations can provide a natural process for "interband transfer." A subsequent manuscript presents evidence that collective octupoles can facilitate similar transfers at higher energies with another three orders of magnitude increase in cross section.

HAFIUM

As can be seen from Table I, ^{179}Hf is an isotope for which the spectrum for activation is even more complex than ^{167}Er or ^{77}Se. Having five distinct (γ,γ') reactions for the production of isomers, it places even greater demands upon the self-consistency of the five critical nuclear parameters in Table I. Moreover, it is particularly curious that the published transition energies for the excitation step in Table I correspond to no individual transitions in the scheme of currently accepted levels[4] shown in Fig. 2. They evidently represent the sums of excitations through gateway levels whose average positions in Fig. 2 would lie at the energies listed in Table I. It is also of considerable interest that no absorption transitions in the energy range 375 - 1500 keV from the ground state are listed in accepted databases.[4] From this perspective it is almost surprising that experimental results approached the model predictions of Eq. (1) to within the factor of 2.0 - 2.7 actually observed.

The fluorescence spectrum obtained from a single irradiation of 4.71 g foil of hafnium in natural isotopic abundance is shown in Fig. 10. Also shown is the comparative value obtained from Eq. (1) using the parameters of Table I placed into the same units of detected counts by multiplying Eq. (1) by the number of ^{79}Br excitations times the relative efficiencies for fluorescence, escape, and detection. While indicating that one or more of the parameters for ^{179}Hf in Table I are underestimating the actual value of integrated cross section, the suggested discrepancy of 2.0 - 2.7 is more of the magnitude which might be reasonably expected to result from a direct remeasurement of such derived parameters.

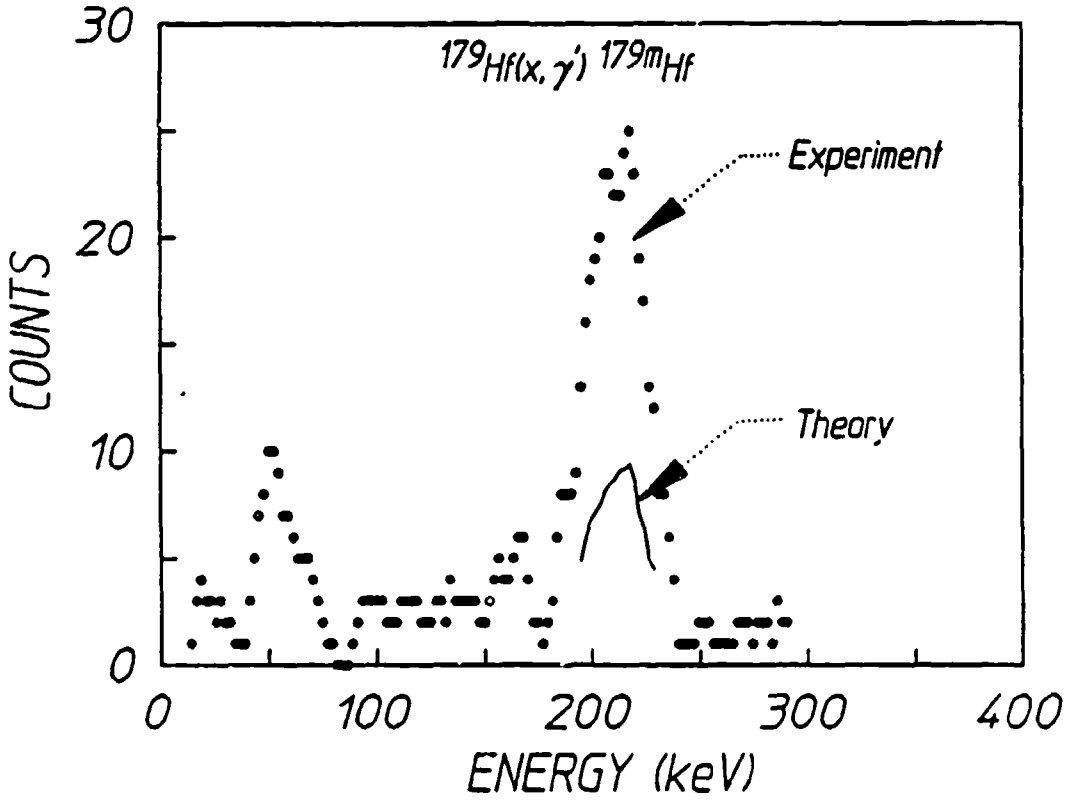

Figure 10: Arrows identify the nuclear component of the spectrum of fluorescence of Hf in comparison with model predictions based upon nuclear parameters input from the extant database. Points were obtained from a single irradiation of 4.71 g of metal in natural isotopic abundance.

As in the case[2] of ^{77}Se, attempts to identify the extra contribution should begin with a computation of the residue Δ between the measured ratios of the numbers of ^{179m}Hf to ^{79m}Br,

$$\Delta = R(exp) - R(model) \quad , \tag{7}$$

where the R is as defined in Eq. (1). This was not done in this case because R(exp) >> R(model) so that the observed ratio could be reasonably expected to show the same correlations with experimental variables as would the residue Δ.

If it were assumed that the observed value,

$$R(^{179}Hf) = 0.094 \quad , \tag{8a}$$

for

$$V_{max} = 1360 \quad , \tag{8b}$$

were dominated by a single unknown gateway, then the integrated cross section could be determined as a function of the energy assumed for the gateway, just as was done with the ^{167}Er. The graph of the possible values of cross section that result is shown in Fig. 11.

Attempts to use APEX-I to determine the gateway energy in a manner analogous to what succeeded with ^{167}Er failed to produce measureable activation of the sample. In this case the combination of a low natural abundance of 13.6% and a relative excitation ratio of more than an order of magnitude less than found with ^{167}Er prevented any useful limits from being extracted from the null result. The gateway could be at any energy in Fig. 11 and be consistent with the null result.

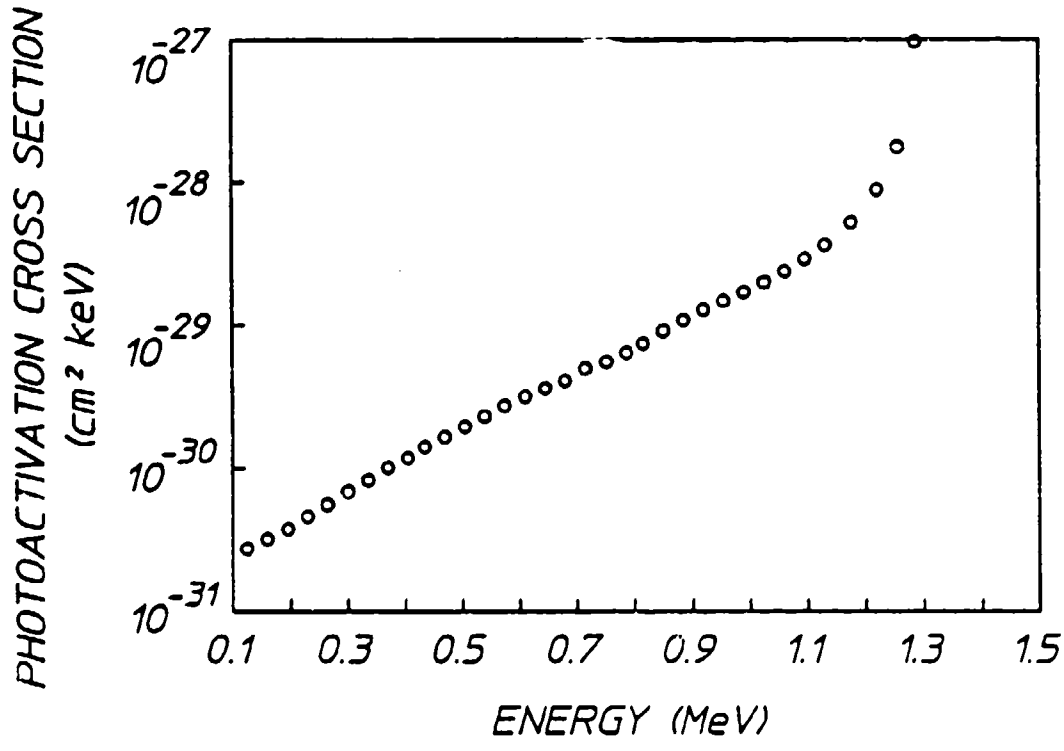

Figure 11: The integrated cross section for the photoactivation of ^{179m}Hf through a single dominant gateway state as a function of the energy at which it could be assumed to lie.

IRIDIUM

The most drastic inconsistency in this group was found for ^{191}Ir, which should have the simplest scheme for excitation. The spectrum of (γ,γ') reactions leading to the production of the ^{191m}Ir isomer is reported to be monoenergetic,[4] as shown in Fig. 2. If so, this would place a very high importance on ^{191}Ir as a material contributing another clearly selective line for sampling energies in the XAN procedure.

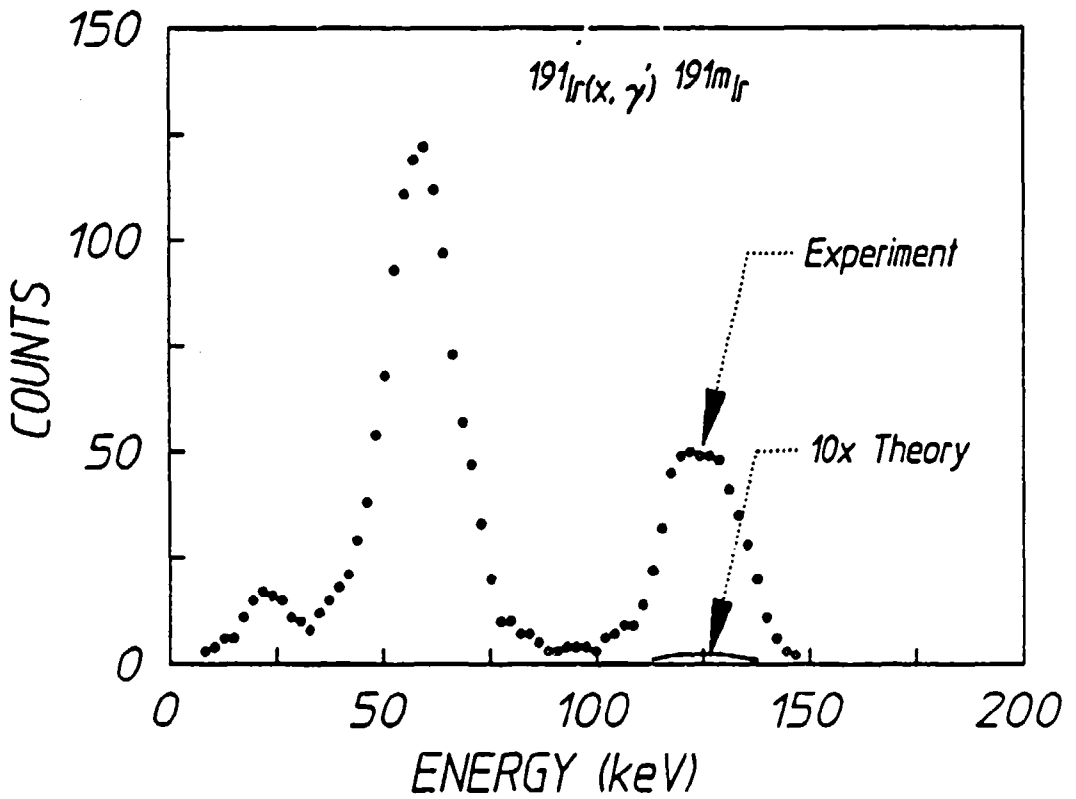

Figure 12: Arrows identify the nuclear component of the spectrum of fluorescence of Ir in comparison with model predictions based upon nuclear parameters input from the extant database. Points were obtained from a single irradiation of 1.82 g of metal in natural isotopic abundance.

The iridium sample used in these experiments had the form of 1.82 g of metallic powder in natural isotopic abundance sealed into a flat planchet. The fluorescence spectrum is shown in Fig. 12, and its time decay positively identified the source as ^{191m}Ir. Self-absorption of the fluorescence at 129 keV represented a significant effect in this

geometry and data were corrected appropriately. In the units of the left hand side of Eq. (1), the measured value in the peak was

$$R(exp) = 1.86 \quad , \tag{9a}$$

for

$$V_{max} = 1300 \text{ keV} \quad , \tag{9b}$$

in comparison to the values near 0.1 encountered in the previous example. This immediately identifies ^{191}Ir as possessing a path for (γ,γ') reactions of major importance.

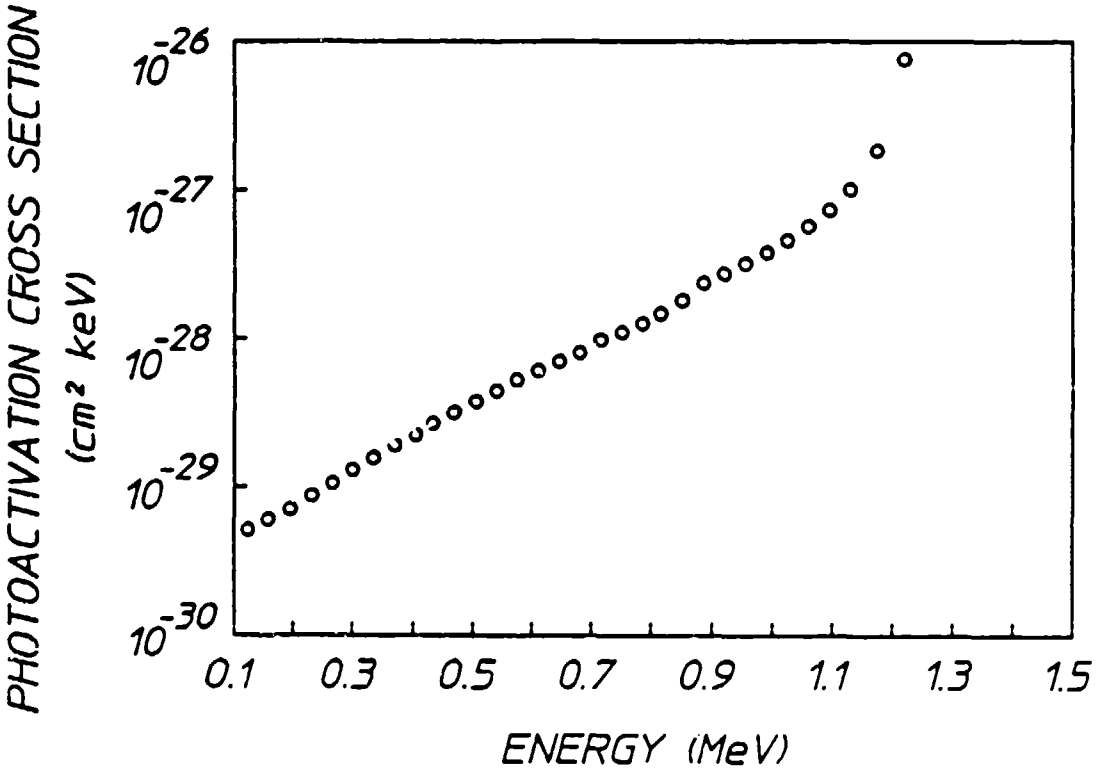

Figure 13: The integrated cross section for the photoactivation of ^{191m}Ir through a single dominant gateway state as a function of the energy at which it could be assumed to lie.

As before, if it is assumed that the reaction proceeds predominantly through a single gateway, the possible values of integrated cross section can be obtained as shown in Fig. 13. For iridium, as well as hafnium, irradiation with APEX-I failed to produce measurable activation. However, in this case the negative is indicative. The excitation ratio of Eq. (9a) from PITHON is comparable to that of Eq. (3a) for

^{167}Er, and the fractional abundance for ^{191}Ir is 37.3%. The inescapable conclusion is that had the gateway been at the same energy as for ^{167}Er, we would have seen fluorescence from the iridium. In this case the null result implies the gateway lies above the 900 keV value for ^{167}Er. Thus, only the part of the curve in Fig. 13 above 900 keV need be considered.

If we arbitrarily suppose that the reaction proceeds through $^{191}Ir(1000\ keV, \gamma')^{191m}Ir$, then the solution of Eq. (4) in that case for Eq. (9a) would give an even larger integrated cross section of

$$\pi b_a b_o \sigma_o \Gamma/2 \sim 40 \times 10^{-29}\ cm^2\ keV \quad , \qquad (10)$$

a very large value for a total spin change of $\Delta J = -4$ between ground and isomeric states.

Evidently, there is a shockingly broad funneling state for such an unfavorable spin change, and the ^{191}Ir isotope spotlights itself as an important candidate for a more extensive investigation.

GOLD

The system of known (γ,γ') channels for the production of isomeric gold nuclei is the simplest possible -- there are none.[4] Nevertheless, samples of gold activate quite strongly, at a qualitative level comparable to ^{179}Hf.

In this survey, a gold foil of 2.41 g was mounted in a shuttle target with the same geometry as characterized the hafnium experiments. Commercial gold foil was used in which the ^{197}Au isotope occurs with natural 100% abundance. The spectrum of a single irradiation is shown in Fig. 14 and identification was confirmed by the time dependence of the fluorescence. As in previous examples, data were reduced to ratios of the numbers of isomeric nuclei per unit concentration; and the level of excitation on this scale was of the order of the results with hafnium,

$$R = 0.09 \quad , \tag{11a}$$

and

$$V_{max} = 1480 \text{ keV} \quad . \tag{11b}$$

Another irradiation was also obtained under almost ideally contrasting values of end point energies for the bremsstrahlung. Both experimental values of R from Eq. (1) are plotted in Fig. 15 for the two available shots. Statistical uncertainty of counting is much smaller than the size plotted for the data points.

As is readily seen from Eq. (4), if a single reactive channel is dominant, the dependence of the data points upon end point energy should correlate with the variations of the relative intensity $\varsigma(E)$, where E is the energy of the gateway state. The shapes of curves of $\varsigma(E)$ as functions of end point energy differ drastically[2] for different excitation energies E. As in the case[1,2] of ^{77}Se, a simple visual comparison of data with the different shapes[2] can give a clue to the value of the excitation energy E of the gateway state. Of course, a substantial number of data points is needed for such comparisons to be unequivocal.

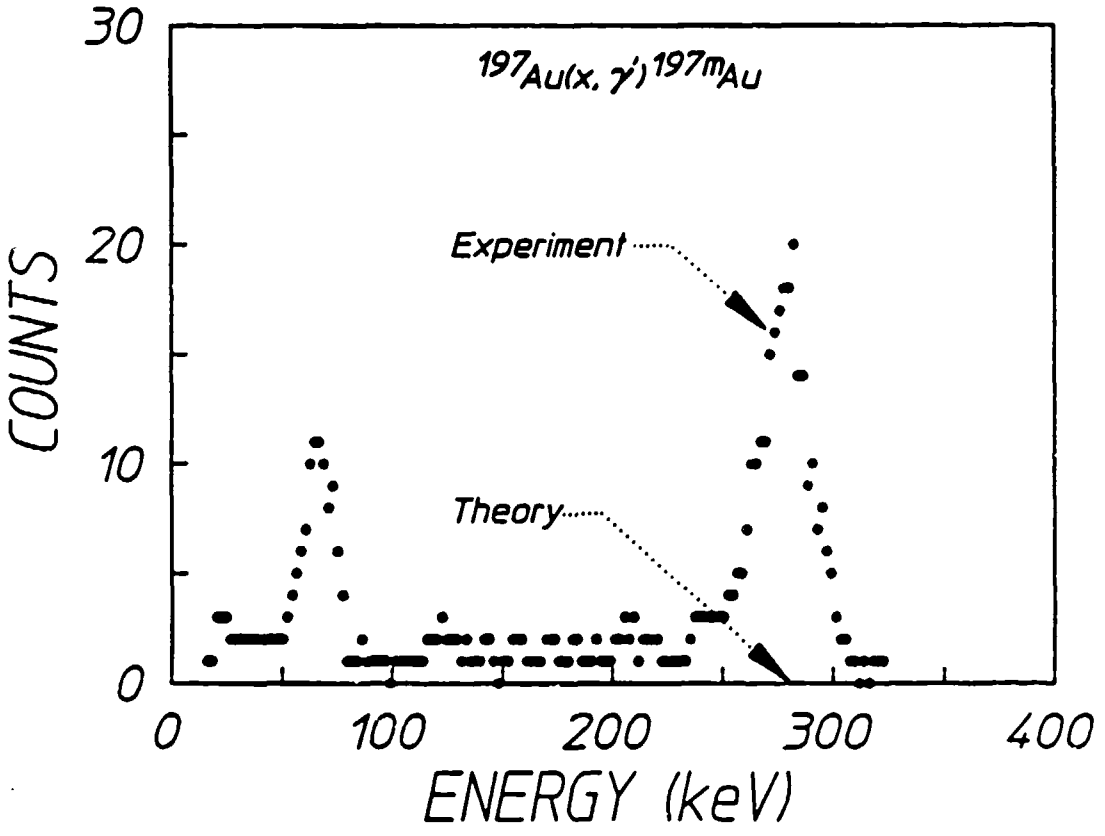

Figure 14: Arrows identify the nuclear component of the spectrum of fluorescence of Au in comparison with model predictions based upon nuclear parameters input from the extant database. Points were obtained from a single irradiation of 2.41 g of metal in natural isotopic abundance.

Shown in Fig. 15 are two typical curves of $\zeta(E)$ for a high value of excitation energy and for a lower value. For the higher values they tend to "point" to an intercept near the gateway energy.

In the case of Fig. 15, it is tempting to identify the gateway as occurring in the cluster of levels near 900 keV. However, also as suggested by the placement of the curve of $\zeta(E)$ for a lower energy threshold, a contribution from a second gateway at lower energy could displace the apparent intercept to lower values, giving a quite erroneous conclusion were a system with two gateways analyzed as having only one. Nevertheless, it is interesting to estimate the magnitude of the integrated cross section for excitation were it to arise from a single level in ^{197}Au near 900 - 1000 keV. In that case $\zeta(1000) \sim 0.26$ for an end point energy near 1.4 MeV. Then from the analog to Eq. (4),

$$\xi_{1000}(\mathrm{Au}) \sim 2.8 \times 10^{-32}\ \mathrm{cm}^2 \quad , \tag{12}$$

and for ^{197}Au(1000 keV, γ')^{197m}Au,

$$\pi b_e b_o \sigma_o \Gamma/2 \sim 2.8 \times 10^{-29}\ \mathrm{cm}^2\ \mathrm{keV} \quad , \tag{13}$$

provided excitation actually occurs through a single gateway in the 900 - 1000 keV range of energies.

Attempts to activate gold with the APEX-I device proved fruitless, but this is not surprising given the smaller excitation ratio of Eq. (11a) and higher probable gateway energy indicated by Fig. 15. As in the case of ^{179}Hf, these null results convey no limits and are consistent with Eq. (13).

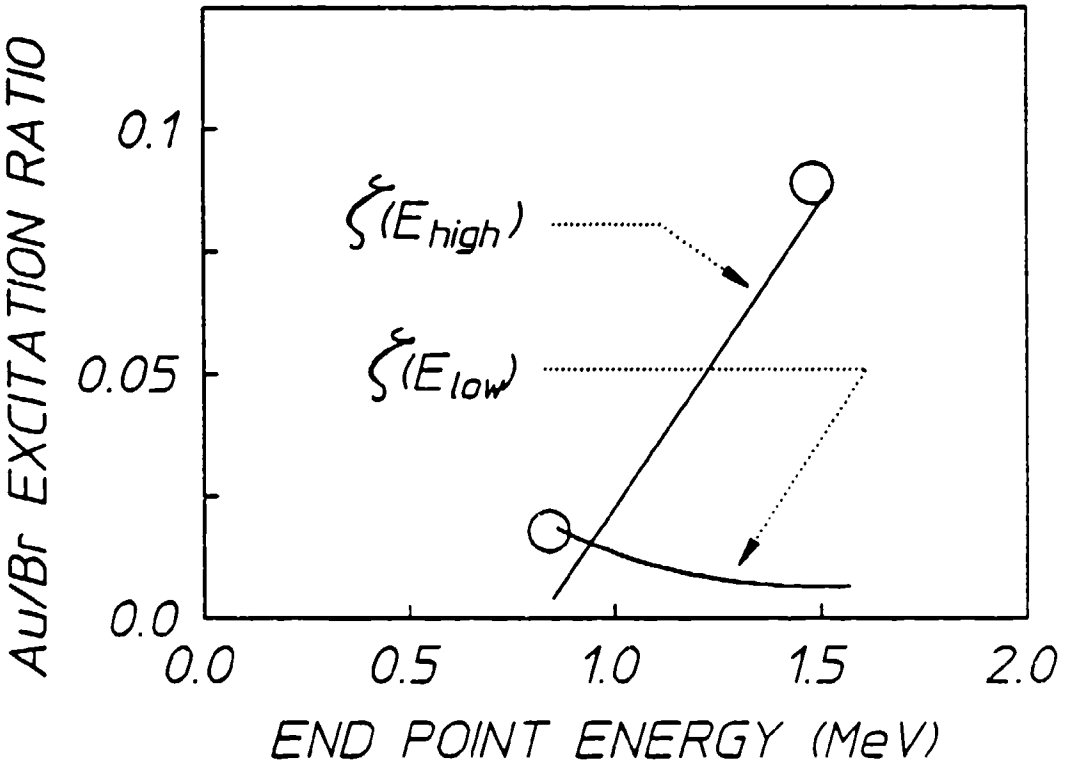

Figure 15: Relative numbers of isomers ^{197m}Au and ^{79m}Br normalized to equal numbers of initial targets plotted as functions of the end point energy of the bremsstrahlung. Curves show the variations of the intensities at high and low pump energies relative to the intensity pumping the ^{79m}Br.

Conclusions

The discovery of cross sections for (γ,γ') reactions which are orders of magnitude greater than theoretical expectations is obviously of great significance both for nuclear physics and for the development of a gamma-ray laser. However, a posteriori, attempts to extract from the survey data new lines for the XAN procedure for calibrating intense pulses of bremsstrahlung highlighted the experimental difficulties of this work. Not nearly enough data were available for the sort of painstaking analyses of residues proven effective in the reconciliation of the nuclear data for ^{77}Se.

Whereas existing values of nuclear parameters were found to be 83% self-consistent in the best set of isotopes, ^{77}Se, ^{79}Br, and ^{115}In, in this new group of four, ^{167}Er, ^{179}Hf, ^{191}Ir, and ^{197}Au, extant parameters were consistent in fewer than 50% of the cases. Moreover, discrepancies were drastic. Fluorescence from ^{167}Er should have been hindered by the same punative K-selection rules which have been used to downgrade priorities of some laser candidates, but actual measurement showed 17 times more yield than expected. Experimental excitation evidently finds a real path around the K-rules, which should have been the most restrictive for this ^{167}Er nucleus because that is the stable isotope most nearly conforming to input assumptions to the theory. It is the most elongated stable nucleus.

Fluorescence from ^{179}Hf was 2.0 to 2.7 times more than predicted from seemingly complete data spanning the range of energies up to 1.4 MeV. Negligible within the context of the more extreme discrepancies found in this group of four, it is an unaccountable excess far greater than was observed in ^{77}Se, the worst example in the previous group studied.

In ^{191}Ir the largest finite excess of experiment over theory was found. Either representing an error of 20,000% in accepted values or the dominance of a new gateway of tremendous width, the results with this isotope merit description as being shockingly unexpected. Such results offer an extreme contrast to the smooth agreement obtained in the first group of isotopes with 83% of the important parameters.

For ^{197}Au the results described in the work came close to providing insight into the discrepancy which is becoming the majority result --

experimental excitation of isomeric fluorescence is much more effective than indicated by the "accepted" database. This case benefited from the largest variation of input spectrum and so suggested a trend. Far from compelling belief, nevertheless the two data points for ^{197}Au suggest a threshold behavior. If so, the gateway state would be one of the cluster in the 900 - 1000 keV range and support an integrated cross section for funneling to the isomer of 2.8 ($\times 10^{-29}$ cm^2 keV) units in the system generally employed. This is a surprisingly large value to find so easily for a completely unexpected pumping sequence spanning a change of angular momentum of $\Delta J = 4$. In a sense, for gold, the experimental yield is infinitely greater than theory because accepted models[4] provide no channels for such an excitation.

Such results as presented here spotlight the drastic inadequacies of the existing database for the purposes of screening candidates for a gamma-ray laser. These earliest results cast severe doubt onto the validity of generally accepted procedures invoking K-selection rules for reducing the slate of candidates by elimination. It appears that instead of narrowing the field of candidate laser isotopes, these experiments are widening the field. Much more study is needed to see whether the experimental production of yields from heavy nuclei that are drastically in excess of theory will prove to be a general phenomenon.

References

1. J. A. Anderson and C. B. Collins, Rev. Sci. Instrum. (pending).

2. J. A. Anderson and C. B. Collins, Proof of the Feasibility of Coherent and Incoherent Schemes for Pumping a Gamma-Ray Laser, University of Texas at Dallas, Report #GRL/8701, Innovative Science and Technology Directorate of Strategic Defense Initiative Organization, July 1987, pp. 11-34.

3. C. B. Collins, F. W. Lee, D. M. Shemwell, B. D. DePaola, S. Olariu, and I. I. Popescu, J. Appl. Phys. 53, 4645 (1982).

4. Evaluated Nuclear Structure Data File (Brookhaven National Laboratory, Upton, New York, 1986).

5. Table I of Ref. 1.

6. C. B. Collins and J. A. Anderson, Proof of the Feasibility of Coherent and Incoherent Schemes for Pumping a Gamma-Ray Laser, University of Texas at Dallas, Report #GRL/8701, Innovative Science and Technology Directorate of Strategic Defense Initiative Organization, July 1987, pp. 35-53.

7. J. A. Anderson and C. B. Collins, Proof of the Feasibility of Coherent and Incoherent Schemes for Pumping a Gamma-Ray Laser, University of Texas at Dallas, Report #GRL/8602, Innovative Science and Technology Directorate of Strategic Defense Initiative Organization, April 1987, pp. 29-46.

8. A. deSchalit and H. Feshbach, Theoretical Nuclear Physics Vol. I: Nuclear Structure (J. Wiley, New York, 1974) Ch. 6, Section 14.

9. M. E. Bunker and C. W. Reich, Rev. Mod. Phys. 43, 348 (1971).

10. Table IV.16 of Ref. 9 suggests the $1/2^-[510]$ and the $5/2^-[521]$ are present in about equal amounts, the former contributing about 40% of the total state.

ACTIVATION OF ^{115m}In BY SINGLE PULSES OF INTENSE BREMSSTRAHLUNG

by C. B. Collins, J. A. Anderson, Y. Paiss, C. D. Eberhard,
University of Texas at Dallas
R. J. Peterson,
University of Colorado
W. L. Hodge,
High Energy Laser Associates

For the study of (γ,γ') reactions that produce isomeric products, ^{115}In has a particularly favorable combination of characteristic properties. Having only a few channels for reaction at energies below 1.4 MeV, it nevertheless displays a large integrated cross section for excitation of the 269 minute isomer at 336 keV. For these pragmatic reasons ^{115}In has served as the archetype material for the study of this type of reaction, and a number of efforts have been reported[1-13] in the past 48 years.

The relevant part of the energy level diagram[14] of ^{115}In is shown in Fig. 1, indicating only three levels through which a (γ,γ') reaction of multipolarity E1, M1, M2, or E2 could proceed to populate the isomeric state for photons below 1.4 MeV. The importance of the lowest dipole gateway level at 941 keV is negligible because it has a particularly small integrated cross section[15] for excitation in comparison to that of the nearby 1078 keV level, and the 934 keV 7/2$^+$ level has a yet smaller cross section because of its longer lifetime.

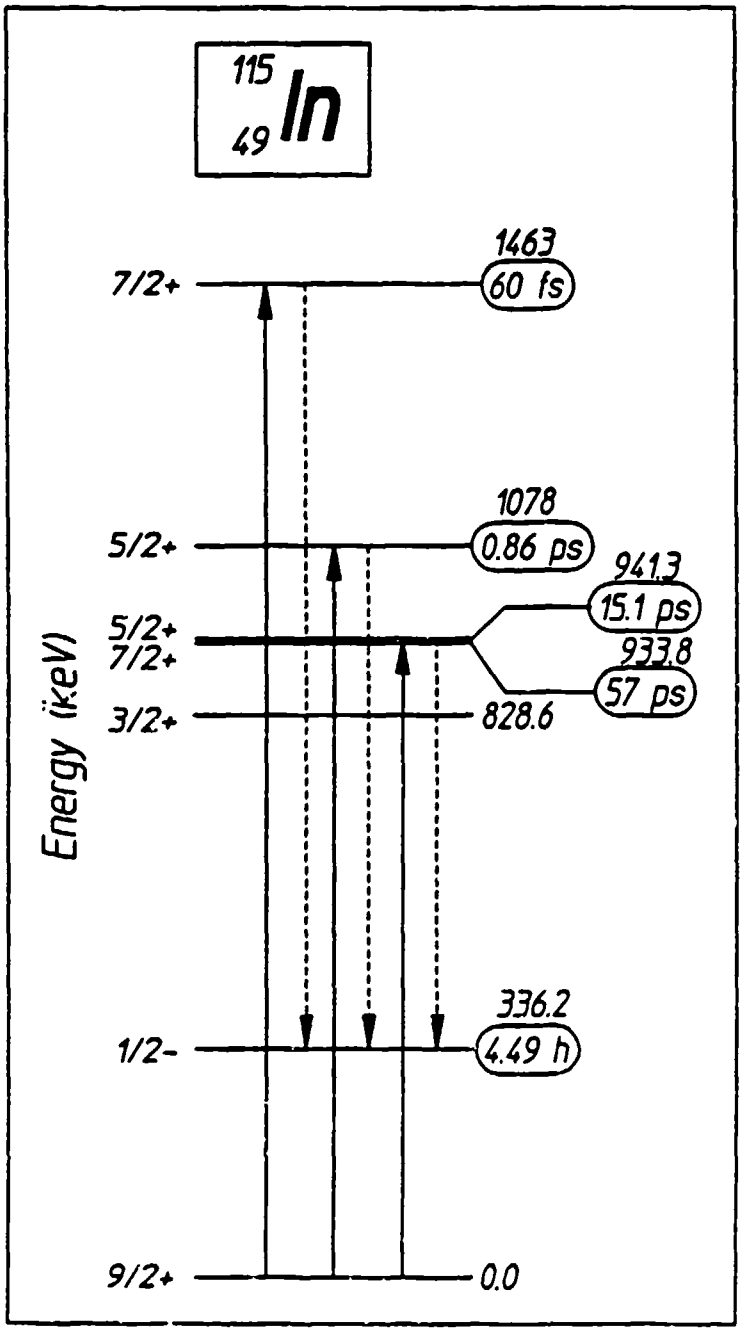

Figure 1: Energy level diagram of the excited states of ^{115}In important in the production of populations of the isomer.[14] Half-lives of the states are shown to the right of each, and sequences of (γ,γ') reactions leading to the isomer are shown by the arrows. Dashed γ' transitions occur by cascading through levels not shown.

Table I

Summary of integrated cross sections reported for the reaction $^{115}In(\gamma,\gamma')^{115m}In$ through the 1078 keV $J^{\pi} = 5/2^{+}$ level.

Cross Section $\pi b_a b_o \sigma_o \Gamma/2$ ($\times 10^{-29}$ cm^2 keV)	Reference
23 ± 4	Ikeda and Yoshihara (Ref. 4)
20 ± 4	Veres (Ref. 5)
7.1 ± 2.3	Chertok and Booth (Ref. 6)
11.5 ± 4.0	Booth and Brownson (Ref. 7)
30 (+40,-20)	Boivin, Cauchois, and Heno (Ref. 8)
10.5 ± 2.7	Lakosi, Csuros, and Veres (Ref. 9)
19 ± 1	Watanabe and Mukoyama (Ref. 10)
5.39 ± 0.64	Ljubicic, Pisk, and Logan (Ref. 11)
18.1 ± 1.5	Yoshihara et. al. (Ref. 12)
18.7 ± 2.7	This work

In practical cases in which ^{115}In samples are excited either with gamma rays from a source or by bremsstrahlung from an accelerator operating below 1.4 MeV, the absorption spectrum for (γ,γ') reactions producing isomers is essentially monochromatic at 1078 keV. Nevertheless, quantitative measurements of the integrated cross section have shown a chaotic level of contradiction between theory and experiment and among the experiments themselves. Table I presents a summary of values reported in the literature together with the results of this measurement, in terms of the integrated cross section as usually reported,[16] $\pi b_a b_o \sigma_o \Gamma/2$, where Γ is the natural width in keV of the pump band; where the branching ratios b_a and b_o give the probabilities for the decay of the gateway level back into the initial and isomeric level, respectively; and σ_o is the Breit-Wigner cross section for the absorption transition.

$$\sigma_o = \frac{\lambda^2}{2\pi} \frac{2I_e+1}{2I_g+1} \frac{1}{\alpha_p+1} , \quad (1)$$

where λ is the wavelength in cm of the gamma ray at the resonant energy E_i; I_e and I_g are the nuclear spins of the excited and ground states, respectively; and α_p is the total internal conversion coefficient for the absorption transition.

It has been recently argued[16] that the principal cause of such a large degree of variance among previous measurements of the ^{115}In excitation has been the generally inadequate level of characterization of the spectrum of the pump source. In a subsequent paper[13] we showed that the spectrum from a pulsed source of intense bremsstrahlung could be determined to a level of accuracy sufficient for the quantitative description of the reactions $^{77}Se(\gamma,\gamma')^{77m}Se$ and $^{79}Br(\gamma,\gamma')^{79m}Br$. In doing so, an important new channel for the excitation of ^{77m}Se was found through the 1005 keV $J^\pi = 3/2^-$ level.

It is the purpose of this paper to report the reexamination of the reaction $^{115}In(\gamma,\gamma')^{115m}In$ with the same pulsed bremsstrahlung source used for the reconciliation of the absorption cross sections to ^{79m}Br and ^{77m}Se. Results for ^{115}In were found in this work to be consistent with that reconciliation. Moreover, the quantitative value for the integrated cross section we report can be seen to be in good agreement with the other value reported most recently as the result of excitation with a radioactive source.[12]

Methods and Apparatus

In a previous report[13,16] it was shown that the uncertainty in the absolute value of the geometric coefficient coupling the source of pump radiation to the absorbing target could be eliminated by normalizing both the pump fluence and the fluorescence counts to some standard material having a monochromatic excitation spectrum. The reaction $^{79}Br(\gamma,\gamma')^{79m}Br$ was found to be an ideal standard, having an integrated cross section of 6.2×10^{-29} cm^2 keV and a convenient radioactivity in the isomer. Following the formalism reported earlier,[13] the number of ^{115m}In nuclei, S(In), which could be excited by a flash of intense bremsstrahlung can be conveniently expressed as a ratio,

$$\frac{S(In)}{S(Br)} = \frac{N(In)}{N(Br)} \frac{\xi_{1078}(In)}{\xi_{761}(Br)} \zeta(1078) \quad , \qquad (2)$$

where S(x) and N(x) are the number of nuclei produced and the number of target nuclei of material x, respectively; $\zeta(1078)$ is the ratio of pumping intensity at 1078 keV to the intensity at 761 keV; and the $\xi_E(x)$ are the combinations of nuclear parameters involved in the excitation of the gateway level at energy E,

$$\xi_E(x) = \frac{(\pi b_e b_o \sigma_o \Gamma/2)_E}{E} \quad . \qquad (3)$$

The collection of terms in parentheses in Eq. (3) comprises the integrated cross section for excitation as usually reported, and the calibration value for ^{79}Br is $\xi_{761}(Br) = 8.2 \times 10^{-32}$ cm^2.

The source of excitation in these experiments[13] was the bremsstrahlung produced by the DNA PITHON nuclear simulator at Physics International. The usual end point energy of the electrons producing the bremsstrahlung was 1.3 MeV with small shot-to-shot variance. For these particular experiments, the nominal firing parameters were deliberately perturbed so that successive irradiations could be obtained with end point energies varying from 0.9 to 1.5 MeV.

Intensities at the target were determined by measuring the nuclear activation of the ^{79}Br component of a sample of LiBr containing isotopes in natural abundance. This calibrating target was run in a pneumatic transfer system which enabled the population of ^{79m}Br produced by a single irradiation to be subsequently counted at a quiet location 30 m removed from the source. Activation lost during the 1.0 s transit time could be readily corrected during analysis.

The ^{115}In sample under study was in the form of a thin foil taped to a fiduciary mark near the pneumatic system. Since the ^{115m}In had a substantially longer half-life, it could be manually detached after exposure and transferred to the spectrometer, which consisted of a 3" x 3" NaI(Tl) detector with associated electronics. In typical cases, a counting time of one hour gave better than 2% statistical accuracy in the ^{115m}In peak after removal of background. In the course of this experimental series, twelve shots were obtained for sufficiently high

end point energies to yield statistically significant numbers of fluorescent isomeric activity.

To confirm that the fluorescence being detected resulted only from decay of the ^{115m}In activity, additional foils were irradiated and then examined with an intrinsic Ge spectrometer, carefully shielded. In Fig. 2 we show spectra from an In foil irradiated by bremsstrahlung with an end point of 1.3 MeV. The fluorescence peak is at 336.2 keV, with a half-life seen to be consistent with a tabulated value of 4.49 hours.

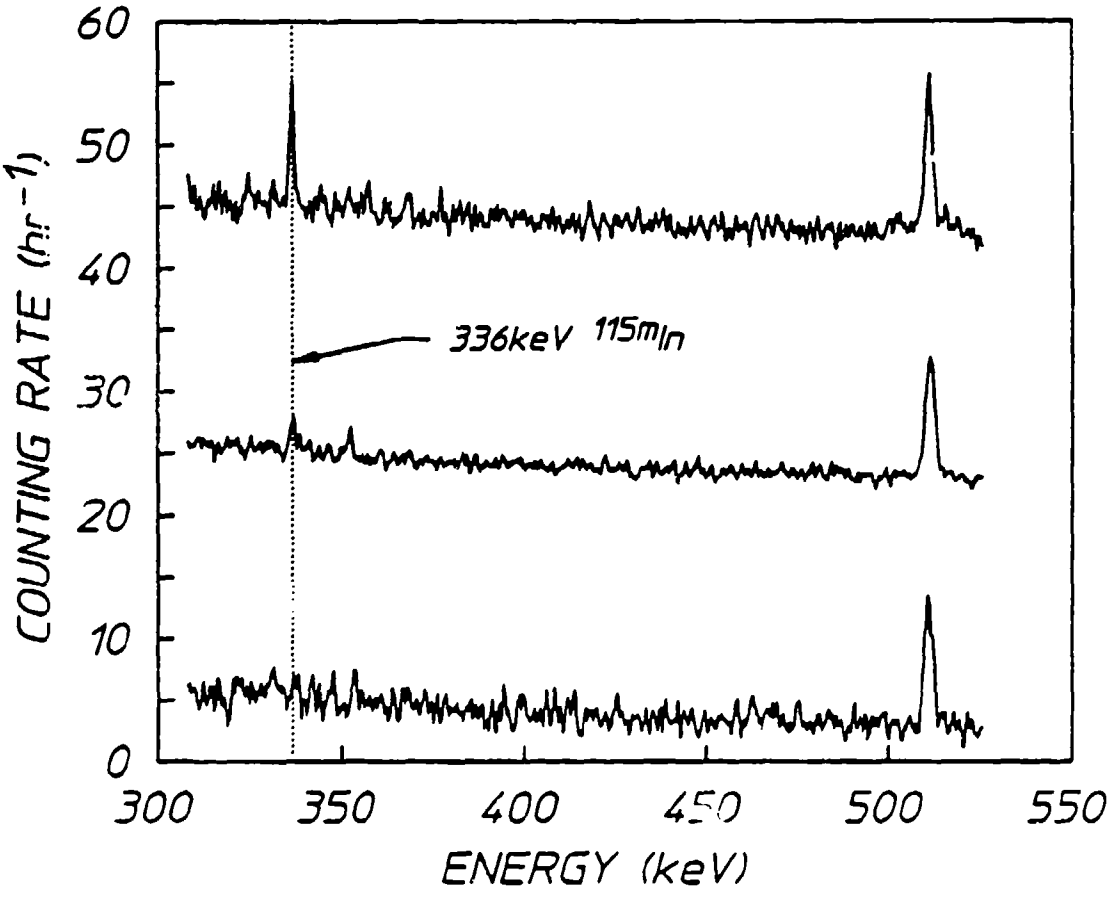

Figure 2: Three sequential spectra from an intrinsic Ge detector begun at times 6.5, 9.2, and 19.0 hours after the irradiation with a flash of bremsstrahlung with a 1.3 MeV end point. Data have been offset by 40, 20, and 0 counts/h, respectively. The 336.2 keV peak is seen to decay with the appropriate half-life of 4.49 hours for ^{115m}In. The other structure is the annihilation peak at 511 keV.

The relative bremsstrahlung intensity emitted at 1078 keV was a strong function of the end point energy of the accelerator as shown in Fig. 3. These data were obtained by numerically fitting theoretical computations of bremsstrahlung spectra. As reported previously,[13] confidence was established by examining quantitatively the number of fluorescent nuclei produced by successive irradiations of samples of ^{79}Br and ^{77}Se at a variety of end point energies.

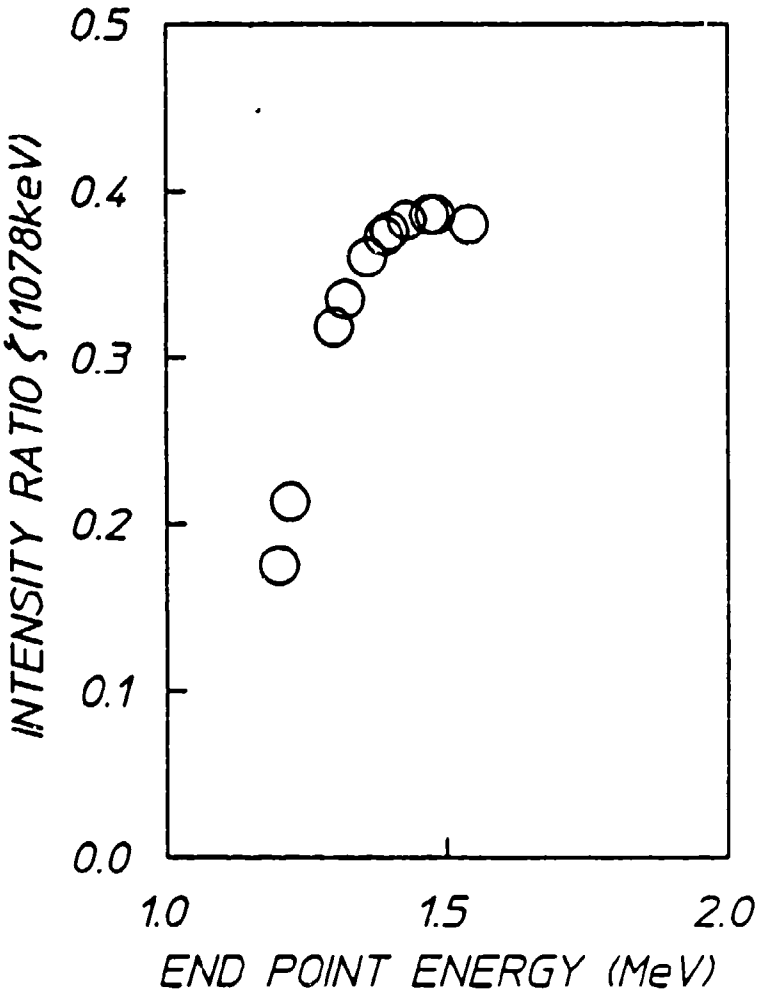

Figure 3: Plot of the ratio of intensities of the bremsstrahlung spectrum at 1078 keV to that at 761 keV as a function of the end point energy of the electron beam producing the photons.

Results

Because of a small physical displacement of the ^{115}In sample from the mixed $^{79}Br/^{77}Se$ target providing calibration, the actual number of fluorescent photons counted from the former had to be corrected for the extra path length from the source point to the absorber. This was done by mounting thermoluminescent diodes (TLD's) at both positions and then comparing the total dose recorded at the different points for each shot. The number of photons from ^{115m}In was scaled by the value of relative dose received at the ^{115}In and at the calibrating positions.

The indium sample was optically thin at the 336 keV energy of the fluorescence from the ^{115m}In, thus obviating corrections for self-absorption. Data were corrected for fluorescence and detector efficiencies. The resulting values of S(In)/S(Br) are obtained from Fig. 4 by multiplying the ratios of fluorescent counts shown there by 0.75, the ratio of correction factors for these effects.

The linear form of the dependence of the relative yield of fluorescence from the indium isomers seen in Fig. 4 between 1.0 and 1.45 MeV is a strong indication of the dominance of a single channel of excitation through a gateway level lying at an energy given by the value of intercept. From the data of Fig. 4, it is seen that the intercept lies between 1000 and 1200 keV in agreement with the known state at 1078 keV. Also shown in Fig. 4 is the energy of the next higher gateway state, $7/2^+$ at 1.463 MeV. It is interesting to observe that for end point energies above this value there may be a tendency of the data to depart from the simple linear fit because of the availability of this additional gateway. A greater number of measurements at successively higher end point energies would be needed to confirm this indication.

Once most of the data are established as being consistent with the model of excitation through a single level at 1078 keV, Eq. (2) provides a means of determining the absolute cross section for the excitation. In Fig. 5, data for the measured values on the left side of Eq. (2) are plotted as functions of the relative intensities $\zeta(1078)$ appearing on the right.[17] As can be seen from Eq. (2), the best slope around which the data of Fig. 5 scatter would represent our experimental determination of the product of the first two terms on the right of Eq. (2).

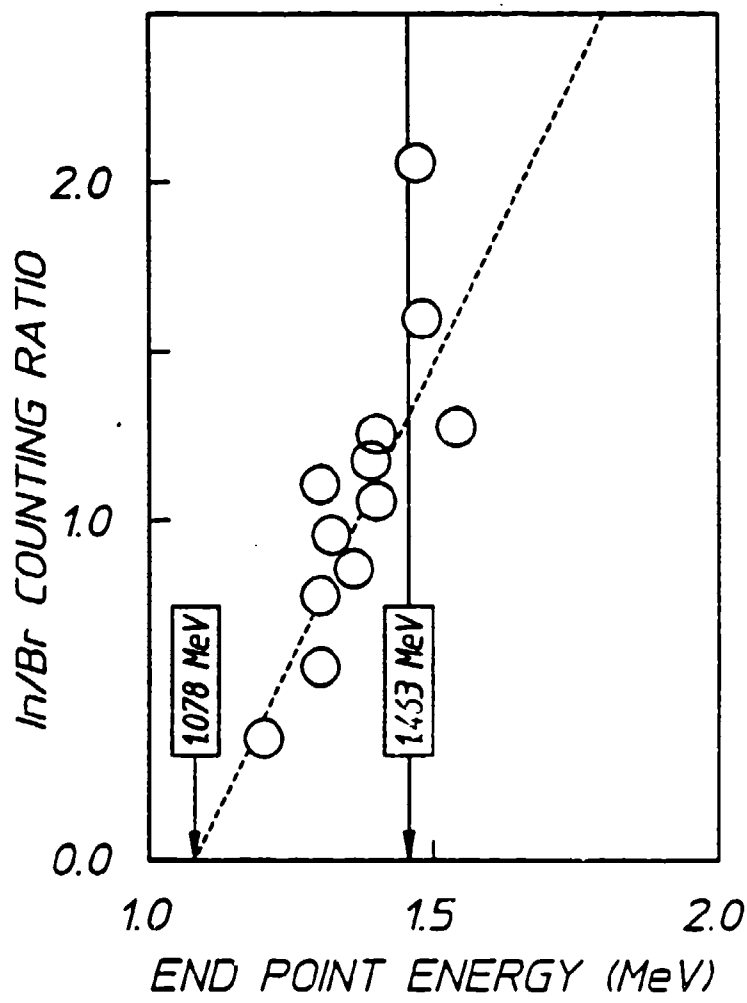

Figure 4: Ratios of fluorescent photons from ^{115m}In to those from ^{79m}Br, produced by single discharges from PITHON, as corrected for the finite duration of the counting interval and plotted as a function of the end point energies of the electrons producing the bremsstrahlung. The dashed line shows a linear fit to the data intercepting the x-axis at a gateway energy of 1.078 MeV. Excitation energy of the next higher gateway is shown at 1.463 MeV.

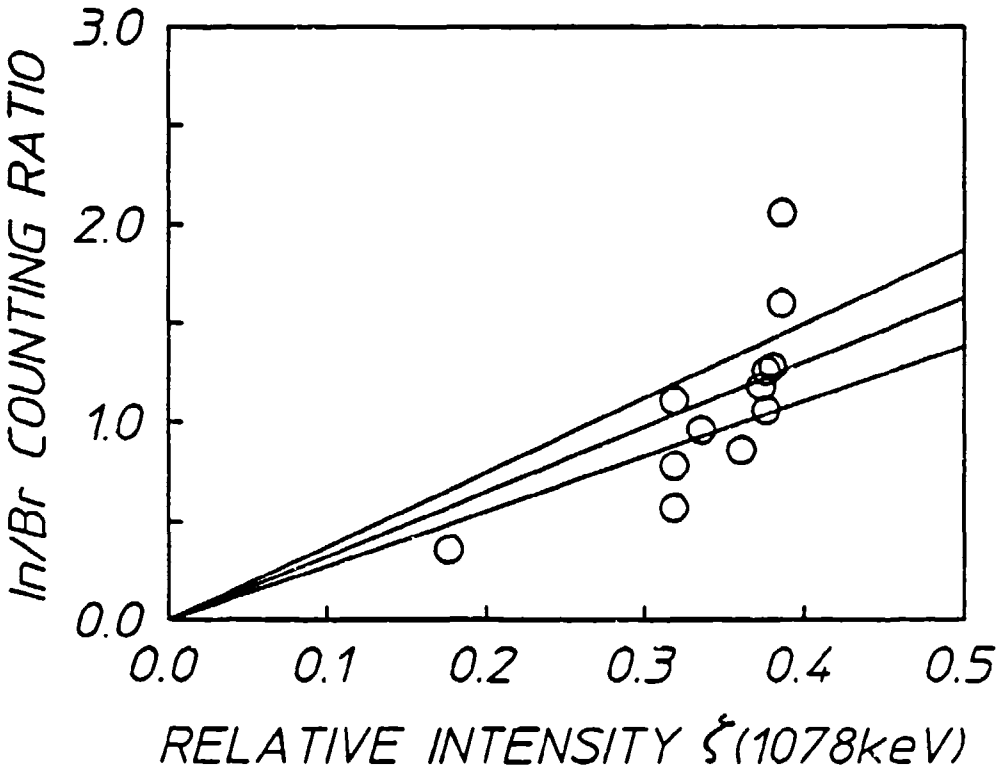

Figure 5: Plot of the ratios of ^{115m}In to ^{79m}Br fluorescence observed as a function of the relative intensity of irradiation at 1078 keV normalized to the intensity at 761 keV. The center line shows the least squares fit including the origin and the outer lines bound uncertainty in such a fit introduced by varying the characterization of the intensities of Fig. 3 over acceptable limits.

From the linear fit to the data of Fig. 5 shown as the center line, Eqs. (2) and (3), and the value of the integrated cross section for ^{79}Br mentioned earlier, we obtain

$$\zeta_{1078}(\text{In}) = (17.3 \pm 2.5) \times 10^{-32}\ \text{cm}^2 \quad . \qquad (4)$$

The uncertainty was obtained from application of the same analyses to the outer lines in Fig. 5 reasonably bounding the scatter from the least squares fit to the data. The lines actually shown were obtained by determining the extent to which data points of Fig. 5 would be displaced horizontally if the corresponding abscissae were varied by the maximum extent of the uncertainty in the value of $\zeta(1078)$ arising from the nature of the calibration and the interpolations being employed.[13] The

statistical scatter in the data is within the bounds established by the uncertainty in intensity.

Finally, substituting Eq. (4) into Eq. (3) and solving for the integrated cross section give for the 1078 keV transition in ^{115}In,

$$\pi b_a b_o \sigma_o \Gamma/2 = (18.7 \pm 2.7) \times 10^{-29} \text{ cm}^2 \text{ keV} \quad . \quad (5)$$

This is the value we report in Table I.

Conclusions

The detailed characterization of the spectrum emitted by the intense source of pulsed bremsstrahlung described earlier[13] has been found to be sufficient to describe the quantitative yield of the reaction ^{115}In$(\gamma,\gamma')^{115m}$In, for the value of integrated cross section given by Eq. (5).[18] Table I shows that value to agree with some of the prior measurements. In this work there was no need to invoke any nonresonant reaction channels of the type sometimes used[11] in the description of this reaction.

In addition to providing further evidence against the occurrence of nonresonant reactions in ^{115}In, the results of this work have important implications for the calibration of intense sources of pulsed continua. By providing a means for storing a sample of the illuminating intensity at a single well-defined energy of 1078 keV for subsequent measurement at a later, quieter time, a sample of ^{115}In can readily complement the information supplied[13,16] by ^{79}Br about the intensity at 761 keV. Moreover, both together can be used to identify the component of excitation contributed by the higher energy lines of ^{77}Se so that the remainder can be used to characterize the intensities at lower energies.[13]

Finally, it seems this technique of using single pulses of intense continua to measure integrated cross sections for the production of measurable populations of isomers can provide data of use in astrophysical modeling. Cross sections at energies as low as 1 MeV are quite large for such elements as Se, Br and In and might provide viable photonuclear channels for the production of enough isomeric population to be important in cosmic nucleosynthesis. It seems that the experiments reported here give evidence that it is possible to advance the precision for the characterization of (γ,γ') reactions toward that enjoyed by other types of particle reactions at comparable energies.

References

1. B. Pontecorvo and A. Lazard, C. R. Acad. Sci. 208, 99 (1939).
2. G. B. Collins, B. Waldman, E. M. Stubblefield, and M. Goldhaber, Phys. Rev. 55, 507 (1939).
3. G. Harbottle, Nucleonics 12, 64 (1954).
4. N. Ikeda and K. Yoshihara, Radioisotopes 7, 11 (1958).
5. A. Veres, Int. J. Appl. Radiat. Isot. 14, 123 (1963).
6. B. T. Chertok and E. C. Booth, Nucl. Phys. 66, 230 (1965).
7. E. C. Booth and J. Brownson, Nucl. Phys. A98, 529 (1967).
8. M. Boivin, Y. Cauchois, and Y. Heno, Nucl. Phys. A137, 520 (1969).
9. L. Lakosi, M. Csuros, and A. Veres, Nucl. Instrum. and Meth. 114, 13 (1974).
10. Y. Watanabe and T. Mukoyama, Bull. Inst. Chem. Res., Kyoto Univ. 57, 72 (1979).
11. A. Ljubicic, K. Pisk, and B. A. Logan, Phys. Rev. C 23, 2238 (1981).
12. K. Yoshihara, Zs. Nemeth, L. Lakosi, I. Pavlicsek, and A. Veres, Phys. Rev. C 33, 728 (1986).
13. J. A. Anderson and C. B. Collins, Rev. Sci. Instrum. (pending).
14. Evaluated Nuclear Structure Data File (Brookhaven National Laboratory, Upton, New York, 1986).
15. In the units usually employed, the integrated cross section $\pi b_a b_o \sigma_o \Gamma/2$ for the 941 keV level is computed from Ref. 14 to be 0.72×10^{-29} cm^2 keV.
16. J. A. Anderson and C. B. Collins, Rev. Sci. Instrum. (to be published Nov. 1987).
17. Data actually plotted in Figs. 4 and 5 are ratios of the numbers of detected photons corrected for the finite period of counting, while the analyses of Eq. (2) are written in terms of the ratios of the numbers of active nuclei produced in the target. Slopes obtained from the figures must be multiplied by 0.75, the product of the ratios of corrections for detector and fluorescence efficiencies and for self-absorption in the target before being used in the equations.
18. The value of $\pi b_a b_o \sigma_o \Gamma/2$ was determined in this work relative to the calibration value for ^{79}Br taken from the literature and confirmed in recent experiments described in Ref. 13.

ACTIVATION OF ^{111m}Cd BY SINGLE PULSES OF INTENSE BREMSSTRAHLUNG

by J. A. Anderson, M. J. Byrd, and C. B. Collins

Fifty years ago it was first reported[1] that (γ,γ') reactions could produce isomeric nuclei. It is interesting to note that even after such an advance of technology as has occurred over the intervening time, attempts at quantitative measurement still do not converge. For example, the most recent three measurements[2-4] of the integrated cross sections for the reaction $^{111}Cd(\gamma,\gamma')^{111m}Cd$ were conducted in 1979, 1982 and 1987 with results of 35, 5.8, and 14, respectively, in the usual units of 10^{-29} cm^2 keV. Probable errors were quoted as varying only from 7 to 14%, and yet, no two of the measurements were even within a factor of two of each other.

The ^{111m}Cd isomer at 396 keV has a 48.6 minute half-life and is readily detected by observing the 150.6 keV and 245.4 keV gammas radiated in the cascade from the isomer. Experimentally this is an almost ideal vehicle for the study of (γ,γ') reactions, since the lifetime of the isomer is long enough to collect a substantial dose from a variety of excitation sources during the activation cycle and short enough to count with reasonable signal-to-background ratio afterward. Experiments appear to have been carefully executed, and the drastic disagreement in the results has been attributed[3] to the controversial[4] proposal that some mechanism of nonresonant nuclear absorption dominates the excitation step. However, the data that support this intriguing proposal[3] and the data that seem to refute[4] it agree only in indicating that the (γ,γ') reaction producing ^{111m}Cd is not well understood.[2-8]

The relevant part of the energy level diagram[9] of ^{111}Cd is shown in Fig. 1. All of the adopted levels[9] between 1000 and 1500 keV are shown together with the gamma transitions that have been observed[10] in reactions other than (γ,γ'). Additional transitions to the 1190 and 1330 keV levels have been inferred[5,6] from (γ,γ') studies, but those reports depend upon the validity of arguments which are weakened by the controversy. Moreover, even the existence of the 1330 keV level might reasonably be questioned, since it is based upon a single report[11] of a reaction not dependent upon the interpretations of (γ,γ') data.

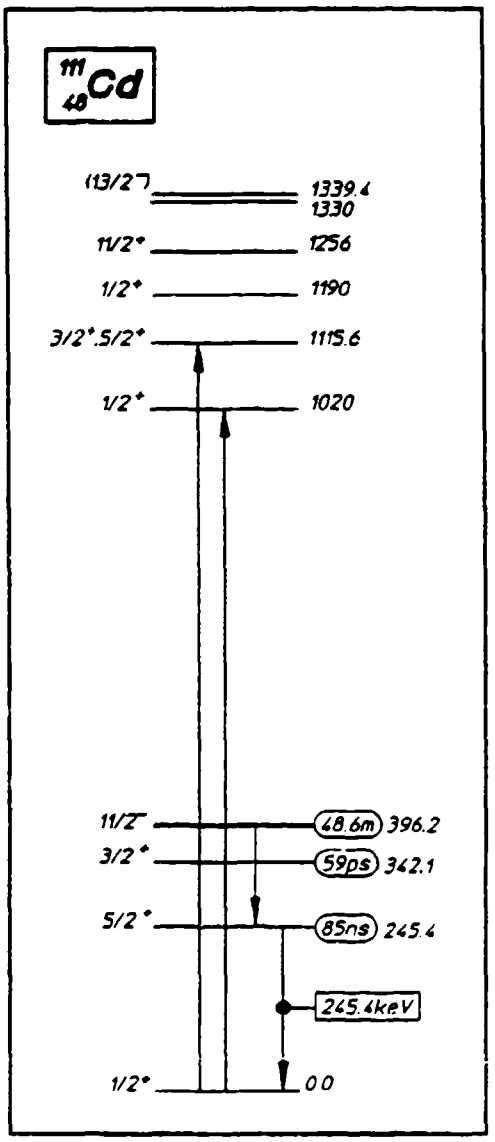

Figure 1: Energy level diagram of the excited states of ^{111}Cd between 1000 and 1500 keV which may be important in the production of the 48.6 m isomer. Also shown are all excited states below 400 keV. Half-lives of the states are shown to the right of each state and known[10] gamma transitions are shown by the arrows. Populations of the 48.6 m isomer are most conveniently detected by the 245.4 keV fluorescent transition as indicated.

For levels in Fig. 1 which might be excited by photons with energies in the range 1000 to 1500 keV, there are a number of possible cascades to the $11/2^-$ isomer through levels below 1000 keV which are not shown. However, no particular path has been proposed.

It has been recently argued[12] that the principal cause of such a large degree of variance among previous measurements of isomeric excitation has been the generally inadequate level of characterization of the spectrum of the pump source. In a subsequent paper[13] we showed that the spectrum from a pulsed source of intense bremsstrahlung could be determined to a level of accuracy sufficient for the quantitative description of the reactions $^{77}Se(\gamma,\gamma')^{77m}Se$ and $^{79}Br(\gamma,\gamma')^{79m}Br$. In doing so, an important new channel for the excitation of ^{77m}Se was found through the 1005 keV, $J^\pi = 3/2^-$ level.

Subsequently we reexamined[14] the reaction $^{115}In(\gamma,\gamma')^{115m}In$ with the same pulsed bremsstrahlung source used for the reconciliation of the absorption cross sections to ^{79m}Br and ^{77m}Se. Results for ^{115}In were found to be consistent with that reconciliation. Moreover, the quantitative value for the integrated cross section we reported was in good agreement with the other value reported most recently as the result of excitation with a radioactive source.[15] Reported here is an extension of this technique to the reaction $^{111}Cd(\gamma,\gamma')^{111m}Cd$. We find an integrated cross section of $(9.8 \pm 2.5) \times 10^{-29}$ cm^2 keV for reaction through a gateway level near 1200 keV.

Methods and Apparatus

As usually reported[12] the integrated cross section for a (γ,γ') reaction yielding an isomeric product state is $\pi b_a b_o \sigma_o \Gamma/2$, where Γ is the natural width in keV of the pump band; where the branching ratios b_a and b_o give the probabilities for the decay of the gateway level back into the initial and isomeric level, respectively; and σ_o is the Breit-Wigner cross section for the absorption transition,

$$\sigma_o = \frac{\lambda^2}{2\pi} \frac{2I_e+1}{2I_g+1} \frac{1}{\alpha_p+1} , \qquad (1)$$

where λ is the wavelength in cm of the gamma ray at the resonant energy E_i; I_e and I_g are the nuclear spins of the excited and ground states, respectively; and α_p is the total internal conversion coefficient for the absorption transition.

Unlike our previous study of ^{115}In from which this present work has been extended, none of the elementary nuclear properties entering into the computation of the integrated cross section were known for ^{111}Cd. Although it is uniformly assumed[2-8] that the dominant gateway level lies at 1330 keV, this is not strongly supported by prior data. Early experiments[5,6,16,17] using bremsstrahlung from accelerators with variable end point energies indicated that the reaction turns on between 1200 and 1400 keV. However, the apparent sharpness seen in some early data at 1330 keV is strongly affected by the logarithmic presentation of a linear threshold and the sensitivity of the instrumentation to low levels of activation. In more recent experiments using ^{60}Co sources, the high level of activation produced and the proximity of the 1330 keV level of ^{111}Cd to the strong 1332 keV line of ^{60}Co made it attractive to identify the (γ,γ') reaction as occurring through the 1330 keV level of undetermined symmetry. Since the experiments reported here were conducted with an accelerator producing a known[13] bremsstrahlung spectrum, it was decided to try to determine experimentally the energy of the gateway needed, as well as the integrated cross section.

In a previous report[12,13] it was shown that the uncertainty in the absolute value of the geometric coefficient coupling the source of pump radiation to the absorbing target could be eliminated by normalizing both the pump fluence and the fluorescence counts to some standard material having a monochromatic excitation spectrum. The reaction ^{79}Br$(\gamma,\gamma')^{79m}$Br was found to be an ideal standard, having an integrated cross section of 6.2×10^{-29} cm^2 keV and a convenient radioactivity in the isomer. Following the formalism reported earlier,[13] the number of ^{111m}Cd nuclei, S(Cd), which could be excited through a single gateway state at an energy E by a flash of intense bremsstrahlung can be conveniently expressed as a ratio,

$$\frac{S(Cd)}{S(Br)} = \frac{N(Cd)}{N(Br)} \frac{\xi_E(Cd)}{\xi_{761}(Br)} \zeta(E) \quad , \qquad (2)$$

where S(x) and N(x) are the number of nuclei produced and the number of target nuclei of material x, respectively; $\zeta(E)$ is the ratio of pumping

intensity at the gateway energy E in keV to the intensity at 761 keV; and the $\xi_E(x)$ are the combinations of nuclear parameters involved in the excitation,

$$\xi_E(x) = \frac{(\pi b_a b_o \sigma_o \Gamma/2)_E}{E} \quad . \tag{3}$$

The collection of terms in parentheses in Eq. (3) comprises the integrated cross section for excitation as usually reported, and the calibration value for ^{79}Br is $\xi_{761}(Br) = 8.2 \times 10^{-32}$ cm^2. Still more convenient for analysis is the weighted activation ratio R obtained by multiplying Eq. (2) by the ratio of the number of target nuclei,

$$R = \frac{N(Br)S(Cd)}{N(Cd)S(Br)} = \frac{\xi_E(Cd)}{\xi_{761}(Br)} \zeta(E) \quad . \tag{4}$$

The source of excitation in these experiments[13] was the bremsstrahlung produced by the PITHON nuclear simulator at Physics International. The typical end point energy of the electrons producing the bremsstrahlung was 1.3 MeV with small shot-to-shot variance. For these particular experiments, the nominal firing parameters were deliberately perturbed so that successive irradiations could be obtained with end point energies varying from 1.3 to 1.54 MeV.

Intensities at the target were determined by measuring the nuclear activation of the ^{79}Br component of a sample of LiBr containing isotopes in natural abundance. This calibrating target was run in a pneumatic transfer system which enabled the population of ^{79m}Br produced by a single irradiation to be subsequently counted at a quiet location removed from the source. Activation lost during the 1.0 s transit time could be readily corrected during analysis.

The ^{111}Cd sample under study occurred in natural isotopic abundance in a thin Cd foil taped to a fiduciary mark near the pneumatic system. Since the ^{111m}Cd had a substantially longer half-life than the calibrating Br, it could be manually detached after exposure and transferred to the spectrometer, which consisted of an intrinsic Germanium detector with associated electronics. In typical cases a counting time of one hour gave better than 5% statistical accuracy in the area of the ^{111m}Cd peak. In the course of this experimental series, six shots were obtained for sufficiently high end point energies to yield statistically significant numbers of fluorescent isomeric activity.

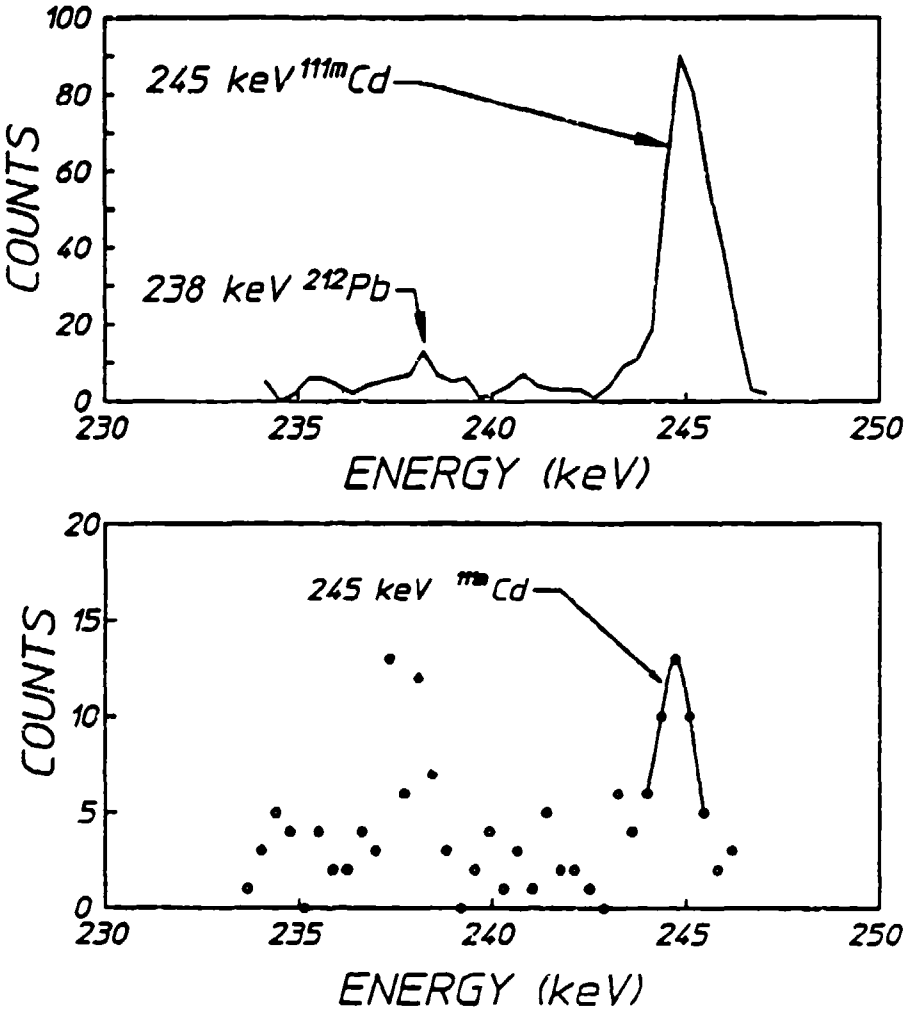

Figure 2: Spectra showing the 245 keV line from the decay of ^{111m}Cd. The spectra were obtained from an 8.02 gm, natural Cd foil sample. The small peak near 238 keV is due to the decay of naturally occurring ^{212}Pb in the counting environment.
(a) Fluorescence from ^{111m}Cd following irradiation with a single bremsstrahlung pulse having an end point energy of 1.4 MeV. Counting time was 3600 sec.
(b) Fluorescence following excitation with an end point of 1.3 MeV. Counting time was 2700 sec.

To confirm that the fluorescence being detected resulted only from decay of the ^{111m}Cd activity, the spectra from irradiated foils were first examined for traces of interference from the 238 keV line from ^{212}Pb in the counting environment. The clear separation of the 238 keV line from the 245 keV line obtained from ^{111m}Cd following irradiation with a 1.4 MeV end point bremsstrahlung pulse is shown in Fig. 2(a). At

an end point energy of 1.3 MeV, where the spectral intensity at the 1330 level in ^{111m}Cd should be negligible, the 245 keV line is weak but clearly observable, as shown in Fig. 2(b).

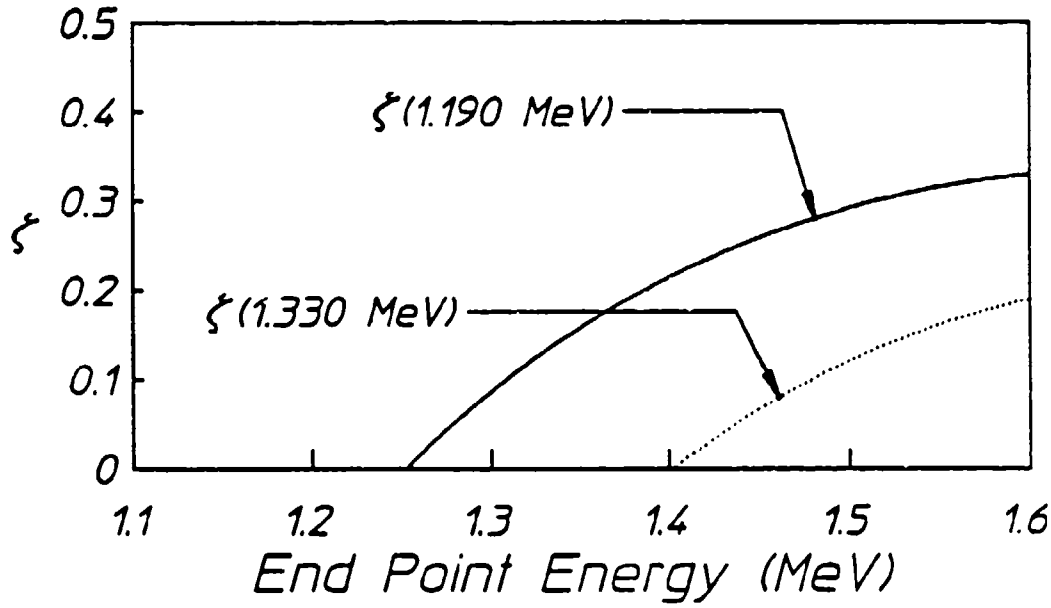

Figure 3: Plots showing the ratio of the spectral density at energy E normalized to the spectral density at the 761 keV gateway of ^{79m}Br for varying end point energies. The solid and dotted lines show the ratio for energies E = 1.190 and E = 1.330 MeV.

In order to determine an experimental value of the ξ_ε(Cd) by fitting Eq. (4) to measurements of the fluorescence yields from the sample and from the LiBr calibrator, the relative bremsstrahlung intensity ζ(E) emitted at E must be known. For these experiments, these data were obtained by numerically fitting theoretical computations of bremsstrahlung spectra. As reported previously,[13] confidence was established by examining quantitatively the number of fluorescent nuclei produced by successive irradiations of samples of ^{79}Br and ^{77}Se at a variety of end point energies. The relative bremsstrahlung intensity emitted at a particular energy was found to be a strong function of the end point energy of the accelerator; two examples are shown in Fig. 3.

Results

Because of a small physical displacement of the ^{111}Cd sample from the mixed $^{79}Br/^{77}Se$ target providing calibration, the observed number of fluorescent photons counted had to be corrected for the different source intensities. This was done by mounting thermoluminescent diodes (TLD's) at both positions and then comparing the total dose recorded at the different points for each shot. The number of photons from ^{111m}Cd was scaled by the value of relative dose received at the ^{111}Cd and at the calibrating positions.

The cadmium sample was optically thin at both the 150 keV and the 245 keV fluorescence energies, requiring relatively small factors of 1.645 and 1.222 for the self-absorption correction. Data were corrected for fluorescence and detector efficiencies, as well as for variations in measurement time. Good agreement was found between corrected counts due to each of the fluorescence lines, and their weighted average was taken for each exposure. The resulting values of the weighted activation ratio R from Eq. (4) are shown in Fig. 4.

The linear form of the dependence of the relative yield of fluorescence from the cadmium isomers seen in Fig. 4 between 1.[illegible] and 1.6 MeV is a strong indication of the dominance of a single channel of excitation through a gateway level lying at an energy given by the value of the x-intercept. From the data of Fig. 4, it is seen that the intercept lies near 1200 keV in agreement with the known state at 1190 keV. Also shown in Fig. 4 is the energy of the next higher gateway state not excluded by an unacceptable J^{π}, the poorly characterized level at 1330 keV. It is interesting to observe that for end point energies above this value there seems to be no clear tendency of the data to depart from the simple linear fit because of the availability of this additional gateway. A greater number of measurements at successively higher end point energies would be needed to confirm this indication that the 1330 keV level has no particular role in the excitation of ^{111m}Cd.

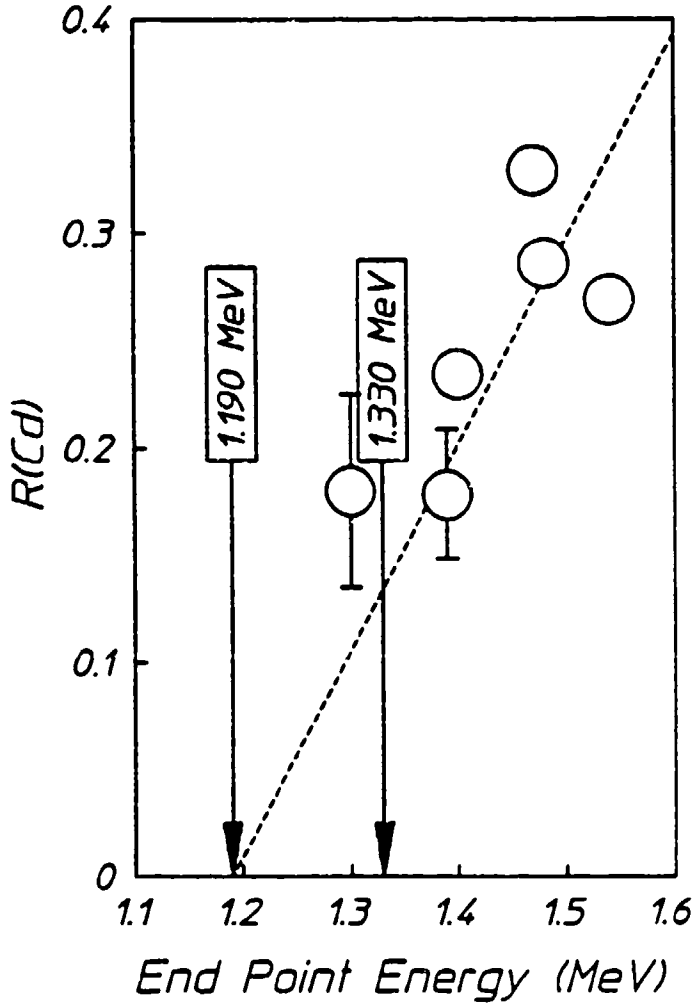

Figure 4: Ratios of isomeric fractions produced in ^{111m}Cd to those in ^{79m}Br, as corrected for the finite duration of the counting interval and plotted as a function of the end point energy of the bremsstrahlung. The dashed line shows a linear fit to the data intercepting the x-axis at a gateway energy of 1.19 MeV. Excitation energy of the next higher gateway is shown at 1.33 MeV. In this figure and in Fig. 5, the error bars for the two least precise points have been shown. The statistical errors for the other points are commensurate with the plotting symbols in the figures.

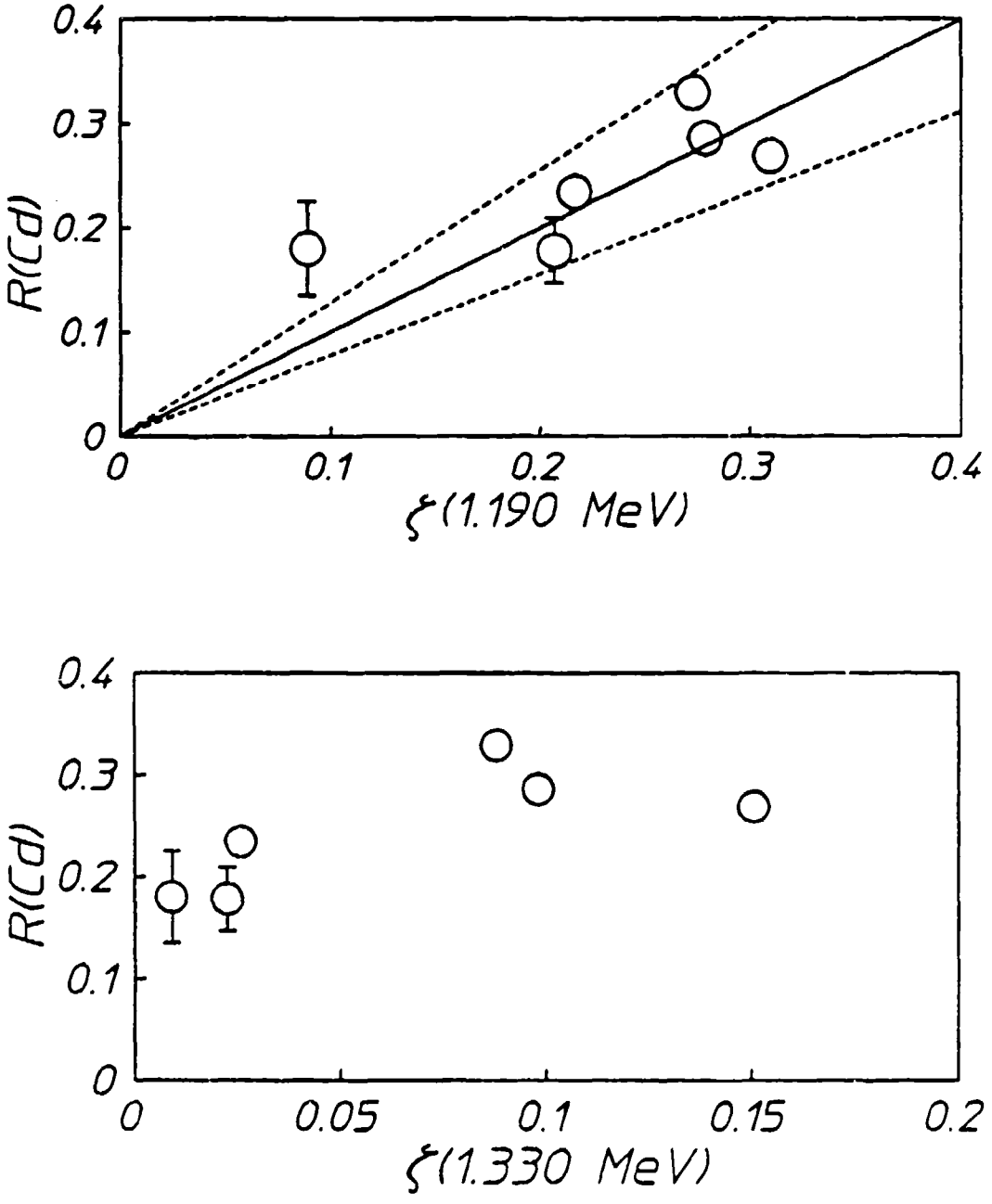

Figure 5: Plots of the weighted activation ratio R(Cd) as a function of the spectral intensity at energy E normalized to the intensity at the 761 keV gateway in ^{79m}Br.
(a) Plot for E = 1190 keV. The heavy line shows the least squares fit through the origin, and the dashed lines bound the uncertainty in such a fit.
(b) Plot for E = 1330 keV, showing the absence of a reasonable fit that would include the origin.

Once most of the data are established as being consistent with the model of excitation through a single level at 1190 keV, Eq. (4) provides a means of determining the absolute cross section for the excitation. In Fig. 5(a) data for the measured values on the left side of Eq. (4) are plotted as functions of the relative intensities $\zeta(1190)$ appearing on the right. As can be seen from Eq. (4), the best slope around which the data of Fig. 5(a) scatter would represent our experimental determination of the product of the first two terms on the right of Eq. (4). For comparison, the same approach is repeated in Fig. 5(b) to show the difficulty in attempting to force the interpretation that the principal gateway level is the state at 1330 keV. In Fig. 5(b) the weighted activation ratios are plotted as functions of $\zeta(1330)$. It is difficult to consider these data as approximating a linear dependence of R upon ζ, and particularly one which extrapolates to the origin as required by Eq. (4).

From the linear fit to the data of Fig. 5(a) shown as the heavy line, Eqs. (3) and (4), and the value of the integrated cross section for ^{79}Br mentioned earlier, we obtain

$$\xi_{1190}(\mathrm{Cd}) = (8.2 \pm 2.1) \times 10^{-32}\ \mathrm{cm}^2 \quad . \qquad (5)$$

The uncertainty was obtained from application of the same analyses to the dashed lines in Fig. 5(a) reasonably bounding the scatter from the least squares fit to the data. The statistical scatter in the data is within the bounds established by the uncertainty in intensity.

Finally, substituting Eq. (5) into Eq. (3) and solving for the integrated cross section give for the 1190 keV transition in ^{111}Cd,

$$\pi b_a b_o \sigma_o \Gamma/2 = (9.8 \pm 2.5) \times 10^{-29}\ \mathrm{cm}^2\ \mathrm{keV} \quad . \qquad (6)$$

This is the value we report in Table I.

Table I

Summary of integrated cross sections reported for the reaction $^{111}Cd(\gamma,\gamma')^{111m}Cd$ through a level near 1200 keV.

Cross Section $\pi b_a b_o \sigma_o \Gamma/2$ ($\times 10^{-29}$ cm^2 keV)	Reference
8 (+4,-0.5)	Cauchois, Heno and Boivin (Ref. 5)
6 ± 2	Boivin, Cauchois and Heno (Ref. 6)
15 ± 3	Yoshihara (Ref. 7)
10.2 ± 2.6	Lakosi, Csuros, and Veres (Ref. 8)
35 ± 4	Watanabe and Mukoyama (Ref. 2)
5.8 ± 0.8	Krcmar et. al. (Ref. 3)
14 ± 1	Bikit et. al. (Ref. 4)
9.8 ± 2.5	This work

Conclusions

The detailed characterization of the spectrum emitted by the intense source of pulsed bremsstrahlung described earlier[13] has been found to be sufficient to describe the quantitative yield of the reaction $^{111}Cd(\gamma,\gamma')^{111m}Cd$, for the value of the integrated cross section given by Eq. (6).[18] Table I shows that value to fall within the interval over which the prior measurements have scattered. In this work there was no need to invoke any nonresonant reaction channels of the type sometimes used[3] in the description of this reaction.

In addition to providing further evidence against the occurrence of nonresonant reactions in ^{111}Cd, the results of this work have important implications for the calibration of intense sources of pulsed continua. By providing a photoactivation channel with a well-defined gateway at 1190 keV, a sample of ^{111}Cd can readily complement the information supplied[12,13] by ^{79}Br about the intensity at 761 keV and by ^{115}In at 1078

keV.[14] Moreover, the results of this work may indicate why previous work gave such disparate results, no matter how carefully done. The most recent experiments[3,4] with ^{60}Co sources were strongly model dependent. In those efforts, the irradiating intensity and its dependence upon experimental variables were assumed to be a result of Compton scattering from the ^{60}Co line at 1332 keV to the absorption energy at 1330 keV. From Fig. 4 it can be seen that the actual excitation energy is nearer 1200 keV. In the ^{60}Co experiments, the intensities at the real gateway must have differed drastically from what had been calculated because of the substantial differences in energies assumed for the gateway.

Finally, it seems this technique of using single pulses of intense continua to measure integrated cross sections for the production of measurable populations of isomers can provide data of use in astrophysical modeling. Cross sections at energies as low as 1 MeV are quite large for such elements as Se, Br, In and Cd and might provide viable photonuclear channels for the production of enough isomeric population to be important in cosmic nucleosynthesis. It seems that the experiments reported here give evidence that it is possible to advance the precision for the characterization of (γ,γ') reactions toward that enjoyed by other types of particle reactions at comparable energies.

References

1. B. Pontecorvo and A. Lazard, C. R. Acad. Sci. 208, 99 (1939).

2. Y. Watanabe and T. Mukoyama, Bull. Inst. Chem. Res., Kyoto Univ. 57, 72 (1979).

3. M. Krcmar, A. Ljubicic, K. Pisk, B. Logan and M. Vrtar, Phys. Rev. C 25, 2097 (1982).

4. I. Bikit, J. Slivka, I. V. Anicin, L. Marinkov, A. Rudic, and W. D. Hamilton, Phys. Rev. C 35, 1943 (1987).

5. Y. Cauchois, Y. Heno, and M. Boivin, C. R. Acad. Sci. Ser. B 262, 503 (1966).

6. M. Boivin, Y. Cauchois, and Y. Heno, Nucl. Phys. A137, 520 (1969).

7. K. Yoshihara, Isot. Radia. Technol. 3, 464 (1960).

8. L. Lakosi, M. Csuros, and A. Veres, Nucl. Instrum. and Meth. 114, 13 (1974).

9. B. Harmatz, Nuc. Data Sheets 27, 453 (1979).

10. Evaluated Nuclear Structure Data File (Brookhaven National Laboratory, Upton, New York, 1986).

11. B. Rosner, Phys. Rev. 136, B664 (1964).

12. J. A. Anderson and C. B. Collins, Rev. Sci. Instrum. (to be published Nov. 1987).

13. J. A. Anderson and C. B. Collins, Rev. Sci. Instrum. (submitted).

14. C. B. Collins, J. A. Anderson, Y. Paiss, C. D. Eberhard, R. J. Peterson, and W. L. Hodge, Phys. Rev. C (pending).

15. K. Yoshihara, Zs. Nemeth, L. Lakosi, I. Pavlicsek, and A. Veres, Phys. Rev. C 33, 728 (1986).

16. M. L. Wiedenbeck, Phys. Rev. 67, 92 (1945).

17. E. C. Booth and J. Brownson, Nucl. Phys. A98, 529 (1967).

18. The value of $\pi b_a b_o \sigma_o \Gamma/2$ was determined in this work relative to the calibration value for ^{79}Br taken from the literature and confirmed in recent experiments described in Ref. 13.

PHOTONUCLEAR EXCITATION FOR THE CALIBRATION OF PULSED BREMSSTRAHLUNG SPECTRA

by Y. Paiss, C. D. Eberhard, and C. B. Collins

Photoactivation, the absorption of a high energy photon to form an excited nuclear state, has been studied for the last 50 years.[1] However, only a few tens of papers have appeared in the literature and those dealt only with the excitation of relatively long-lived isomers. The more recent development of intense pulsed x-ray devices has made it possible to extend those studies to the excitation of isomeric states with lifetimes below one second. This, in turn, has made it practical to use photonuclear activation as a means of quantitatively characterizing the spectra emitted by such sources.

It is very difficult to calibrate x-ray continuua above 200 keV if the source is pulsed for periods of microseconds or less. Recently we suggested a technique that has since proven successful[2] in which the (γ, γ') reactions are used to sample a pump continuum at discrete energies. By determining the activation induced by a single flash of x-rays, the intensity over the relatively narrow absorption width of the sample nuclei can be determined. Perhaps the most surprising aspect of this technique is that usable signal-to-noise ratios can be realized despite the modest sizes of the integrated absorption cross sections for such nuclear transitions.

The purpose of this paper is to quantify the photoactivation technique and to describe the most favorable set of nuclear species suitable for calibrating pulsed continuua over ranges not covered by existing techniques. To identify the appropriate span of energies, it is useful to first review the extant technology.

1. For machines capable of high repetition rates such that each burst is "cheap," the problem is particularly tractable. From every burst, a small sample (one photon or less) of the radia-

tion is taken, measured with a solid state detector such as intrinsic Ge, stored and added up over many bursts to make a spectrum. Of course, this is possible only if all bursts are equivalent.

2. The second method of determining the spectrum of an x-ray source utilizes diffraction by a suitable crystal. This method is viable for photon energies to about 150 keV. Above this, no crystal gives good dispersion over a wide spectral range because wavelengths are invariably smaller than lattice spacings. In a considerable advance to the state-of-the-art, a crystal monochromator was recently used up to one MeV under constrained circumstances.[3]

3. The third method employs the energy dependencies of the gamma ray absorption coefficients of various elements by analyzing the response of thermoluminescent devices (TLDs) or emulsions located behind sample shields composed of these elements. One can unfold the spectrum from the TLD responses. Unfortunately, for photon energies greater than 200 keV, all elements have very similar ratios of the absorption coefficients considered as functions of photon energy. For this reason, this method is limited to energies less than 200 keV. Efforts to push this limit to higher energies have met with rather limited success because they have required prior knowledge of the shape expected for the source spectrum.[4]

4. The most complex instrumentation for such measurements is the Compton spectrometer which uses time-of-flight or electromagnetic separation of the Compton electrons. For quasi-relativistic electrons, the time-of-flight technique requires extremely long tubes. However, in both electromagnetic and time-of-flight techniques, it is possible that the measurement time will not be sufficiently delayed to avoid the radiofrequency noise of the source machine, compromising the usefulness of this device for large sources producing many kilojoules of photons. A variation of the Compton spectrometer in which the electrons follow helical trajectories may reduce the required tube length by two orders of magnitude, thus reducing the size of the spectrometer, and delay the analysis until after the machine noise subsides. This is a promising method,

and future utility may be expected.[5] However, since for each energy, there is spread in the time of flight, much data analysis is required to unfold the spectrum from the response, and errors may accumulate.

5. Above 1.67 MeV, the threshold for Be(γ,n) reactions, photonuclear reaction techniques based upon neutron activation or (γ,n) reactions may be used.

Here we propose to use the accumulated nuclear data on photoactivation to develop a calibration technique suitable for large x-ray machines. We consider a small number of nuclear species chosen to have lifetimes from a fraction of a second to several minutes. Longer lifetimes would mean lower signal-to-background ratios and thus would be of limited utility for x-ray bursts of laboratory scale. Shorter lifetimes offer greater sensitivities but at the cost of much greater complexity of the mechanisms needed to cycle targets between sites of irradiation and measurement.

Each nuclear species being considered has a known isomeric level which can be populated through decay from higher levels. These gateway levels above the isomeric state must be connected by electromagnetic transitions to both the ground state and the isomeric state. To be useful they should have orders of magnitude shorter lifetimes and therefore much wider absorption widths. Thus if several nuclear species are used, the determination of the number of nuclear isomers formed, coupled with knowledge of the electromagnetic decay schemes ending on the metastable levels, enables the determination of the x-ray spectrum in one shot.

Resonance Pumping Of Nuclei By X-Rays

In the following discussion of nuclear resonance absorption, we shall make use of these definitions:

$$\sigma_o = \frac{2I_f + 1}{2I_i + 1} \frac{\lambda^2}{2\pi} \frac{1}{\alpha_p + 1} \quad , \qquad (1)$$

where

σ_o = integrated Breit-Wigner cross section for absorption of a resonant photon,

I_i, I_f = initial and final angular momenta of the nucleus, respectively,

λ = the photon wavelength,

$\Gamma_s = b_s\Gamma/(1+\alpha_p)$ = partial width of the excited state for electromagnetic transitions to the ground state,

Γ = total level width of the excited state,

b_s = the branching ratio of the excited state to ground, and

α_p = total internal conversion coefficient for the absorption transition. This nuclear absorption cross section σ_o is the same as that used in the Mössbauer spectroscopy community.

Resonant nuclear absorption cross sections as functions of the photon energy may be described by the Breit-Wigner formula

$$\sigma_{BW}(E) = \frac{\lambda^2}{8\pi} \frac{2I_f + 1}{2I_i + 1} \frac{\Gamma_s\Gamma}{[\,(E-E_r)^2 + (\Gamma/2)^2\,]} \quad , \qquad (2a)$$

$$= \frac{\sigma_o}{4} \frac{b_s\Gamma^2}{[\,(E-E_r)^2 + (\Gamma/2)^2\,]} \quad , \qquad (2b)$$

which has the Lorentzian shape. When pumping a level by resonant monochromatic radiation where the linewidth of the photon spectrum is much narrower than the absorption line and where its center coincides

with the center of the absorption line, the effective absorption cross section is,

$$\sigma_{eff} = \sigma_o b_a \quad , \tag{3}$$

which depends only on the branching ratio and not explicitly on the linewidth. This must be modified when irradiating nuclei with a continuous spectrum which is conventionally given in terms of a flux per unit energy. If the flux is assumed to be constant over the width of the nuclear absorption line,

$$\phi(E_r) = \phi_o \text{ photons/cm}^2 \text{ s keV} \quad , \tag{4}$$

the effective cross section is found by integrating the Breit-Wigner cross section over the energy,

$$\sigma_{eff} = (\pi/2)\sigma_o b_a \Gamma \text{ cm}^2 \text{ keV} \quad . \tag{5}$$

It can be seen to increase with increasing level width.

In the region where the spectrum of the incident x-rays is continuous and above the characteristic lines of the device, this formulation for "white spectra" is applicable. An additional assumption is implicit in Eq. (5), namely that the irradiated sample is assumed to be thin and with no modifications of the spectrum due to self-absorption or scattering within the target. Here, and throughout the following discussions, the internal conversion (IC) is assumed to be negligible. Exceptions will be noted.

As a point of nomenclature it should be emphasized that in the e-beam community, spectra are conventionally described by the spectral density $\Phi(E)$ in units of keV/keV cm^2 s or time-integrated keV/keV cm^2. In this paper, the flux $\phi(E)$ is the photon flux per unit energy, which is related to the spectral density through the relation $\Phi(E) = E\phi(E)$.

If the excited gateway state produced according to Eq. (5) then decays to the metastable level being detected, the cross section for the production of the metastable is the effective cross section of Eq. (5) multiplied by the branching ratio for decay into the metastable state, b_m.

$$\sigma = (\pi/2)\sigma_o b_a b_m \Gamma \text{ cm}^2\text{-keV} \quad . \tag{6}$$

One should note that the dimensions of this cross section are (energy) × (area). The rate of formation of the metastable R in a layer dx perpendicular to the x-ray beam is, then

$$R = N_0\phi(E)\sigma_0 b_a b_0 \Gamma \quad dx \ cm^{-2}\ s^{-1} \quad , \tag{7}$$

where N_0 is the number of target nuclei/cm^3.

To show that direct pumping into the metastable level is negligible, let us assume that a nucleus having the a level scheme shown in Figure 1a is irradiated by a white spectrum $\phi(E)$. The rate at which level 1 is populated via the gateway state, level 2 is $N_0\phi(E_2)\sigma_0(2)b_a b_0\Gamma_2$, and the rate from direct population is $N_0\phi(E_1)\sigma_0(1)\Gamma_1$. The ratio of the two population rates is

$$\frac{N_0\phi(E_2)\sigma_0(2)\ b_a b_0\Gamma_2}{N_0\phi(E_1)\sigma_0(1)\ \Gamma_1} = K\,\frac{\Gamma_2}{\Gamma_1} \quad , \tag{8}$$

where

$$K = \frac{\phi(E_2)\sigma_0(2)}{\phi(E_1)\sigma_0(1)}\ b_a\ b_0 \quad . \tag{9}$$

The value of K can vary by few orders of magnitude; but, if level 1 is metastable and level 2 is not, the quantity (Γ_2/Γ_1) is a very large number. This fact, as described in the previous reports,[2] is the reason for looking for indirect pumping, or bandwidth funneling through a gateway state. Direct population of the isomeric level is practically nonexistent.

When the lifetime of the metastable state is long compared to the duration of the excitation pulse, as it is in the current application, the rates may be integrated over time so that concentrations and time integrated spectra are used. If more than one excited state can funnel population into the metastable state, then the equation for the metastable population becomes more complicated. A typical level scheme of this type is shown in Figure 1b. If N is the concentration of metastable nuclei formed by a particular nuclear species, then for each nuclear species we may write

$$N = N_0 \Sigma_i\ \sigma_i\ \phi(E_i) \quad , \tag{10}$$

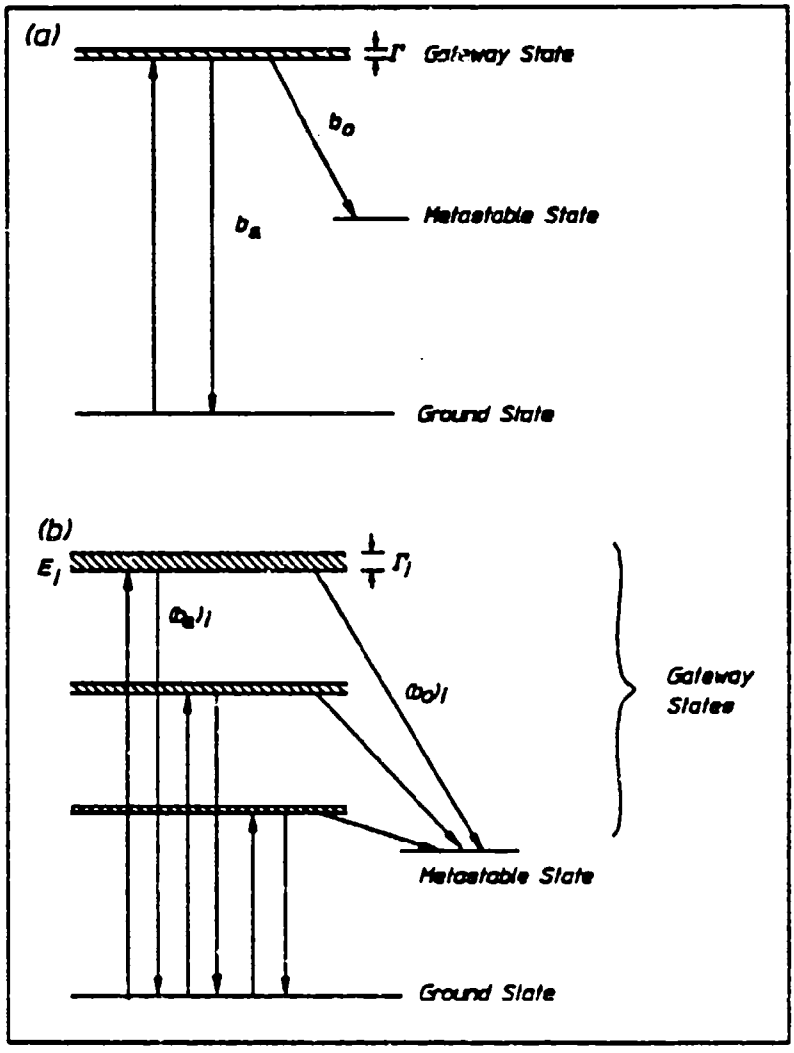

Figure 1(a): Energy level diagram of a single gateway isotope.
(b): Energy level diagram of a multiple gateway istope.

where

σ_i - the cross section for the activation of the metastable state by the absorption of a photon leading to the i^{th} excited state followed by decay to the metastable state, as defined in Eq. (6),

E_i - the energy relative to the ground state of the i^{th} excited state, and

$\phi(E_i)$ - the time integrated photon flux per unit energy at E_i.

The summation over i is the summation over the gateway states, and a few restrictions must be appreciated. The energy of the gateway state, E_i, must be less than the end point energy of the x-ray machine. Deexcitation may occur by direct decay to the metastable state or by a cascade to the metastable state and may be accompanied by the emission of photons or conversion electrons. In addition, there are other competing decay schemes not involving the metastable level. Each nuclear species must be evaluated separately. In the event of several possible cascade paths, the relative probabilities of the different chains must be summed to determine b_e, the branching ratio for decay to the metastable.

The most desirable situation is one in which each nuclear species has only one possible funneling level in the range of energies covered by the source spectrum. Then the intensity of the x-ray machine at the particular energy E_i of the gateway could be found simply by dividing the concentration of metastables formed (which is measurable) by the product of the known cross section σ and the number of exposed target nuclei to find the value of $\phi(E_i)$.

When calibrating spectra in the region between 433 and 1191 keV, we can make use of the isotopes in which this arrangement exists. The values of $\phi(E_i)$ are found and, together with the known end point energy, yield four points on the spectrum. Using this spectrum as a first approximation, additional data points obtained from the analysis of the activation of isotopes with more complicated level systems can be used to provide a better fit of the spectrum produced by the machine.

The data shown in Tables I and II have been taken from the most recent Nuclear Data Sheets dealing with these mass numbers[6-10] and supplemented by the results of recent experiments, as indicated.

Table I

Properties of single gateway isotopes

E(keV)	Jπ	b_o (metastable)	b_g (ground)	$\sigma(10^{-29}cm^2\text{-keV})$
A. Properties[6] of ^{79}Br				
761	7/2-	0.035	0.337	6.0
207*	9/2+			
0	3/2-			
B. Properties[7] of ^{111}Cd				
1190	1/2+			9.8 (measured)[12]
396*	11/2-			
0	1/2+			

*Metastable level

The Single Gateway Isotopes

The properties of the isotopes possessing only a single gateway state below 1.3 MeV are summarized in Table I. Simple calculations as described above can yield the time-integrated photon flux at the energy of the gateway states from a measurement of the number of isomeric nuclei produced by an irradiation.

Unfortunately, of the candidate isotopes described in Table I, only ^{79}Br can be recommended in an unqualified manner for use in calibrating high flux devices. Experience with ^{79}Br indicates that it is indeed very useful in calibrating high flux devices.[2,10,11] The energy levels are known, and the branching ratios of the electromagnetic transitions have been measured.

Experimental data has been accumulated about the properties of the lowest gateway state of ^{111}Cd. Although ^{111}Cd has not yet been used extensively in calibrations, the data indicates that this isotope may become very useful in providing one of the high energy points on the spectrum.[12]

Table II

Properties of multiple gateway isotopes

E(keV)	Jπ	b_o	b_a	$\sigma(10^{-29}$ cm^2-keV)
A. Properties[8] of ^{113}In				
1191	7/2+	0.216×10^{-2}	0.979	4.42×10^{-2}
1131	5/2+	0.141	0.850	10.2
1024	5/2+	0.105	0.895	2.62
392*	1/2-			
0	9/2+			
B. Properties[9] of ^{115}In				
1078	5/2+			20 (measured)[11]
941	5/2+	0.102	0.898	7.20×10^{-1}
934	7/2+	2.3×10^{-5}	1.000	6.5×10^{-5}
336*	1/2-			
0	9/2+			
C. Properties[10] of ^{77}Se				
1005	3/2-			30 (measured)
433[a]				1.7×10^{-29}
162*	7/2+			
0	1/2-			

*Metastable level
[a]The effects of the transitions at 250 keV, 440 keV and 818 keV have been combined.[10]

The Multiple Gateway Isotopes

In addition to the single gateway isotopes described above, we have considered three having multiple gateway states in the region below 1.3 MeV. These are also shown in Fig. 2 together with the single gateway isotopes. The properties of ^{113}In, ^{115}In, and ^{77}Se are summarized in Table II.

The usefulness of ^{113}In is compromised by its low abundance of 4.3% compared with its more useful partner ^{115}In (95.7%). Since both isotopes yield information about the spectrum around 1 MeV, it is more practical to use the information derived from ^{115}In activation.

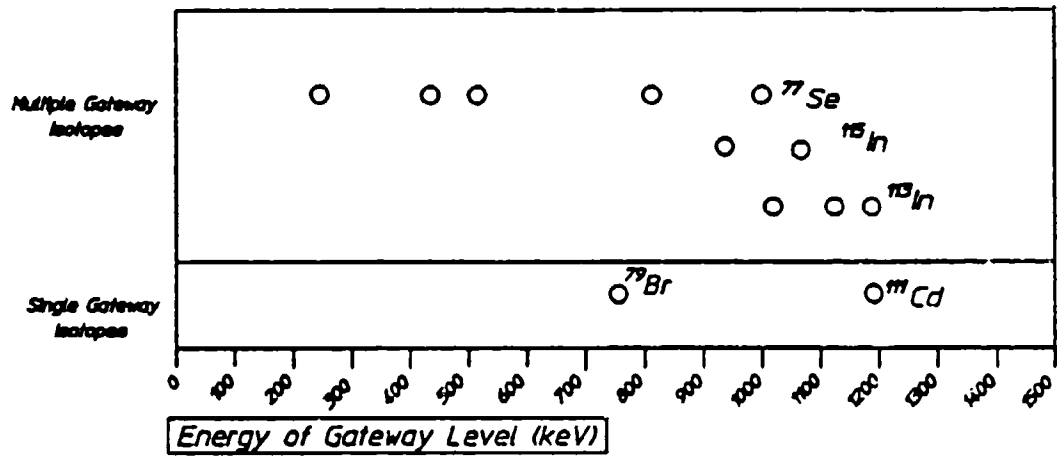

Figure 2: Single and multiple gateway isotopes proven useful in calibrating pulsed, broadband x-ray sources.

In analyzing the ^{115}In data, the contribution due to the weak absorption line at 933.8 keV for which $\sigma = 6.5 \times 10^{-34}$ cm^2 keV is considered negligible compared to that of the stronger line at 941 keV for which $\sigma = 0.720 \times 10^{-29}$ cm^2 keV. However, both are usually negligible in comparison to contribution of the 1078 keV absorption line whose measured cross section[11] is 20×10^{-29} cm^2 keV. In this respect ^{115}In may be considered a single gateway isotope.

Thus far, the isotopes ^{79}Br, ^{111}Cd, and ^{115}In described above are all useful for providing calibrations of the photon flux at energies in excess of 761 keV. To obtain an estimate of the flux at lower energies, it is necessary to utilize an isotope with a more complex excitation scheme. The isotope ^{77}Se has four low energy absorption lines at 250, 440, 521, and 818, as well as the higher energy transition at 1005 keV. These may be used to sample the low energy photon flux.[10]

Derivation Of The Spectrum

Let us now consider the results that would be obtained from exposing optically thin targets composed of individual samples, each 1 gram, of the isotopes described in Tables I and II, to a pulse of high intensity bremsstrahlung such as might be produced by a nuclear simulator of the type used in a preliminary demonstration of the method.[2,10,11,13] Specifically we assumed a typical burst from the DNA/PITHON high flux x-ray device operating with an end point energy of 1.35 MeV. The spectrum used to calculate the expected yields of metastables is a three-point average result from the TIGER code Monte Carlo simulation for a target distance of 3 cm. This spectrum is shown in Fig. 3. It should be noted that the output of the TIGER code becomes time-integrated spectral density, that is, keV/keV cm^2 which must be converted into the time-integrated flux ϕ of Eqs. (4) through (10) which is the number of photons per keV per unit area, or keV^{-1} cm^{-2}. When the measured counting rate of the decay of the metastables has been corrected for finite counting time, efficiency of a typical detector (including geometry) and any time lapse between excitation and counting, the total number of metastables activated can be determined.

The photoactivation cross sections of ^{111}Cd, ^{115}In, and ^{77}Se have been measured experimentally.[10,11,12] The effective cross sections shown in Tables I and II were used with Eq. (10) to generate the number of metastables formed. The uncertainties were generated by the standard uncertainty in the number of counts which would be observed. The numbers of target nuclei were calculated for an optically thin target of 1 gram in the natural isotopic abundances. The results of these calculations are shown in Table III. For ^{115}In and ^{77}Se, all of the gateway states described in Tables IIB and IIC were used to generate the number of metastables formed.

The flux at 761 keV may be found immediately as the quotient

$$\phi(761) = N_{meta}/N_o\sigma = (1568 \pm 8.3) \times 10^8 \text{ cm}^{-2} \text{ keV}^{-1} . \quad (11)$$

Similarly from the activation of ^{111}Cd, the flux at 1190 keV is found to be

$$\phi(1190) = (156 \pm 4.8) \times 10^8 \text{ cm}^{-2} \text{ keV}^{-1} \quad (12)$$

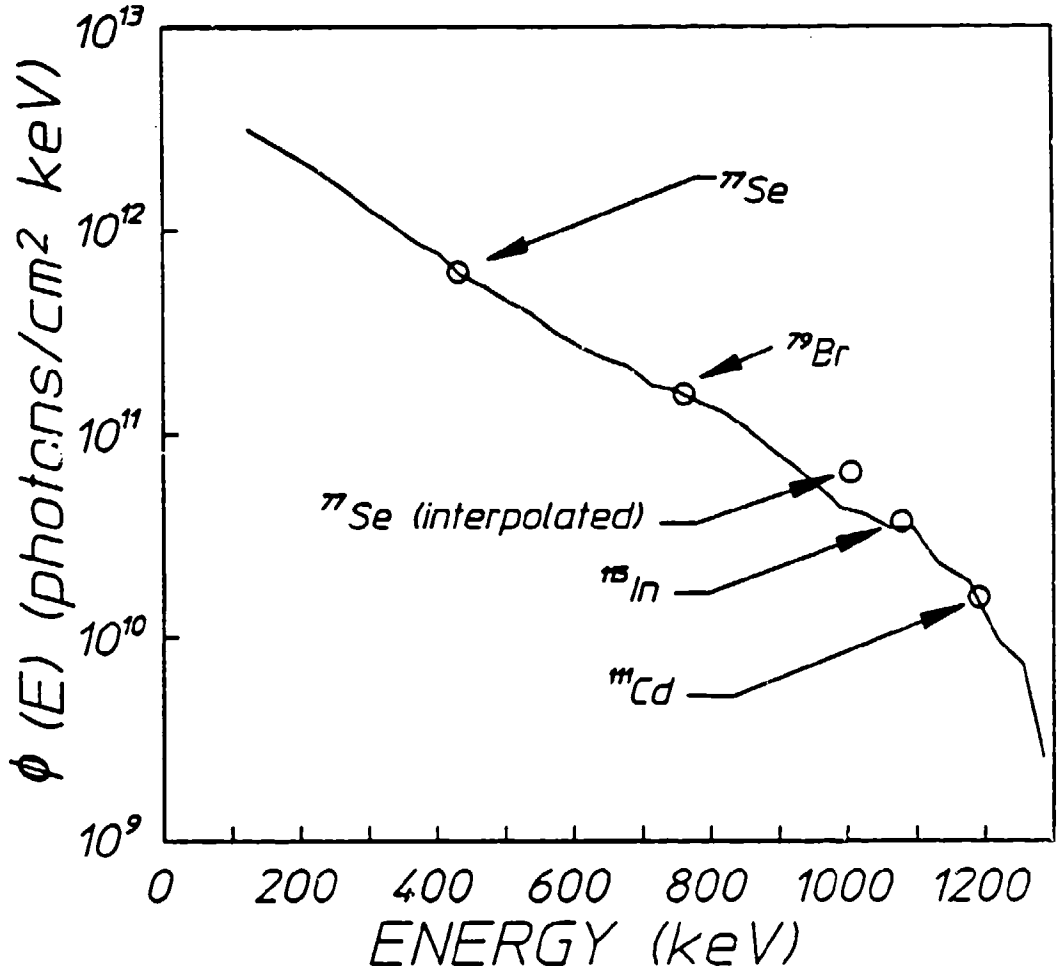

Figure 3: A sample calibration of the DNA/PITHON device. The solid line represents the flux as calculated with the TIGER Monte Carlo code. The circles represent the values of the flux which would be obtained using the calibration method presented in this paper. The uncertainty due to counting statistics is approximately 1%.

Table III

Parameters leading to the calculated number of metastables

Isotope	N_o	$E_{gateway}$(keV)	N_{meta}
^{79}Br	3.82×10^{21}	761	$3.59 \times 10^4 \pm 190$
^{111}Cd	6.86×10^{20}	1190	$1.049 \times 10^3 \pm 32$
^{115}In	5.02×10^{21}	934,941,1078	$3.70 \times 10^4 \pm 192$
^{77}Se	5.80×10^{20}	433,1005	$1.70 \times 10^4 \pm 130$

If the absorption in ^{115}In is attributed only to the absorption line at 1078 keV, the flux at 1078 keV is also given by a simple quotient,

$$\phi(1078) = (369 \pm 1.9) \times 10^8 \text{ cm}^{-2} \text{ keV}^{-1} \quad . \qquad (13)$$

This simple approach, which attributes the contribution of the absorption at 941 keV to the 1078 keV state, overestimates the flux at 1078 keV by only about 7%, which justifies the use of the "one-line approximation."

It is not possible to make this simplifying assumption in the case of ^{77}Se. However, if the three lowest absorption lines are combined into a weighted average,[10] the result is equivalent to a single absorption line at 433 keV with an effective cross section of 1.7×10^{-29} cm^2 keV. The flux at 1005 keV, the principle absorption line, may be found by linear interpolation between the data at 761 and 1078 keV. Then the flux at 433 keV may be inferred after the contribution of the 1005 keV absorption line has been subtracted from the total. This provides a useful low energy estimate. Numerically, in ^{77}Se the number of metastables found, N_{meta}, is derived from the equation

$$N_{meta} = N_o[(\phi\sigma)_{250} + (\phi\sigma)_{480} + (\phi\sigma)_{818} + (\phi\sigma)_{1005}] \qquad (14a)$$

$$= (9628 \pm 9.8) \times 10^2 \quad . \qquad (14b)$$

However, in order to use the simplification of combining the lower energy absorption lines, N_{meta} is assumed to be given by

$$N_{meta} = N_o[(\phi\sigma)_{433} + (\phi\sigma)_{1005}] \quad . \qquad (15)$$

The flux at 1005 keV, found by linear interpolation between the values obtained at 761 keV by ^{79}Br activation and 1078 keV by ^{115}In activation, is $(646 \pm 8.5) \times 10^8$ cm^{-2} keV^{-1}, and

$$N_o(\phi\sigma)_{1005} = (112.4 \pm 1.5) \times 10^2 \quad . \qquad (16)$$

When this value is substituted into Eq. (15) and the weighted cross section of the combined transition is used, the value of the flux at 433 keV is found to be $6.22 \times 10^{11} \pm 198$ cm^{-2} keV^{-1} which is in extremely good agreement with 6.17×10^{11} cm^{-2} keV^{-1}, the value obtained by linear interpolation of the results of the TIGER code.

The derived values at 433, 761, 1005, 1078 and 1190 keV are also shown on Fig. 3.

Experimental Procedure

The irradiated target used for resonant absorption is nevertheless a Compton scatterer. Since Compton scattering in the absorber can scatter off-resonance gammas into the resonance bandwidth, the total absorption depends on the physical dimensions of the absorber. When the Klein-Nishina equation is used to calculate the ratio of the Compton scattered flux to the original flux within the resonance line, this ratio is found to be around unity for an infinitely thick bromine target and a 1 to 2 MeV end point x-ray machine. The Doppler broadened resonance absorption cross section for strong lines is in the range of hundreds of kilobarns while the Compton cross section is of the order of barns. A thin target, whose depth is only a few mean free paths for resonance absorption, will scatter only a negligible number of photons into the resonance line. Thus bromine target having only a few mg/cm^2 thickness will absorb the photons from the original beam almost exclusively.

Therefore, a recommended procedure would be to place thin targets of the isotopes in the volume in which we want to measure the spectrum.[2,10,11] Nuclei with short-lived metastable states could be located in "rabbits," targets which are pneumatically transferred out of the noisy irradiation environment. After irradition, these rabbits would be propelled into counting facilities where the spectra of the gammas produced by the decay of the metastable levels would be determined. By

extrapolating the decay of metastable population, the initial number of metastables could be determined. These initial numbers would then be used in the data analysis to provide an estimate of the output spectrum of the x-ray machine. When used in the intense x-ray machines, the intensities would be sufficient to calibrate the machine on a single shot basis at[4,5] discrete energies using the data of Tables I and II.

Problems To Be Solved

Attempts to extend the resolution of this method by increasing the number of sampled energies are frustrated at the present time. In principle, intensities can be determined at three more energies, 659, 598, and 1229 keV, by adding ^{191}Ir, ^{193}Ir, and ^{87}Sr to the target sample, but only after the integrated cross sections for the excitation of the respective isomers are remeasured to a high level of precision. Then, photonuclear activation can yield an eight point sample of the spectral intensity radiated in a single flash of bremsstrahlung spanning the range of photon energies from 400 to 1400 keV.

In spite of the accumulated research data, the excitation energies of some potential gateway levels for additional samples are not well defined nor have their angular momentum and parity assignments been determined. Even in cases where the energies of the levels are known, until recently[10] no straightforward method has existed to evaluate the level width from this knowledge because different models yield very different calculated transition probabilities. For example, the single particle Weisskopf model sometimes overestimates the transition probability for E1 transitions by more than five orders of magnitude and underestimates some E2 transitions by two orders of magnitude. In some promising cases, such as ^{197}Au, the connecting gamma transitions have not been identified, although the activation of ^{197}Au has been reported.[13]

There are many discrepancies in other systems which initially appear attractive. When dealing with distorted nuclei, an additional set of selection rules governing transitions exists. The contributions of indirect reactions, such as pair production which provides positrons which in turn make inelastic collisions with K electrons at the same time producing energy to excite the isomeric state,[14] must be evaluated.

By solving the above problems either theoretically or experimentally, it is possible to apply the nuclear methods to measure the characteristic spectral intensity of the output of a large x-ray machine within a few minutes after a single shot with considerably better resolution than has been reported in preliminary reports.[2,10,11,13]

References

1. K. Yoshihara, Zs. Nemeth, L. Lakosi, I. Pavlicsek, and A. Veres, Phys. Rev. C, 33, 728 (1986). Contains useful list of references.

2. J. A. Anderson and C. B. Collins, Rev. Sci. Instrum. (to be published Nov. 1987).

3. Crystal Relectivity for Bent Crystal Spectrometer, P. H. M. Van Asche and E. Kaerts, G. L. Green and R. D. Deslattes, Paper Df.1, 1987 Spring Meeting APS.

4. X-Ray Spectra from Various Flash X-Ray Simulators, Steven G. Gorgics, Nino R. Pereira, Private Communication.

5. George T. Baldwin and James R. Kee, IEEE Trans Nucl. Sci., Vol. NS-33, 6 (December, 1986).

6. B. Singh and D. A. Viggars, Nucl. Data Sheets 371, 393 (1982).

7. B. Harmatz, Nucl. Data Sheets 27, 453 (1979).

8. J. Lyttkens, K. Nilson and L. P. Ekström, Nucl. Data Sheets 33, 1 (1981).

9. B. Harmatz, Nucl. Data Sheets 30, 413 (1980).

10. J. A. Anderson and C. B. Collins, Rev. Sci. Instrum. (pending).

11. C. B. Collins, J. A. Anderson, Y. Paiss, C. D. Eberhard, R. J. Peterson, and W. L. Hodge, Phys. Rev. C. (pending).

12. J. A. Anderson, M. J. Byrd, and C. B. Collins, Phys. Rev. C. (pending).

13. J. A. Anderson and C. B. Collins, Proof of the Feasibility of Coherent and Incoherent Schemes for Pumping a Gamma-Ray Laser, University of Texas at Dallas, Report #GRL/8701, Innovative Science and Technology Directorate of Strategic Defense Initiative Organization, July 1987, pp. 11-34.

14. R. S. Raghavan, A. P. Mills, Jr., Phys. Rev. C, 24, 1814 (1981).

PHOTOACTIVATION OF INDIUM AND CADMIUM INTO ISOMERIC STATES PUMPED BY BREMSSTRAHLUNG RADIATION FROM A MEDICAL LINEAR ACCELERATOR

by C. D. Eberhard, J. W. Glesener, Y. Paiss, J. A. Anderson, and C. B. Collins,
University of Texas at Dallas
W. L. Hodge,
High Energy Laser Associates
E. C. Scarbrough and P. P. Antich,
University of Texas Southwestern Medical Center at Dallas

Because electromagnetic transitions tend to occur with small changes of angular momenta, (γ,γ') reactions have the potential of offering insights into nuclear structure that could be rather unique. Although the literature on such reactions spans nearly 50 years,[1] experimental results are disappointing when measured against the levels of precision routinely achieved with other types of processes at low energies. The cross sections for (γ,γ') reactions are often small in cases where the product is required to have a lifetime convenient for detection, and so intense sources or accelerators must be used. In turn, these are poorly characterized; and it has been argued[2,3] that the cause of the general lack of agreement in the results reported for (γ,γ') reactions has been the deviation of the pump spectrum from expectations.

Only recently has technology been able to support the direct measurement[2,3] of the spectrum of a pulsed source of bremsstrahlung sufficiently intense in the 0.5 - 1.5 MeV range to insure a product yield large enough for accurate characterization of the (γ,γ') reactions being excited. With such a system it was found that both[4] $^{115}In(\gamma,\gamma')^{115m}In$ and[5] $^{111}Cd(\gamma,\gamma')^{111m}Cd$ occurred through the resonant excitation of a state near 1 MeV broadened by its relatively short

lifetime as would have been reasonably expected but has been recently disputed.[6,7] The sharp onset of the (γ,γ') reaction with increasing energy of the γ relegated to less than 3% any contributions from nonresonant channels that are sometimes considered dominant.[6,7,8] Thus it can be reasonably concluded that the results of the studies of the (γ,γ') reactions in ^{115}In and ^{111}Cd were able to convey information about the particular gateway state in each system, namely that it was reasonably well-connected by radiative transitions to both initial and final states of the reaction.

The integrated cross sections for excitation of the isomers such as those of ^{115}In and ^{111}Cd are usually expressed as $\pi b_a b_o \sigma_o \Gamma/2$, where Γ is the natural width in keV of the i-th pump band,

$$\Gamma = \hbar/\tau_p \quad , \tag{1}$$

and the branching ratios, b_a and b_o, give the probabilities for the decay of the broad level back into the initial and fluorescence level, respectively. The pump energy E_i is in keV and σ_o is the Breit-Wigner cross section for the absorption transition,

$$\sigma_o = \frac{\lambda^2}{2\pi} \quad \frac{2I_e+1}{2I_g+1} \quad \frac{1}{\alpha_p+1} \quad , \tag{2}$$

where λ is the wavelength in cm of the gamma ray at the resonant energy, E_i; I_e and I_g are the nuclear spins of the excited and ground states, respectively; and α_p is the total internal conversion coefficient. Cross sections for the archetype cases of ^{115}In and ^{111}Cd were of the order of 10 in the conventional units of 10^{-29} cm^2 keV. Such values for excitation through a gateway near 1 MeV are characteristic of products of branching ratios $b_a b_o$ somewhat degraded from the optimal value of 0.25. One transition is primarily responsible for the favorable width of the gateway; and the other is parasitic, contributing lesser additional width. Whether this is simply coincidental for these two cases or the result of a general principle is not known.

Very early data[9,10] indicated that yields from (γ,γ') reactions increased as higher energy gateway states were accessed. Evidence was accumulated[9,10] in the form of increases in the slopes of curves showing product yields as functions of the end point energies of the bremsstrahlung used to pump the reactions, but the changes were not dramatic. Morever, the more recent insistences[6,7] that nonresonant

channels dominated such excitations cast some doubt on the appropriate interpretation of that early data.

Systematic studies[11] have shown that collective octupole oscillations of the nuclear core can unhinder E1 transitions, making very short lived states available for (γ,γ') reactions excited from ground states at energies between 1 and 2 MeV. However, the literature[12] suggests that the branching from such a collective state would almost entirely favor the initial transition so that a diminishing product, $b_a b_o$, would largely offset the greatly increased width Γ in expressions for the integrated cross section for a (γ,γ') reaction excited through such a collective state. Such an expectation is supported by the early data mentioned above.

Since the density of states is considerably elevated at energies of 1 to 2 MeV above the ground state, an alternate hypothesis is attractive. A strong octupole oscillation of the core might serve to mix enough single particle states so that radiative branches to several different lower levels might become comparable. In this case a very large integrated cross section of (γ,γ') reactions producing isomers from ground state nuclei might be found to be only slightly dependent upon the detailed single particle assignments of neighboring nuclei. Just such an effect is reported here. Integrated cross sections of the order of 10,000 in units of 10^{-29} cm^2 keV are reported for the excitation of isomers of ^{111}Cd, ^{113}In and ^{115}In through resonant gateways pumped by bremsstrahlung from a linear accelerator producing most of its intensity near 2 MeV.

Experimental Procedure

Figure 1 shows the energy level diagram for the three nuclei of interest in these experiments, ^{111}Cd, ^{113}In and ^{115}In, together with the lifetimes of the isomers and the transitions convenient for detection. Excited states of the ^{111}Cd result primarily from promotion of the odd neutron, while those of the In isotopes arise from the odd proton. The two indiums differ only by a pair of neutrons, implying that their energy levels and angular momenta assignments should be very similar, while those of the cadmium are quite different, as seen in Fig. 1.

In these experiments, foils were used containing natural isotopic abundances of 12.8, 4.3 and 95.7%, respectively, for the ^{111}Cd, ^{113}In and ^{115}In isotopes. Two complex target assemblies including thin rectangular samples of indium and cadmium were exposed to the output of a Varian Clinac 1800 linear accelerator at the Department of Radiology of the University of Texas Southwestern Medical Center. This linear accelerator has an end point energy of 6 MeV.

The indium sample was irradiated for 121 minutes, and the cadmium sample for 240 minutes. The foils were removed to the counting facility at the Center for Quantum Electronics at the University of Texas at Dallas, where the decay of the isomeric products of the (γ,γ') reactions were measured with an HPGe spectrometer system. Only the results from indium and cadmium will be considered in this paper, although other isomers were produced in additional foils in the target package. Figures 2 and 3 show the measured counting rates as a function of time. By experimentally measuring the decay of the count rate, the decay constant of the observed peaks was determined in order to verify the identity of the peaks.

Figure 1: (Opposite) Energy level diagrams of the excited states of ^{111}Cd, ^{113}In and ^{115}In important in the production of populations of the isomers. Half-lives of the states are shown to the right of each, and sequences of (γ,γ') reactions leading to the isomer are shown by the arrows. Dashed γ' transitions occur either directly or by cascading through levels not shown. The greater width of the new gateway state formed in this work is implied by the rectangle at the higher energies of each system.

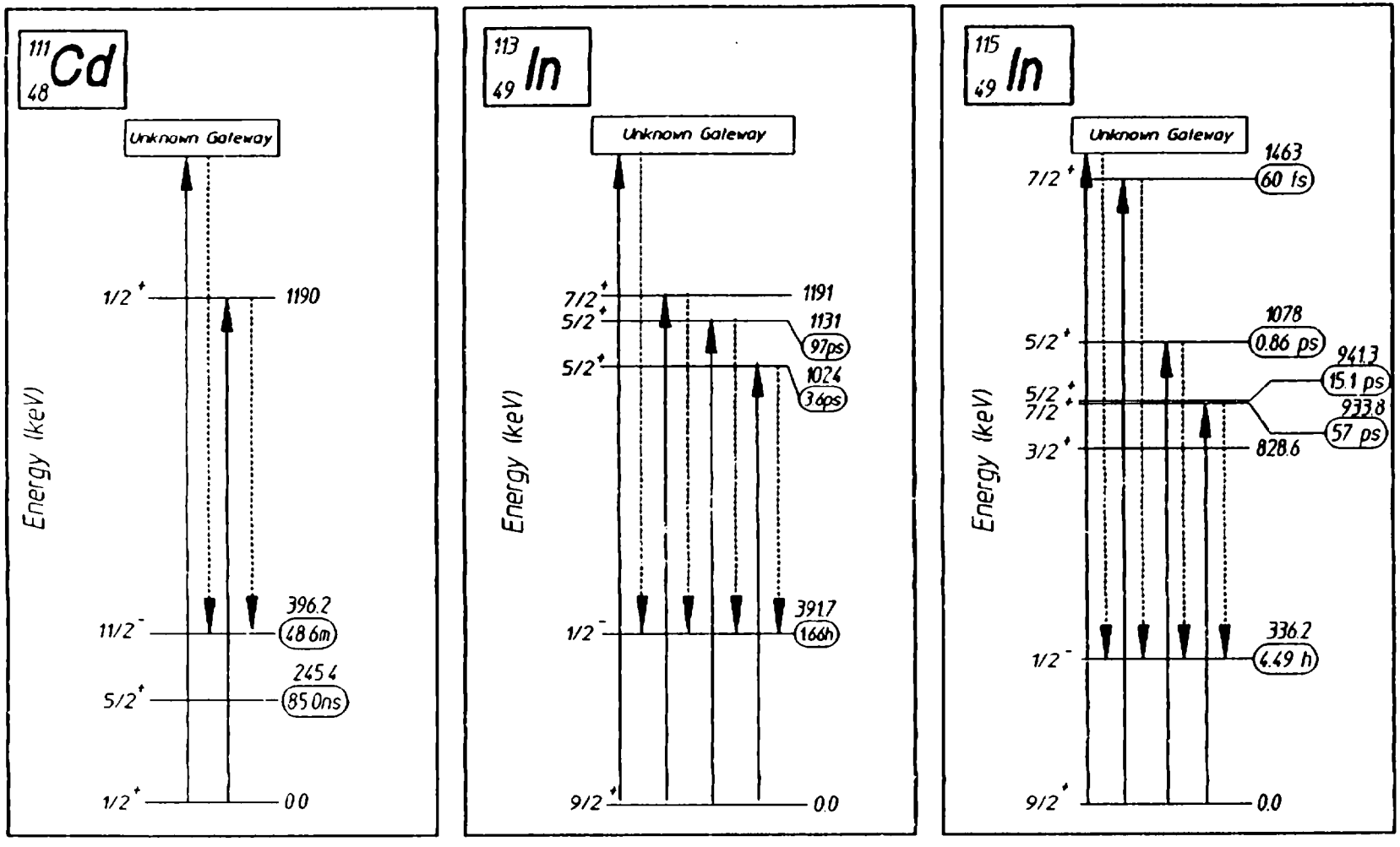
111 48 Cd
Unknown Gateway
Energy (keV)
1/2+ 1190
11/2- 396.2 48.6m
5/2+ 245.4 85.0ns
1/2+ 0.0
113 49 In
Unknown Gateway
Energy (keV)
7/2+ 1191
5/2+ 1131 97ps
5/2+ 1024 36ps
1/2- 391.7 166h
9/2+ 0.0
115 49 In
Unknown Gateway
Energy (keV)
7/2+ 1463 60 fs
5/2+ 1078 0.86 ps
5/2+ 941.3 15.1 ps
7/2+ 933.8 57 ps
3/2+ 828.6
1/2- 336.2 4.49 h
9/2+ 0.0

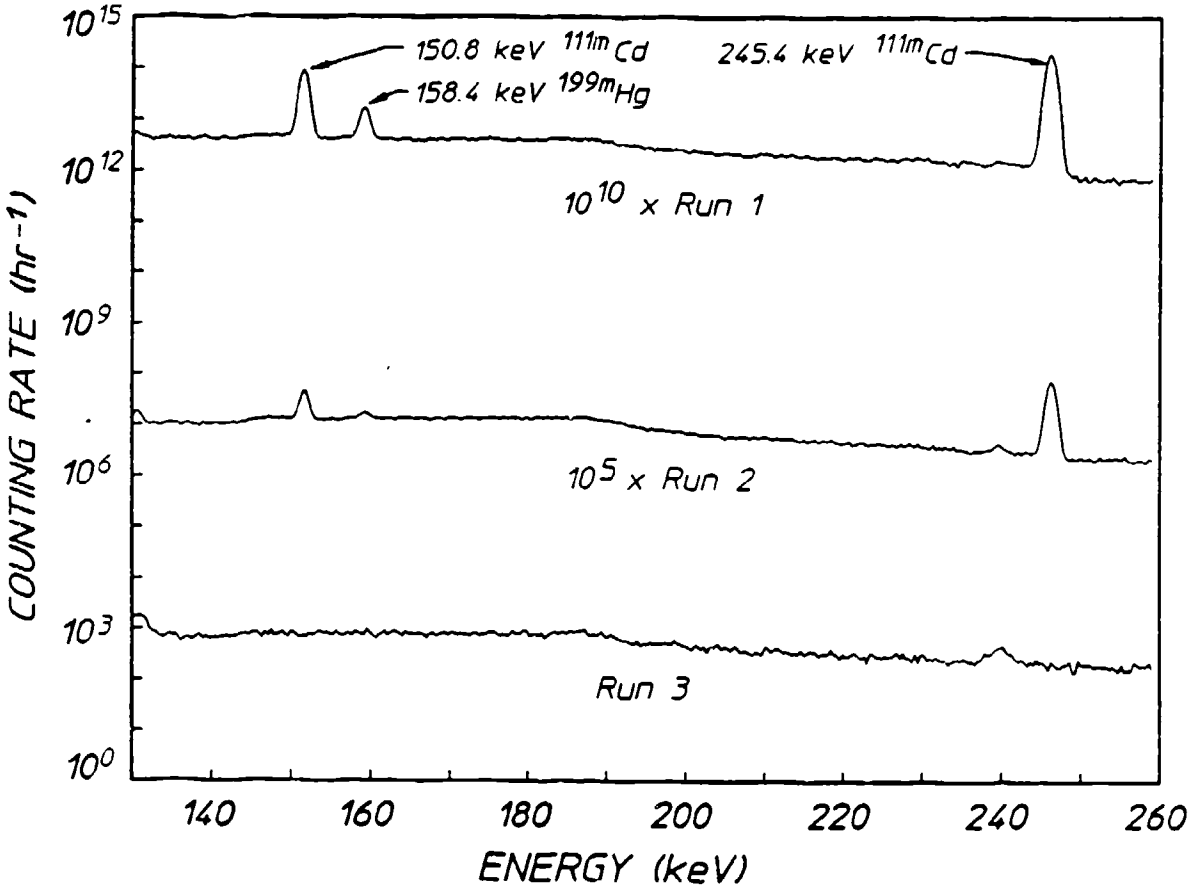

Figure 2: Three sequential spectra from an intrinsic Ge detector emphasizing the lower range of energies shown. The elapsed time from the end of the irradiation to the start of each of the counting intervals of 123, 600, and 600 m was 75, 203, and 1331 m for Runs 1, 2 and 3, respectively. Data have been offset vertically for clarity.

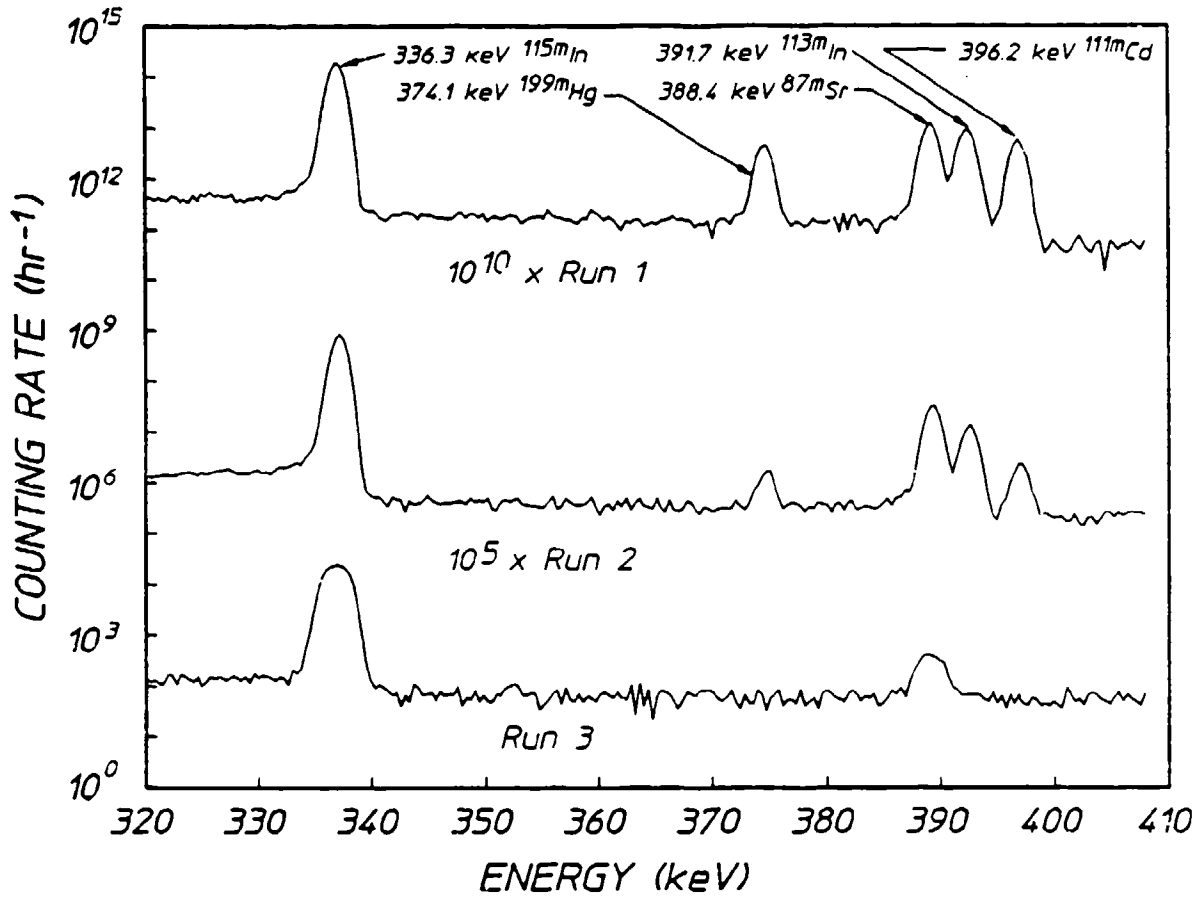

Figure 3: Continuation of the spectra of Fig. 2 to the higher energy range shown.

During the irradiation of a target which is thin in comparison to the mean free path of a pump photon, at time t the total number of metastables formed of a given isotope, $N_m(t)$, is given by

$$N_m(t) = N_o\tau \left[\Sigma_i(\sigma\Phi)_i\right] \left[1 - \exp(-t/\tau)\right] \qquad (3)$$

where

N_o = the total number of target nuclei,

$\tau = (\tau_{1/2}/\ln 2)$ = the natural lifetime, and

$(\sigma\Phi)_i = (\pi b_e b_o \sigma_o \Gamma/2)_i\ \Phi(E_i)$ = the product of the effective cross section for the excitation and subsequent decay to the isomer of the i^{th} gateway state located at the energy E_i and the flux of photons with energy E_i. The summation is carried out over the gateway states below the end point energy of the bremsstrahlung spectrum.

After the samples have been irradiated for a time T and removed from the irradiation source, the total number of counts accumulated in the interval from T_1 to T_2 is given by

$$\Delta C = K\ N_m(T)\ \exp(-T_1/\tau)\ \left[1 - \exp\left(-(T_2-T_1)/\tau\right)\right] \quad , \qquad (4)$$

where T_1 is the time elapsed from the end of the irradiation to the beginning of the counting interval, and K is the net detection efficiency factor. By measuring the accumulated counts in a given time interval and correcting for detector efficiencies, branching ratios, and self absorption, $N_m(T)$ may be determined. If the photon spectrum is known, the effective integrated cross section may be extracted.

The shape of the expected output spectrum of the linear accelerator as calculated by Monte Carlo methods[13] is shown in Fig. 4. The function describing the probability per unit energy for the emission of a photon, F(E), is normalized such that the integral under the curve is unity. In usage it must be multiplied by the total photon flux density of the linear accelerator which was 1.74×10^{12} photons/cm^2 min for the indium exposure and 1.54×10^{12} photons/cm^2 min for the cadmium exposure. The spectrum has been shown to be quite uniform over the field of exposure used in the irradiation, becoming somewhat harder near the beam centerline.[14]

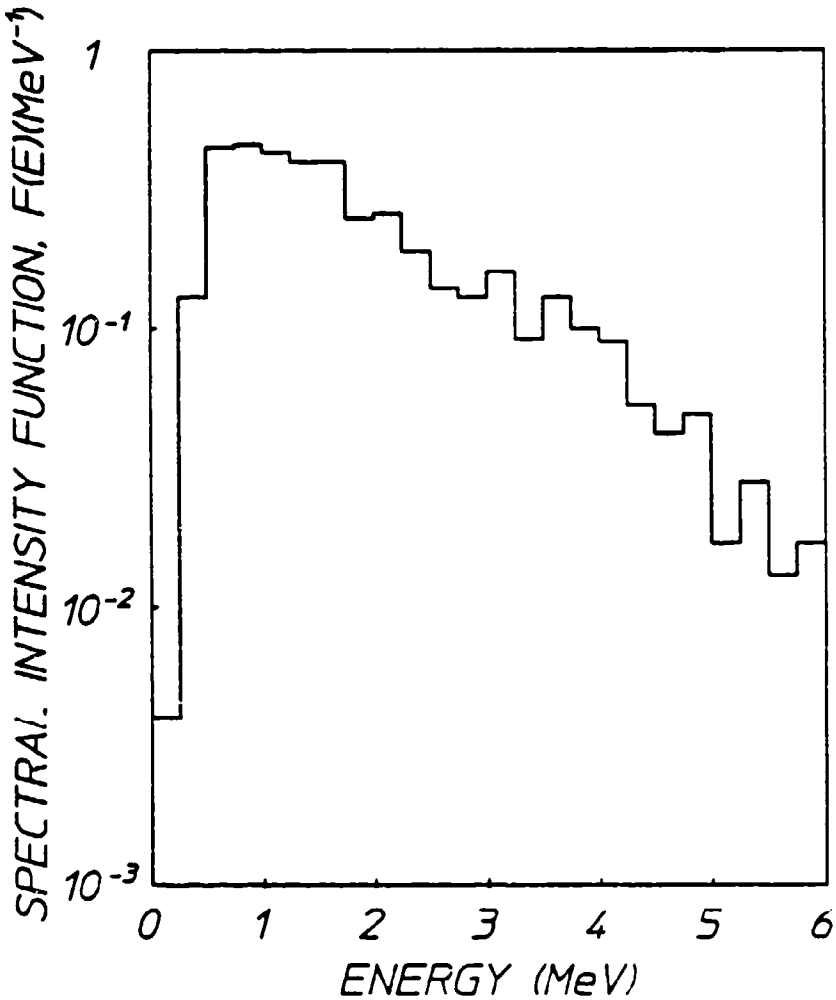

Figure 4: Relative spectral intensities of the bremsstrahlung used for irradiation in these experiments normalized so that the integral under the curve is unity.

Results

The total numbers of metastables formed, $N_m(T)$, are listed below:

$$N_m(121 \text{ min}) = 2.86 \times 10^7 \text{ for } ^{115}\text{In} \quad (5a)$$

$$N_m(121 \text{ min}) = 4.61 \times 10^5 \text{ for } ^{113}\text{In} \quad (5b)$$

$$N_m(240 \text{ min}) = 8.24 \times 10^6 \text{ for } ^{111}\text{Cd} \quad (5c)$$

The 2.2 g indium foil contained 1.10×10^{22} nuclei of ^{115}In and 4.60×10^{20} nuclei of ^{113}In. The isotope ^{115}In has a known gateway state[4] at 1078 keV for which

$$(\pi b_a b_o \sigma_o \Gamma/2) = 20 \times 10^{-29} \text{ cm}^2 \text{ keV} \quad . \quad (6)$$

The contribution of the absorption at the relatively narrow gateway at 941 keV is negligible compared to that at 1078 keV.

The isotope ^{113}In has gateways at 1024, 1131, and 1191 keV for which $(\pi b_a b_o \sigma_o \Gamma/2)$ is 2.62, 10.2, and 0.044 in units of 10^{-29} cm^2 keV respectively.[14] These cross sections are estimates based on Breit-Wigner cross sections and measured lifetimes taken from the Nuclear Data Sheets. Figure 4 shows that the flux is nearly constant at 7.5×10^8 photons/cm^2 min keV in this region so that the three gateways may be combined into a single gateway for which

$$(\pi b_a b_o \sigma_o \Gamma/2) = 12.9 \times 10^{-29} \text{ cm}^2 \text{ keV} \quad . \quad (7)$$

The isotope ^{111}Cd has been found to have a gateway state[5] at 1191 keV for which the effective cross section is given by

$$(\pi b_a b_o \sigma_o \Gamma/2) = 9.8 \times 10^{-29} \text{ cm}^2 \text{ keV} \quad . \quad (8)$$

The summation in Eq. (3) may be decomposed into a contribution for the known gateway(s) below 1.3 MeV plus another term $(\sigma\Phi)_x$ representing an unknown gateway state above 1.3 MeV, that is,

$$(N_m(T)/N_o\tau) = [(\sigma\Phi)_{known} + (\sigma\Phi)_x] [1 - e^{(-T/\tau)}] \quad . \quad (9)$$

When the known parameters of ^{115}In are substituted into Eq. (7), the $(\sigma\Phi)$ products are found to be

$$(\sigma\Phi)_{known} = 1.5 \times 10^{-19} \text{ min}^{-1} \quad , \tag{10}$$

which is negligible compared to the contribution to the summation from the unknown gateway state(s) obtained by substituting the results of Eq. (5a) into Eq. (3) and solving for $(\sigma\Phi)_x$, namely

$$(\sigma\Phi)_x = 2.48 \times 10^{-17} \text{ min}^{-1} \quad . \tag{11}$$

The activations due to the known gateway state comprise less than 1% of the total number of activations. If the assumed spectrum of the linear accelerator is that shown in Fig. 4 represented by

$$\Phi(E) = \Phi_o F(E) \quad , \tag{12}$$

the effective cross section $\sigma = (\pi b_e b_o \sigma_o \Gamma/2)$ may be found as a function of the energy of the assumed gateway state,

$$(\pi b_e b_o \sigma_o \Gamma/2) = 1.43 \times 10^{-26}/F(E) \text{ cm}^2 \text{ keV} \quad . \tag{13}$$

This function is plotted in Fig. 5 for ^{115}In. A study[4] of the photoactivation of ^{115}In utilizing a variable end point x-ray source indicated that the assumed gateway state must lie at least as high as 1.4 MeV. Inspection of the energy level diagrams and angular momenta assignments[4] suggests that a second significant gateway state is expected to lie at 1.418 MeV and that this may be the gateway being excited by the linear accelerator, but such an identification is speculative at this time.

For ^{113}In, the $(\sigma\Phi)$ products are found to be

$$(\sigma\Phi)_{known} = 7.63 \times 10^{-20} \text{ min}^{-1} \quad , \tag{14}$$

which again is insignificant compared to the contribution of the unknown gateway state(s),

$$(\sigma\Phi)_x = 1.22 \times 10^{-17} \text{ min}^{-1} \quad . \tag{15}$$

The energy levels and angular momenta assignments below 1.5 MeV imply that the additional gateway state(s) must lie above 1.5 MeV.[14] With the assumption of the single combined gateway state for ^{113}In, the effective

cross section of the gateway state above 1.5 MeV as a function of gateway energy is given by

$$(\pi b_a b_o \sigma_o \Gamma/2) = 6.99 \times 10^{-27}/F(E) \text{ cm}^2 \text{ keV} \quad , \qquad (16)$$

which may be found in Fig. 6. Below 1.9 MeV possible gateway levels occur at 1.510 and 1.631 MeV.[15]

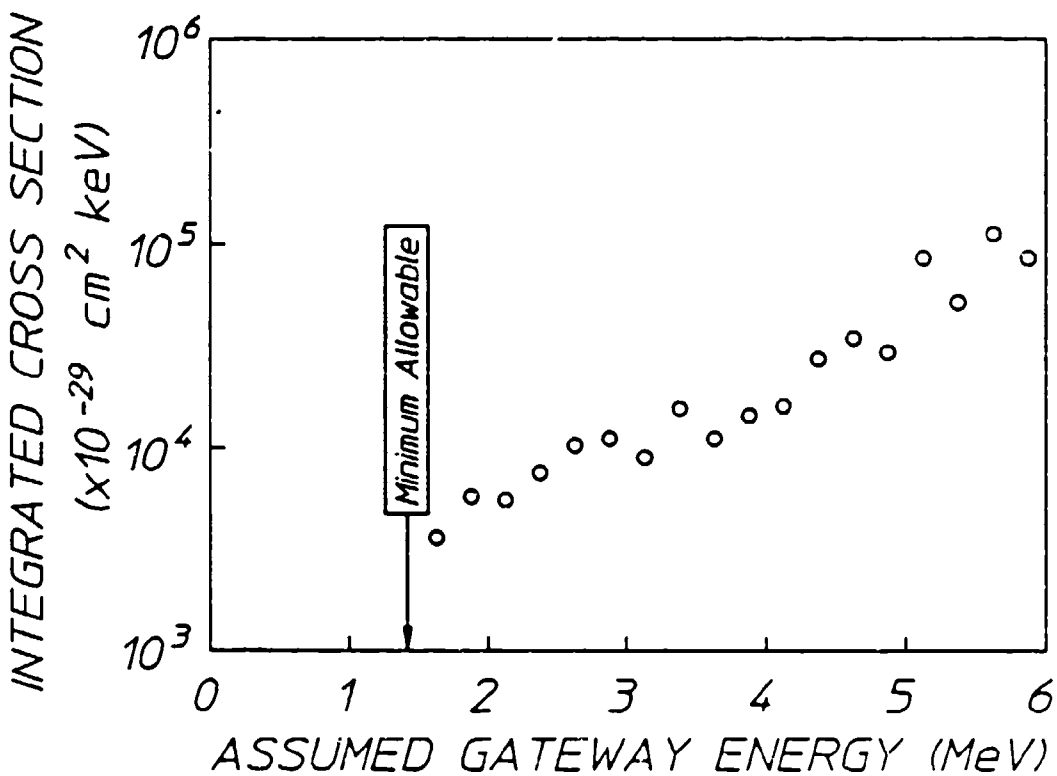

Figure 5: The integrated cross section for the photoactivation of ^{115}In through a single, unknown gateway state above 1.5 MeV as a function of the energy at which it could be assumed to lie.

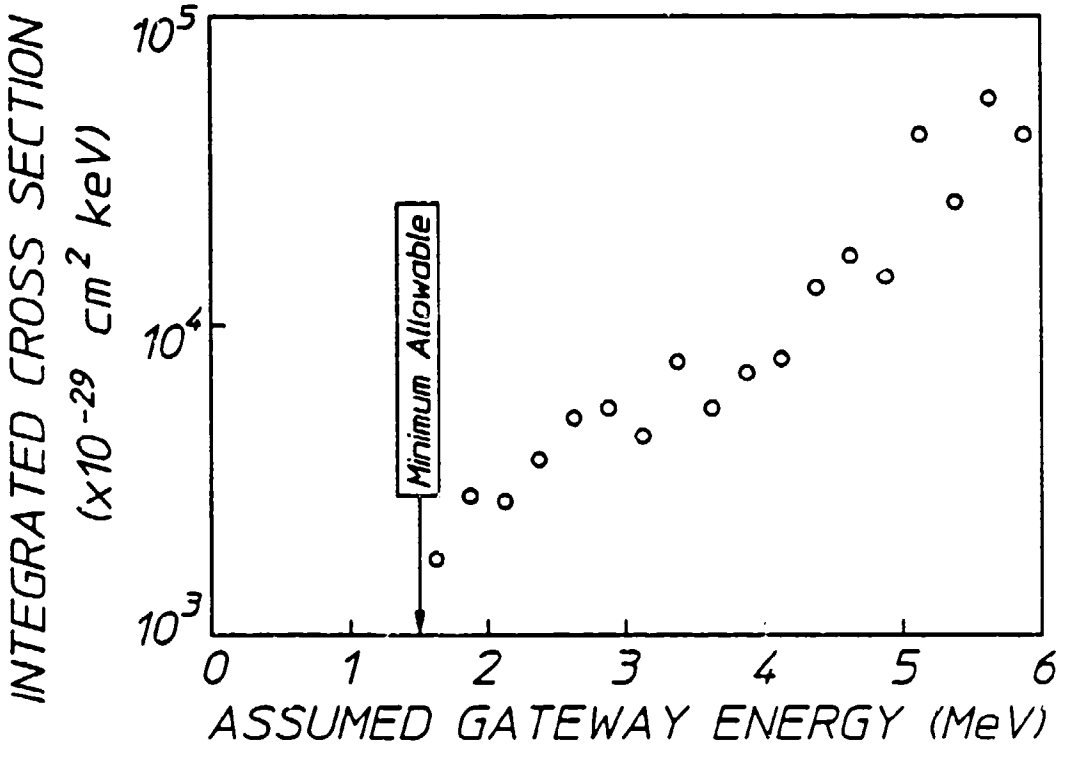

Figure 6: The integrated cross section for photoactivation through a single, unknown gateway state above 1.5 MeV as a function of the assumed gateway energy. This curve approximated the results obtained for the activation of both ^{113}In and ^{111}Cd to within the plotted size of the data points.

The 16.3 g cadmium sample contained 1.12×10^{22} nuclei of ^{111}Cd. The $(\sigma\Phi)$ products are found to be

$$(\sigma\Phi)_{known} = 6.49 \times 10^{-20} \text{ min}^{-1} \quad , \tag{17}$$

and

$$(\sigma\Phi)_{x} = 1.08 \times 10^{-17} \text{ min}^{-1} \quad . \tag{18}$$

The effective cross section of the assumed gateway state as a function of gateway energy is expressed by

$$(\pi b_a b_o \sigma_o \Gamma/2) = 7.01 \times 10^{-27}/F(E) \text{ cm}^2 \text{ keV} \quad , \tag{19}$$

which would plot to be indistinguishable from the curve derived for ^{113}In shown in Fig. 6. The minimum energy of the unknown gateway state is again considered to be about 1.4 MeV.

Conclusions

From Figs. 5 and 6 it can be seen that integrated cross sections for the excitation of isomers of indium and cadmium reach 10^{-25} cm^2 keV for (γ,γ') reactions proceeding through channels open to the bremsstrahlung from a 6 MeV linear accelerator. This is three orders of magnitude greater than values characteristic of excitation with photons of energy below 1.4 MeV. Qualitatively such an increase is of the magnitude expected to result from a change of gateway states with picosecond lifetimes to the femtosecond lifetimes characteristic of E1 transitions at these energies, unhindered by the occurrence of collective octupole vibrations. The similarity of results for nuclei with both similar and dissimilar single particle structures supports the identification of this strong channel for (γ,γ') reactions with some type of core property varying only slowly among neighboring nuclei. In such a case, however, there would need to be a mixing of several single particle states so the decay of the gateway state could occur into several different cascades with comparable probabilities.

References

1. B. Pontecorvo and A. Lazard, C. R. Acad. Sci. 208, 99 (1939).

2. J. A. Anderson and C. B. Collins, Rev. Sci. Instrum. (to be published Nov. 1987).

3. J. A. Anderson and C. B. Collins, Rev. Sci. Instrum. (pending).

4. C. B. Collins, J. A. Anderson, Y. Paiss, C. D. Eberhard, R. J. Peterson, and W. L. Hodge, Phys. Rev. C (pending).

5. J. A. Anderson, M. J. Byrd, and C. B. Collins, Phys. Rev. C (pending).

6. A. Ljubicic, K. Pisk, and B. A. Logan, Phys. Rev. C 23, 2238 (1981).

7. M. Krcmar, A. Ljubicic, K. Pisk, B. Logan and M. Vrtar, Phys. Rev C 25, 2097 (1982).

8. E. B. Norman, S. E. Kellogg, T. Bertram, S. Gil, and P. Wong, Astrophys. J. 281, 360 (1984).

9. M. L. Wiedenbeck, Phys. Rev. 67, 92 (1945).

10. E. C. Booth and J. Brownson, Nucl. Phys. A 98, 529 (1967).

11. A. deShalit and H. Feshbach, Theoretical Nuclear Physics Vol. 1: Nuclear Structure (J. Wiley, New York, 1974) pp. 488-491.

12. C. F. Perdrisat, Rev. Mod. Phys. 18, 41 (1966).

13. R. Mohan, C. Chui, and L. Lidofsky, Med. Phys. 12, 592 (1985).

14. N. C. Ikoro, D. A. Johnson, and P. P. Antich, Med. Phys. 14, 93 (1987).

15. J. Lyttkens, K. Nilson, and L. P. Ekstrom, Nucl. Data Sheets 34, 1 (1981).

ACKNOWLEDGEMENT

We gratefully acknowledge our support by the Innovative Science and Technology Directorate of the Strategic Defense Initiative Organization, under the direction of the Naval Research Laboratory.

The continued achievements of the Center for Quantum Electronics of the University of Texas at Dallas are entirely dependent upon the efforts of our entire staff of research scientists, graduate research assistants and support professionals. We express deepest appreciation for the dedication and hard work of the individuals on our team:

Jon A. Anderson
Denise D. Andrus
Alice C. Barnes
Tracey S. Bowen
Marc J. Byrd
James J. (Jeff) Carroll
James M. (Jim) Carroll
John J. Coogan, Jr.
Patricia A. Currey
Farzin Davanloo
Chizuko M. Dutta
Carol D. Eberhard
John W. Glesener
David R. Jander
Dierdre A. Jones
Eric M. Juengerman
Constance J. Kraus
Raymond K. Krause
John F. McCoy
Charles A. Mize
William R. Osborn
Yehuda Paiss
Peter W. Reittinger
Kyle W. Renfrow
Chester L. Shippy
Timothy W. Sinor
Kenneth N. Taylor
Suhas S. Wagal
Mitchel E. Wright
C. Jennifer Young